Received: 26 March 2021 | Revised: 12 August 2021 | Accepted: 15 August 2021

DOI: 10.1002/jmor.21410

RESEARCH ARTICLE

Journal of morphology WILEY

Anatomy and evolution of the head of *Dorylus helvolus* (Formicidae: Dorylinae): Patterns of sex- and caste-limited traits in the sausagefly and the driver ant

Brendon Elias Boudinot | **Olivia Tikuma Diana Moosdorf** | **Rolf Georg Beutel** | **Adrian Richter**

Friedrich-Schiller-Universität Jena, Institut für Spezielle Zoologie und Evolutionsforschung, Entomology Group, Erbertstraße, Jena, Germany

Correspondence
Brendon Elias Boudinot and Olivia Tikuma Diana Moosdorf, Friedrich-Schiller-Universität Jena, Institut für Spezielle Zoologie und Evolutionsforschung, Entomology Group, Erbertstraße 1, 07743 Jena, Germany.
Email: boudinotb@gmail.com and olivia.moosdorf@uni-jena.de

Funding information
Alexander von Humboldt-Stiftung; Evangelisches Studienwerk Villigst eV

Abstract

Ants are highly polyphenic Hymenoptera, with at least three distinct adult forms in the vast majority of species. Their sexual dimorphism, however, is overlooked to the point of being a nearly forgotten phenomenon. Using a multimodal approach, we interrogate the near total head microanatomy of the male of *Dorylus helvolus*, the "sausagefly," and compare it with the conspecific or near-conspecific female castes, the "driver ants." We found that no specific features were shared uniquely between the workers and males to the exclusion of the queens, indicating independence of male and worker development; males and queens, however, uniquely shared several features. Certain previous generalizations about ant sexual dimorphism are confirmed, while we also discover discrete muscular presences and absences, for which reason we provide a coarse characterization of functional morphology. Based on the unexpected retention of a medial carinate line on the structurally simplified mandible of the male, we postulate a series of developmental processes to explain the patterning of ant mandibles. We invoke functional and anatomical principles to classify sensilla. Critically, we observe an inversion of the expected pattern of male-queen mandible development: male *Dorylus* mandibles are extremely large while queen mandibles are poorly developed. To explain this, we posit that the reproductive-limited mandible phenotype is canalized in *Dorylus*, thus partially decoupling the queen and worker castes. We discuss alternative hypotheses and provide further comparisons to understand mandibular evolution in army ants. Furthermore, we hypothesize that the expression of the falcate phenotype in the queen is coincidental, that is, a "spandrel," and that the form of male mandibles is also generally coincidental across the ants. We conclude that the theory of ant development and evolution is incomplete without consideration of the male system, and we call for focused study of male anatomy and morphogenesis, and of trait limitation across all castes.

KEYWORDS
anatomical atlas, evolutionary developmental biology, sensilla patterning, sexual dimorphism, skeletomusculature

1 | INTRODUCTION

> In short, we can readily perceive a reason for metamorphosis, but how the differences between young and adult have come about, and how two [or more] distinct creatures can develop from one egg are questions difficult to answer. – Snodgrass (1954).
>
> Si les males des [tout animal] ont quelque droit de s'enorgueillir [de n'importe quoi], il n'en est pas de même chez les fourmis. Ce sont des êtres faibles, désarmés, sans intelligence et sans industrie, dont la présence momentanée n'a d'autre but que d'assurer la propagation de l'espèce. Aussi, dès que leur mission fécondatrice est terminée, ce qui a lieu ordinairement peu de jours après la naissance, ils errent au hasard, comme des êtres désormais inutiles, et meurent bientôt misérablement, quand ils ne deviennent pas la proie des oiseaux ou des insectes carnassiers. – André (1885).

Dorylus helvolus (L. 1764) was one of the original 17 ant species recognized by Linnaeus. These ants he knew as massive, hirsute wasps—attributed to the genus *Vespa*—with a cylindrical abdomen, hyaline wings, highly compressed femora, and a brick-red color. So distinct were these winged mysteries that a separate family was designated for them, and confusion reigned over the identity of the female for nearly a century until the fortuitous discovery of males in the raiding ranks of workers (Savage, 1849). Now known as "sausageflies" and "driver ants," for the male and females respectively, the polymorphism and polyphenism of *Dorylus* is so extreme that a third of all species are known only from the males, a fifth only from the aggressive workers, and a tenth only from the gigantic, blind, and wingless queens (Figure 1, Supplementary material, Table S1; Bolton, 2021). How many of these form-specific species are taxonomic synonyms remains a valid biological question. Historically viewed, the parallel taxonomy of the genus *Dorylus* is emblematic of the stark sexual dimorphism widespread in the subfamily Dorylinae, the family Formicidae, and the order Hymenoptera more broadly.

The phenomenon of sexual dimorphism in ants has been known for at least two and a half centuries (Réaumur, [1742–1743]), but it appears largely forgotten or simply neglected as males remain understudied, even for the Hymenoptera as a whole (Boomsma et al., 2005; Stubblefield & Seger, 1994). Post-embryonic developmental patterns resulting in the sexual dimorphism of ants, however, can be generally characterized. Dependent on queen inhibition and juvenile hormone (JH) expression at critical periods in development (Wheeler, 1986,

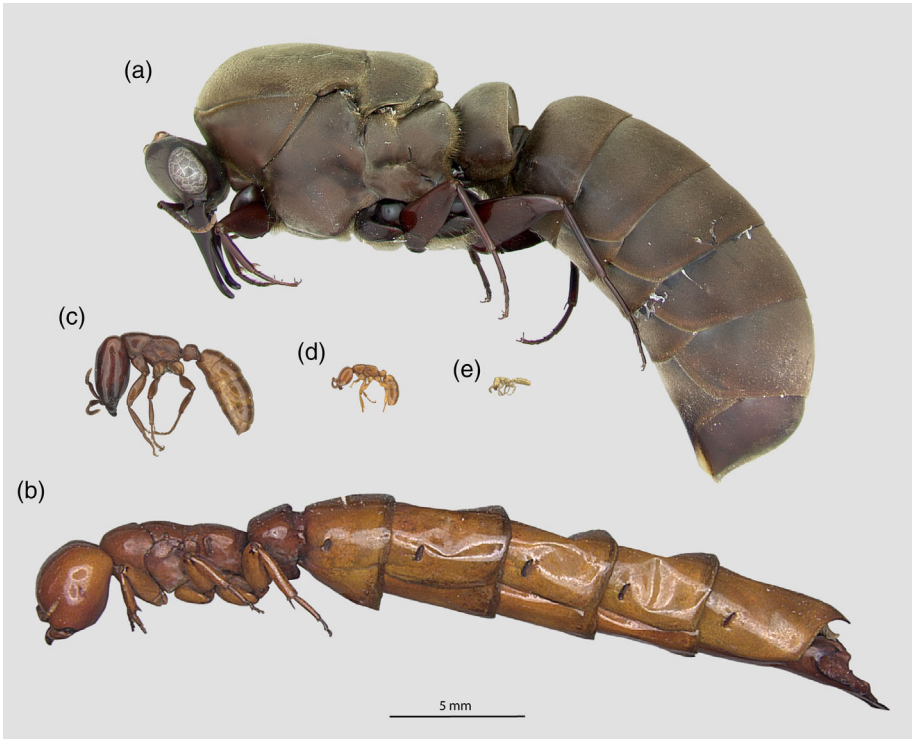

FIGURE 1 Representatives of the three castes of *Dorylus* to scale, demonstrating typical sizes and size range for the genus. (a) *Dorylus nigricans terrificus*, dealated male (CASENT0172650). (b) *Dorylus affinis pulliceps*, apterous queen (CASENT911328). (c–e) *Dorylus helvolus*, workers (CASENT0256791, CASENT0235177, CASENT0235883). Imagers: April Nobile (a), William Ericson (b, e), Bradley Reynolds (c), Shannon Hartman (d)

1991), size is the first clear differentiation of larval morphology, with reproductive-destined larvae having larger bodies (Pontieri et al., 2020). Potential exceptions include those species with "micro-queens" and "micro-males," such as *Formica microgyna* Wheeler, 1903 and *Formica exsecta* Nylander, 1846 (Agosti & Hauschteck-Jungen, 1987; Fortelius et al., 1987), and *Cataglyphis bombycina* (Roger, 1859), which has both discrete micro-queens and discretely large-headed workers (Molet et al., 2014). The larvae of the reproductive castes can be further separated by their genital imaginal discs (Penick et al., 2014) and eventually by development of the gonads (Ortius-Lechner et al., 2003). In the last larval instar, the wing imaginal discs either attain their full size or are degenerated; these discs are crucial for regulating worker caste polyphenism (e.g., Abouheif & Wray, 2002; Koch et al., 2021; Rajakumar et al., 2018), at least in formicines and myrmicines (Béhague et al., 2018), and can also result in winged-wingless polyphenism in males if their development is interrupted (Oettler et al., 2018). The specific structural transformations through metamorphosis in ants are not well understood, but this phase of development results in the anatomically and functionally differentiated adults.

TABLE 1 Summary of general phenotypic differences between the sexes of ants

Character	State: M	State: F	Reference
Ploidy	Haploid	Diploid	–
Body (total size)	Usually smaller	Usually larger	Réaumur, 1926; Divieso et al., 2020
Head (relative size)	Usually smaller	Usually larger	De Andrade & Baroni Urbani, 1999
Body (overall color)	Usually paler	Usually darker	Miyazaki et al., 2014
Cuticular hydrocarbons (CHCs)	Quantitatively dissimilar	–	Strenger & Menzel, 2020
CHCs	Qualitatively dissimilar, sometimes	–	Strenger & Menzel, 2020
Sensilla basiconica on antenna	Not expressed	Expressed	Walther, 1985; Renthal et al., 2003; Okada et al., 2006; Nakanishi et al., 2009; Barsagade et al., 2010; Ghaninia et al., 2018
Antennomere count	Usually F + 1	F	Wheeler, 1910, BEB pers. obs.
Scape length	Shorter in most subfamilies	Longer in most subfamilies	Boudinot, 2015
Pedicel	Sometimes swollen, barrel-shaped	Not swollen, barrel-shaped	Wheeler, 1910; Nakanishi et al., 2009
Flagellum	Sometimes thin, short, whip-like	Thick, longer, not tapering to apex	Wheeler, 1910; Nakanishi et al., 2009
Flagellum	Sometimes massive and elongate	Neither massive nor elongate	Wheeler, 1910; Nakanishi et al., 2009
Johnston's organ	Larger so far as known	Smaller so far as known	Wheeler, 1910
Mandible orientation	Hypognathous	Prognathous	Baroni Urbani et al., 1992; Bolton, 2003
Mandibles	Usually smaller, sometimes rudimentary	Usually larger	Bolton, 2003; Boudinot, 2015
Palpomere count	Often fewer	Often more	Bolton, 2003
Eyes, optical lobes, mushroom bodies	Larger	Smaller	Gronenberg & Hölldobler, 1999; Gronenberg, 2008; Narendra et al., 2011
Mesoscutal notauli	Often developed	Rarely developed	Wheeler, 1910; Boudinot, 2015
Wing venation	Sometimes distinct	–	Perfilieva, 2010
Meso- and metasoma form	Usually distinct	–	Boudinot, 2015
Wings	Almost always present	Diphenic.	Wheeler, 1910
Genitalia	Male	Female	Boudinot, 2013, 2018
Life span	Short-lived	Long-lived	Wheeler, 1910; Shik et al., 2013; Shik et al., 2012

Note: Flagellum variation in males versus females can be considerable, and that male ant genitalia are elaborate, regardless of the degree of simplification. These differences form the framework of expectation for our study, thus patterns not previously observed are remarked upon here as "unexpected"
Abbreviations: M, male; F, female.

Although work focused on ant sexual dimorphism is slim, some general phenotypic qualities are known which distinguish adult males from females, besides the internal reproductive organs (Table 1). The proximal causes of these sex-limited differentiations are, for the most part, untested or purely unknown in the ants. An exception is the color dimorphism of the ant genus *Diacamma*, which was demonstrated to be determined by expression of the gene *yellow* in females via RNA interference, and which has implied that a distinct and as-yet unknown mechanism of *yellow* regulation exists in ants as compared to *Drosophila* (Miyazaki et al., 2014). Through comparison of the hymenopterans *Apis* and *Nasonia*, it has become apparent that although the primary signal for sex determination varies across the universally haplodiploid Hymenoptera, that is, single- or multigene complementary sex determination or maternal imprinting (Asplen et al., 2009; Heimpel & de Boer, 2008), the genetic *doublesex-transformer* pathway does initiate the sex differentiation cascade (general: Sánchez, 2008; Verhulst et al., 2010; Patrella et al., 2019; ants: Nipitwattanaphon et al., 2014; Klein et al., 2016). The downstream patterns of sex differentiation are all but undefined in Formicidae, as are the actual anatomical transformations of the larva through pupation to phenotypic maturity. Given the largely unknown or undemonstrated patterns of development in Formicidae, these facts highlight the value and need of anatomical precision in linking genotype to phenotype (for a brief historical overview, see Appendix).

In the present work, we focus on the head anatomy and sensilla armament of ants, using three recent studies as our empirical and conceptual foundation (Richter et al., 2019, 2020, 2021). These studies have compared the entire head complex of a phylogenetically diverse sample of ant workers, documenting deep conservation of sclerite and soft tissue organization, and establishing Remanean (topological and phylogenetic-distributional) homology hypotheses for the complete head musculature (Remane, 1956). In addition to realizing unappreciated variation of the tentoria (e.g., Kubota et al., 2019), three innovations documented in these studies are here recognized as of key interest for developmental and evolutionary study: the newly discovered torular apodemes (Richter et al., 2020), the "frontal triangle" or "supraclypeal area" (e.g., Keller, 2011), and the highly modified and variable anterior (dorsal) craniomandibular articulation (Richter et al., 2019, 2021). The latter anatomical complex is of special importance due to the critical ecological value and mechanical importance of ant mandibles (Wilson, 1987; Gronenberg et al., 1998; Zhang, Li, et al., 2020). Further anatomical variation was also observed in the development of the pharyngeal and labial muscles, as well as in muscular proportions and origin points. Altogether, these studies make clear that explicit functional and phylogenetic analyses are required (e.g., Keller, 2011; Keller et al., 2014; Paul & Roces, 2019; Peeters et al., 2020; Booher et al., 2021). For our purposes, however, we reiterate that all of these new anatomical discoveries and insights have been limited to workers (i.e., females); this applies for the theory of caste differentiation in ants as well.

Overall, these are many of the generally accepted facts, patterns, and recent discoveries of ant sexual dimorphism and female-specific morphology that are key to our study. Here, we atlas the head anatomy of a male ant for the first time, and provide the first detailed comparison among males, queens, and workers. Our comparisons are of the sausagefly and the subterranean driver ants, representing the species *D. helvolus*, and three distantly related species of known phylogenetic relationship. The primary objectives of this work are threefold: (1) establish the first comparison point for male ant head anatomy; (2) compare the male with the conspecific or near conspecific female castes to understand patterns of sexual dimorphism and the within-sex polyphenism of females; and (3) compare the male with a diverse sample of previously documented workers to develop an understanding of developmental and phylogenetic patterns. At a higher level of synthesis, our objective is to comprehend the head from the perspectives of comparative anatomy, development, and phylogeny. We expected to find sex-specific differences at the outset of this study, similar to those outlined in Table 1, but took a neutral stance for the interpretation of specific patterns, and about whether males would be more similar to queens or would share specific and unique features with workers. Our overarching goal is to guide future anatomical, developmental, and evolutionary studies on ant polyphenism and sexual dimorphism.

2 | MATERIAL AND METHODS

2.1 | Specimens and preparation

Male specimens of *D. helvolus* (Linneus, 1764) were collected by P. Jałoszyński at the Silaka Reserve (−31.6511° 29.5086°, 35 m elev.) in South Africa at a light on November 17, 2019. The identification was confirmed by manual dissection of the genitalia, comparison to imaged specimens on AntWeb.org (AntWeb, 2021), and reference to the primary literature (key to subgenera: Wheeler, 1922, Gotwald Jr, 1982; key to and description of South African species: Arnold, 1915; genital illustration of S. African species *D. attenuatus* Santschi: Santschi, 1939). The specimens were fixed in a formalin-ethyl-acetate-ethanol (FEA) solution and stored in 70% ethanol. After washing in a graded series of ethanol (80%, 90%, 96%, 3 x 100%), two males were soaked in iodine overnight to increase contrast. The specimens were then washed five times in acetone for 15 min, until no more iodine could be seen. They were then critical point dried with liquid CO_2 in an Emitech K 850 Critical Point Drier (Quorum Technologies Ltd., Ashford, England). Voucher specimens are deposited in the collection of the Jena Phyletisches Museum (JPMC; Institut für Zoologie und Evolutionsforschung, FSU Jena); CASENT0753209 was used for genital dissection, −10 for mouthpart SEM, and −11 for head photography (collection data uploaded to AntWeb).

Worker *D. helvolus*, queen *Dorylus*, and other castes and taxa were examined via photomicrographs and scanning electron micrographs (SEMs) available from AntWeb.org (AntWeb, 2021). The SEMs of worker *D. helvolus* are part of the Atlas of Ant Morphology created by Keller (2011). Because images were unavailable for conspecific queens, we evaluated all digitally available specimens and referred to illustrations of *D. helvolus praetoriae* Arnold, 1946 in the literature

(Arnold, 1946). To illustrate the queen phenotype, we chose two species. The first, *Dorylus affinis pulliceps* Santschi, 1917, is a relatively closely related species formerly attributed to the nominotypical subgenus, *Dorylus* (*Dorylus*) Fabricius, 1793, to which both species belong. The second, *Dorylus nigricans molestus* (Gerstäcker, 1859), is a less closely related species formerly attributed to the surface-raiding subgenus *Anomma* Shuckard, 1840. The two respective subgenera are now referred to as the *helvolus* and *nigricans* species groups (Borowiec, 2016, 2019).

2.2 | Imaging and image data processing

2.2.1 | Macrophotography

Two dried heads were affixed to a minuten pin with superglue, then moved into appropriate position with a Patafix roller on a glass slide. Images were taken with a Canon EOS 7 D Mark II with a Canon MP-E65 macro lens with a bellows device. Two flashes were used to provide soft light through a transparent plastic cylinder. Image stacks were montaged using Zerene Stacker (Zerene Systems LLC, Richland, WA).

2.2.2 | Scanning electron microscopy

Antennae and mouthparts were manually dissected for scanning electron microscopy (SEM). Each part was affixed to a minuten pin with superglue then set in a rotatable sample stage (Pohl, 2010). The body parts were sputter coated with gold using an Emitech K 500 (Quorum Technologies). Scanning electron microscopy was performed with a Philips ESEM XL30 (Philips, Amsterdam, Netherlands) with Scandium FIVE software (Olympus, Münster, Germany).

2.2.3 | Micro-computed tomography scanning

For μ-CT, the head of one critical-point dried specimen was inserted into a pipette tip, then scanned with a Bruker SkyScan 2211 (Max-Planck-Institut für Menschheitsgeschichte, Jena, Germany), without a filter, emploaing the CCD camera of the machine. The head of a second specimen was scanned in ethanol in a pipette tip. The energy was 40 kV, current 300 μA, exposure 1.9 s, with a resultant voxel size of 1.10 μm^3 for the dry specimen and 40 kV, current 270 μA, exposure 2.9 s, with a resultant voxel size of 1.70 μm^3 for the ethanol scanned specimen. Both scan sets were performed in microfocus mode with a 0.18° rotation step around 360°.

2.2.4 | 3D-modeling and volume calculation

Segmentation of the μ-CT data set was performed in Amira 6.1 (Visage Imaging GmbH, Berlin, Germany). In order to segment the cuticle, about each tenth image was labeled in Amira then semiautomatic segmentation was carried out with Biomedisa (Lösel & Heuveline, 2016; Lösel et al., 2020). The segmented objects were exported as .tiff image stacks and imported into VG-Studio Max 3.3.6 (Volume Graphics GmbH, Heidelberg, Germany) for modeling. Structures were displayed as Phong volume renders. The specimen scanned in ethanol was visualized in VG Studio Max 3.3.6 without prior segmentation. The raw scan data of the focal critical-point- dried specimen are available at Zenodo.org (doi: 10.5281/zenodo.4776113).

2.2.5 | Image processing

All images were edited and arranged into plates with Adobe Photoshop® CS6 (Adobe System Inc., San Jose, CA) and Adobe Illustrator® CS6 (Adobe Systems Inc.); labels were applied using the latter program.

2.3 | Morphometrics

To compare the size of the maxillolabial complexes (MLC) between the male and worker, we measured the following distances on the specimens subjected to SEM or μ-CT: *Inter-hypostomal width* (IHW), as measured between the apices of the hypostomal teeth; and *oral foramen width* (OFW), as measured between the lateralmost points of the atala ("abductor swelling"). We then divided the IHW by the OFW to obtain the *maxillolabial width ratio* (MWR), an estimate of the relative length of the MLC. We chose to measure the IHW specifically as the hypostoma is a rigid structure which bears the MLC, whereas the MLC itself is a highly mobile set of structures that may not always be preserved in a consistent manner.

2.4 | Concepts and terminology

2.4.1 | Character concept

We are guided in the present work by the concept of developmental characters and states (e.g., McKenna et al., 2021; Wagner, 2014). A developmental character is a discrete phenotypic effect caused by a developmental process and can include individual or iterated (serially homologous) anatomical entities at one level of organization, and entire anatomical systems at a higher level of organization. Anatomical entities are considered to be relatively independent developmentally, and thus evolutionarily individuated structures or structure systems; such entities are expected to be the product of modular and autonomous or semi-autonomous developmental programs (e.g., Wagner, 2007, 2014). A fine-scale example of iterated phenotypic objects are the "ground" and "guard" hairs of mammals. The independent sets of ground and guard hairs would comprise two developmental characters, which can have quantitatively variable states across the body as well as among species, such as length, texture, material composition, and so on. Further

examples of developmental characters specific to Formicidae include the anteromedian clypeal seta of various Myrmicinae (Bolton, 1994), the anterolateral pronotal seta of *Strumigenys* (Bolton, 2000), or the squamiform seta rows or fields of *Rhopalothrix* (Longino & Boudinot, 2013). Pragmatically, developmental characters may be considered as substantive nouns, and the states as descriptive adjectives. In the Results, we set the anatomical nouns, including specified points or surfaces, in **bold-face** font at their key mention.

2.4.2 | General biological terminology

We employ the terms "polymorphism" and "polyphenism" in the strict sense, with the former applied to genetically determined and the latter to environmentally induced phenotypic differentiation (Simpson et al., 2011; Stearns, 1989). While genetic caste polymorphism does exist in various species of ants (e.g., Helms Cahan & Keller, 2003), we treat polyphenism as the null hypothesis for females. We use "reaction norm" and "developmental switch" in the sense of Stearns (1989), that is, phenotypic variation as a continuous function of an environmental signal, versus phenotypic variation as discrete functions of an environmental signal being above or below a given threshold. Also following Stearns (1989), we use the term "canalization" to mean consistent development of a specific phenotype, regardless of environmental variation. We consider males and queens to represent separate castes from workers and soldiers, following Wheeler's (1991) guidelines defining castes as discrete phenotypic sets caused by distinct developmental programs. We prefer the term "queen" to "gyne" in the context of the present work simply for clarity of communication, as there are no intermediate individuals between the worker and queen castes in *Dorylus*. Finally, we employ the antonyms "expected" and "unexpected" as designators for the novelty of observations given the literature and prior experience of the authors. If an observation has been previously documented, it is "expected" (e.g., Table 1); if such an observation has not been previously documented nor made in the prior systematic and anatomical experience of the authors, it is stated to be "unexpected."

2.4.3 | General anatomical terminology

The cuticular and muscular terminology largely follows that of Richter et al. (2019, 2020, 2021), with some slight modifications where necessary to increase the clarity of communication; a subsequent review and synthesis will be made to unify the terminology. Surface sculpturing terminology for the sclerites follows Harris (1979). In general, we tend to employ terms preferred by the Hymenoptera Anatomy Ontology (HAO, Yoder et al., 2010), but do make exceptions. For example, we prefer to refer to the entire line that delimits the clypeus from the cranium as the epistomal sulcus (Keller, 2011; Richter et al., 2019). Muscle label definitions are provided in Supplementary material, Table S2. Note that some concepts and concept sets are left unstated here. Term equivalencies are provided parenthetically throughout the text to clarify potential "jargon" in order to ease the interpretation of the description and discussion (see, e.g., Section 2.4.4).

2.4.4 | Digestive tract

We define the head digestive tract as having these sections and points: the prepharynx, which is that portion orad (oral to) the anatomical mouth opening (AMO), and the pharynx, which is that portion caudad (caudal to) the AMO. The AMO itself is defined by the insertion point of the transneural muscle *M. frontobuccalis anterior* (**0bu2**), and especially the position of the frontal ganglion, which encircles **0bu2** anteriorly. (Transneural = encircled by nervous tissue.) Consequently, the "postpharyngeal" gland of the myrmecological literature is now interpreted as the "pharyngeal" gland (Richter et al., 2020). As the distal portion of the hypopharynx is integrated with the labium, it is treated there. In our terminological system, the hypopharynx is further divided into a medial portion, which forms the infrabuccal pocket, and a proximal portion, which constitutes the ventral wall of the prepharynx. We pragmatically partition the epipharynx into distal, medial, and proximal portions: the distal epipharynx corresponds to the unsclerotized oral surface of the labrum in "Symphyta" (Vilhelmsen, 1996), the medial epipharynx connects to the proximal margin of the labrum, and the proximal epipharynx constitutes the dorsal wall of the prepharynx.

2.4.5 | Sensilla

For the purpose of description and discussion, we refer to "sensilloid" and "sensillum" structures. The former category represents the phenotypic objects that are described based on purely structural observations, while the latter represents structural observations that are combined with experimental (physiological) data and/or functionally relevant anatomy. Because we did not perform histology, our observations of these structures were limited to external surfaces; a further limitation was the obtained SEM resolution, which was not sufficient to observe pore patterning or the absence thereof. Consequently, we describe sensilloid structures in the results section, and integrate sensillar information in the discussion section. This clarification was spurred by conflicting terminology used by the HAO and DAO (*Drosophila* Anatomy Ontology, Costa et al., 2013). For discussion of the higher conceptual terms employed for the sensilla, see Section 4.3.

Stemming from review of the sensilla literature, we apply the term "sensilloid structure" to include potential sensory structures of various form, such as scale- and button-shaped phenotypic objects. In other words, any putative sensilla in our study is referred to as a sensilloid structure. We employ the term "sensilloid patterning" to mean the distribution and form of individual or spatially clustered sensilloid structures. For the appearance of certain hair-like sensilloid patterns, we use the term "villous" in the botanical sense, meaning "long and perhaps shaggy but not matted." Importantly, sensilloid structures can be arranged singularly, in pairs, in rows of three or more, or in fields with various subpatterning; at least in *Drosophila*, sensilla position stereotypy is known to be regulated by lateral inhibition (e.g., Corson et al., 2017). To describe the stature (inclination) of hair-like sensilloid structures (setae), we use the system of Wilson (1955). "Appressed"

setae are flat or prostrate on the cuticular surface (~0–10° angle); "decumbent" setae are standing up higher, but not at a 45° angle (~10–40° angle); "subdecumbent" setae are at about a 45° angle (~40–50° angle); "suberect" setae are inclined above 45° but are not near a right angle (~50–85° angle); and "erect" setae are at about a right angle (~85–95° angle). All statements of stature are based on visual estimation.

2.4.6 | Head orientation

We realized during the process of considering head orientation that the general terminology (e.g., prognathy, hypognathy, orthognathy; see Beutel et al., 2014) does not adequately describe the anatomical conditions observed in ants, which are narrow necked and dynamically flexible as compared to Orthoptera or Coleoptera, for example. Because of this, we chose to apply a neutral terminology specific for the head, and which can be used instead of or in combination with the meso- and metasomal body axes. We recognize three defining axes specific to the head: oral-anal (OA), frontal-abfrontal (FA), and lateromedial (LM). The OA axis extends from the center of the oral foramen to the center of the foramen occipitale; the FA axis extends from the center of the face to the center of the postgenal bridge (effectively the "abfrontal" surface of the head); and the LM axis extends from the left side to the right side of the head. The three planes of the head are formed by the combination of these axes: the frontal plane combines the OA and LM; the sagittal plane combines the OA and FA; and the transverse plane combines the FA and LM. Note that our description treats the antenna as if it were oriented directly away (frontally) from the cranium, thus the antenna is described by the OA, LM, and proximodistal (PD) axes. We also clarify the use of the lateromedial and ectomesal designations; the former defines points, areas, or structures as lateral or medial relative to the sagittal plane, while the latter defines points, areas, or structures that are on the ectal (external) or mesal (internal/lumenal) surfaces of the body wall.

2.4.7 | Phylogenetic classification

For the discussion section, we briefly summarize the phylogeny of the Dorylinae and the Formicidae, with Bolton (2003) as our primary ant taxonomy anchor-point with minor modification, reflecting ongoing revision of the morphological definitions of the Formicoidea (Boudinot, 2020; Boudinot et al., 2020). The Dorylinae are a monophyletic group of crown ants which are sister to the formican clade (Myrmeciomorpha, Dolichoderomorpha, Formicinae, Ectatomminae *s. l.*, and Myrmicinae); the Dorylinae plus formican clade are themselves sister to the poneriine clade (Ponerinae, Paraponerinae, Proceratiinae, Agroecomyrmecinae, Apomyrminae, and Amblyoponinae); these two clades form the poneroformican clade which is sister to the Leptanillomorpha (Martialinae, Leptanillinae), and altogether comprise the crown clade of the Formicidae (Moreau et al., 2006; Brady et al., 2006; Barden & Grimaldi, 2016; Branstetter, Longino, et al., 2017; Borowiec et al., 2019; Barden et al., 2020). Within the Dorylinae there is a polyphyletic grade of numerous genera that were formerly referred to as the Cerapachyinae (Bolton, 2003; Borowiec, 2016); deriving from within the cerapachyine grade are two major clades, the Western (New World) army ants and kin, and the Eastern (Old World) army ants and kin (Borowiec, 2019). The army ant representatives of the Eastern clade include *Aenictus*, *Dorylus*, and *Aenictogiton*, with the latter two forming a clade, while the army ant genera of the Western clade include *Leptanilloides*, *Neivamyrmex*, *Cheliomyrmex*, *Eciton*, *Labidus*, and *Nomamyrmex* (Borowiec, 2019). At the scale of the Aculeata, the Formicidae is sister to the Apoidea, and both the sister to the Scolioidea (Branstetter, Danforth, et al., 2017; Johnson et al., 2013; Peters et al., 2017). Further details of ant phylogeny are provided in the discussion where necessary.

3 | RESULTS

3.1 | Male anatomy

3.1.1 | Head complex, exoskeleton

Head, overall

The **head complex** appears hypognathous, with respect to the mouthparts, as they are directed ventrally relative to the anteroposterior axis of the mesosoma, but it appears prognathous with respect to the mandibles, as they are directed orally (anteriorly) relative to the oral-anal axis; it is transverse, that is, subrectangular in facial view and with the lateromedial width as measured including the eyes being greater than the oral-aboral length (Figure 2a, d). The **cranium** is bulged dorsally relative to the mesosomal anteroposterior axis (Figure 2d,e); the **frontal surface** of the head is broadly convex, with a median **frontal bulge** (fb, Figure 2d,e) that is developed around the ocellar triangle; laterad the bulge, the frontal surface is concave, forming the **antennocranial contact surface**; the **ventrolateral margin of the head**, immediately ventrad the compound eye, is sinuate, with the ventral margin anteroventrally concave and curving through a genal bulge to the posterior head surface (gb, Figure 2b); the **posterior** (anal) **surface of the head** is shallowly concave in each lateral half of the head, and convex around the countersunk **foramen occipitale** (of, Figure 2c,d), that is, the foramen is raised posteriorly by the **postocciput**, which itself arises from a sunken pit. The **postgenal furrow** is short and longitudinal, being present on the posteroventral region of the head capsule, ventrad the foramen occipitale (pgf, Figure 2c,f). The **cuticle** is dull and dark brown.

Eyes

Laterally, the head is almost completely covered by the large, approximately hemispherical **compound eyes** (ca. 1/3 of the surface of the head capsule), which comprise ~4000 **ommatidia** each (ce, Figure 2a, b); the **surfaces of the compound eyes** are glabrous; the **circumocular sulcus** ("ocular suture") is distinctly impressed and slightly emarginate in the anterodorsal third and medial region of the eye (cos, Figures 2a c and 4a). The **three ocelli** (oc, Figure 2a,d) are ca. 0.65 mm in diameter, thus relatively hypertrophied given the size of the head; the

median ocellus is located about one ocellus diameter from either of the lateral ones, and is separated from the compound eyes by about 2.5 × its own diameter; the **lateral ocelli** are situated near the dorsalmost margin of the head, and are separated from one another by about 1.75 × their own diameters and from the compound eyes by about 1.25 x.

Frontotorular complex

The **antennal toruli** are poorly developed, each represented by a low, simple, and even rim, without distinct medial or lateral arches (to, Figure 2e), and are directed frontal–laterally (anterolaterally); they are situated near the extreme oral (anterior) margin of the cranium, and are wide set, being separated from one another at a distance that is about subequal to the distance between the toruli and compound eyes. The **frontal carinae** are poorly developed but can be seen as a short external ridge directly mesad the antennal sockets (Figure 2e).

Tentorial pits

The **anterior tentorial pits** (at, Figures 2e and 5e′) are small and are developed at the oral-lateral (ventrolateral) margin of the toruli. The **posterior tentorial pits** are located directly laterad the moderately sized and approximately round foramen occipitale (diameter ca. 1 mm) in the upper middle region of the slightly convex posterior side of the head (pits not visible in external renders).

Clypeus

The **clypeus**, in anterior (facial) view, is broadly concave between the lateral clypeal shelves (cls, Figure 2d); in oral view, it bears a pair of triangular processes which partially separate the oral and mandibular foramina; the **epistomal sulcus** is weakly differentiated from the remainder of the frontal head surface, making the clypeus difficult to discern externally (es, Figure 2d); the **median portion of the clypeus** is almost entirely situated between the antennal toruli (cm, Figure 2d); the **lateral portions of the clypeus** bear subtriangular processes anterolaterad the antennal toruli (cls, Figure 2d); the **oral margin** is infolded (cam, Figures 2e and 9f), and concealed anteriorly by the **anteromedian clypeal lobe** (cml, Figures 2e and 9f); the **surface of the clypeal infold** is concave between the true anterior margin and anteromedian clypeal lobe (cf. Figure 9f), and it receives the aboral base of the labrum when the labrum is flexed away from the mouth, that is, when the labrum is completely abducted away from the mouth (Figure 10c,f).

Mandibular articulations

The **atalar and ventral mandibular articulations** of both sides are anteromedially convergent in oral view with mandibles removed, that is, lines drawn on the respective sides connecting the lateralmost curves of the concavities, which receive the atala and mandibular condyle, would converge toward the face (dotted line on right side of head in Figure 2e).

Mouth

The medial **oral foramen** is open to the two lateral **mandibular foramina** thus the head has a single ventral **oral-mandibular foramen** (omf, Figure 2e); the oral foramen is small, with an MWR (see "morphometrics" above) of 0.37 ($n = 1$); in oral view, the oral foramen is subequal in lateromedial length to mandibular foramen (Figure 2e), and the **clypeal and hypostomal processes** (clp, hysp, Figure 2e) are closely approaching one another. The **lateral hypostoma**, which margins the mandibular foramen, is long and weakly sinuous in oral view (lhy, Figure 2e); the lateral hypostoma has a shallow **hypostomal hump** (hh, Figure 2e); the **medial hypostoma**, the region between the hypostomal processes, is short and corresponding in lateromedial length to the oral foramen; the **stipital furrow** (sf, Figure 2e) is distinct and margined by the **oral and aboral hypostomal carinae** (hysco, hysca, Figure 2e); the aboral hypostomal carina is not laminar (hysca, Figure 2c); a **hypostomal cavity**, receiving the cardinal bases and cardinal condyles, is present (hyc, cc, Figure 2e).

Sensilloid structures

Patterning overview. The **sensilloid patterning of the cranium** is uniform, covering most of the cranial surface, with two distinct glabrous (bald) patches; the **first glabrous surface** is that which encircles the compound eye dorsally, posteriorly, and ventrally (hg1, Figure 2); the dorsal region of this glabrous surface extends to the lateral ocellus, the posterior region forms a band that is about as wide as the third antennomere (first flagellomere) is long, and the ventral region lies between the compound eye and mandibular articulation; the **second glabrous surface** surrounds the postocciput (hg2, Figure 2).

Sensilloid structure classes. The sensilloid structures are sortable into two classes, both of which are hair-like (thus "setae"): (1) short, denser, and subappressed (hs1, Figure 2c); and (2) long, diluter, and variable in stature (hs2, Figure 2b,c).

Sensilloid pattern. The short, dense setae ***(1-hs1)*** form a plush field that covers the face completely, and most of the posterior head surface; their length decreases near the glabrous surfaces, sometimes apparently discretely so for the first glabrous surface. The long, dilute setae ***(2-hs2)*** form a villous field that covers most of the area that bears the plush vestiture, with the exception of the cranioscapal contact surface; on the posterior surface of the head, the dense setae are restricted to the plush field between the occiput and hypostoma.

3.1.2 | Head complex, endoskeleton

The postgenal furrow corresponds with the internal **postgenal ridge** (pgr, Figure 9f); the postgenal ridge is dorsoventrally tall and completely extends from the ventral base of the foramen occipitale, ventrad the tentorial bridge, to the hypostoma, where it abuts the cardinal concavity; it divides the ventral cephalic region along the midline and forms an attachment area for the mandibular abductor (opener) muscle. The **anterior tentorial arms** (ata, Figures 5c and 9a,c) are massive and nearly perpendicular to the longest axis of the cranium (in this case, the dorsoventral axis, assuming orthognathy); they connect to the cranium anteriorly, at the lateral bases of the toruli,

resulting in the formation of the anterior tentorial pits (atp, Figures 2e and 5e′). The **posterior tentorial arms** are extremely short, originating laterad the foramen occipitale at the posterior tentorial pits (pta, Figure 5c). The narrow and straight **tentorial bridge** connects the tentorial arms shortly anterad the foramen occipitale (tb, Figures 5c and 9c). Two strongly developed **tentorial lamellae**, serving as muscle attachment areas, are developed in the posterior half of each anterior arm; the **anterior (dorsomedial) lamella** is directed dorsally (dl, Figures 5c and 9c) and bears the origins of the extrinsic antennal muscles; the **posterior (ventromedial) lamella** is directed ventrally (vl, Figures 5c and 9c) and receives the origins of the extrinsic maxillolabial muscles, with the exception of 0mx3. The **torular ridge** (tor, Figure 5e′) corresponds to the external antennal torulus, and completely surrounds the **antennal foramen** (af, Figure 5e′); the lateral terminus of the ridge is curled (torc, Figure 5f′), thus cupping the tendons of the lateral tentorioscapal muscles (0an1, 0an3, Figure 5c); the **antennal condyle of the cranium (antennifer)** is developed on the mesal (internal) oral (ventral) surface of the torular ridge (acc, Figure 5f′). The **torular apodeme** encircles the torular ridge ventrally and medially (toa, Figure 5c), giving the internal structure of the antennal foramen a double-rimmed appearance, with duplication of the lateral and medial termini of the rim; it is produced posteromedially and its apex is downcurved at nearly a right angle, effectively embracing the medial tentorioscapal muscles (0an2, 0an4, Figure 5c); its proximodorsal margin is strongly curved, forming the **notch of the torular apodeme** (toan, Figure 5f), over which the lateral vein of the antennal ampulla curves; it also bears the origin of a pharyngeal muscle (0hy9). The **circumocular ridge**, corresponding to the exterior circumocular sulcus (cos, Figure 5a) and surrounding the interior ommatidial foramen, is well-developed (cor, Figure 5a–c).

3.1.3 | Antenna

The scapes are reddish-brown, in contrast to the cranium (head capsule) and similar to the mandibles; the flagellae are slightly yellowed distally, giving them an orange appearance. The **antennae** (bu, sc, pd, fl, Figure 2) are more than twice as long as the dorsoventral length of the head, that is, the distance between the oral (anterior) clypeal margin and dorsal head margin. The **antennal ampulla** (amp, Figure 5e′) is a transverse sac-forming membrane that connects to the lumina of the antennae; it extends across the aboral-most portion of the clypeus, traversing the aboral-most section of the epistomal sulcus (es, Figures 2d and 5e′); in dorsal view, the ampulla is anteroposteriorly thin; in anterior (ectal) or posterior (mesal) view, the **lateral vessel of the antennal ampulla** (ampl, Figure 5e′) is dorsoventrally broad and poorly differentiated from the medial portion of the ampulla; the lateral vessels arch over the dorsal proximal dorsomedial notches of the torular ridges to connect with the lumina of the antennae. Each **bulbus**, that is, the proximal articulatory part of the scapus, is deeply sunk into the **torular acetabulum**, but a considerable part is still visible externally (bu, Figure 2a,d); the **internal surface of the bulbus** forms an attachment area for the extrinsic antennal muscles; the **shaft of the scapus** is smooth, shining, and without distinct punctae over much of its surface, similar to the mandibles; it is about twice as thick as the flagellum, about 1/3 as long as the entire antenna, and somewhat more than half the dorsoventral head length (sc, Figures 2a,d and 3a); it is somewhat lateromedially compressed and proximodistally curved, such that the lateral surface (which contacts the surface at full antennal flexion) is concave, and the medial surface is convex; the **distal rim and lobes of the scapus** enclose almost the entire circumference of the pedicellus (scl, Figures 2a,b and 3a), restricting pedicellar movement to the oral-aboral axis. The **pedicellus** is bell-shaped, with a ball-like proximal articulatory region, and a cone-shaped distal portion which expands distally before narrowly constricting at its distal margin (pd, Figures 2a and 3a). The **flagellum** comprises 11 **flagellomeres** (fl, Figures 2a and 3a); while flagellomere I (antennomere III) is nearly twice as wide as long, flagellomeres II–X are about twice as long as wide, with their lengths increasing distally; the terminal flagellomere is distinctly differentiated, being long and thin, resembling a thick finger.

Sensilloid structures

Patterning overview. The **sensilloid patterning (SP) of the antenna** has a distinct zonation on each of the segments, that is, the scape, pedicel, and multiannulate flagellum. The **SP of the bulbus** (a) is a dense field; the **SP of the scape shaft** (b) varies along its length, with the shaft being densely setose in its proximal 1/7th portion, while the apical 6/7th portion is almost completely glabrous; the **SP of the pedicel** (c) is sparse on the pedicellar bell (c′), except for a proximal patch on its scapal contact surface (c″); the **SP of the flagellum** (d) is asymmetrical, with sensilloid structures largely restricted to the medial surface (apparent anterior surface), which forms a primary sensilloid field (fsf1, Figures 2a and 3a), in contrast to the lateral surface (apparent posterior surface), which forms a secondary sensilloid field (fsf2, Figures 2a and 3a).

Sensilloid structure classes. The antennal sensilloid structures are sortable into seven classes, with variable appearance and stiffness, while an eighth was observed only in workers: (1) short, bristle-like, and erect (as1, Figure 3a); (2) short, hair-like, and approximately decumbent (as2, Figure 3a); (3) short, thin, hair-like, and appressed (as3, Figure 3a,c); (4) short, thin, hair-like, and approximately decumbent (as4, Figure 3d); (5) long, thin, hair-like, approximately erect, and stiff (as5, Figure 3c); (6) long, thin, hair-like, variably erect, and flexuous (as6, Figures 2a and 3a); (7) short, thick, blade-like, and approximately decumbent (as7, Figures 2a and 3d); (8) longer, thick, blade-like, and erect (as8, Figure 12d–f).

Sensilloid pattern. The short and bristle-like setae ***(1-as1)*** form a dense field on the bulbus (a). The short hair-like and leaning setae ***(2-as2)*** occur as a field on the pedicellar contact surface (c″) and are curved, as compared to the bulbus bristle-like setae. The short hair-like and

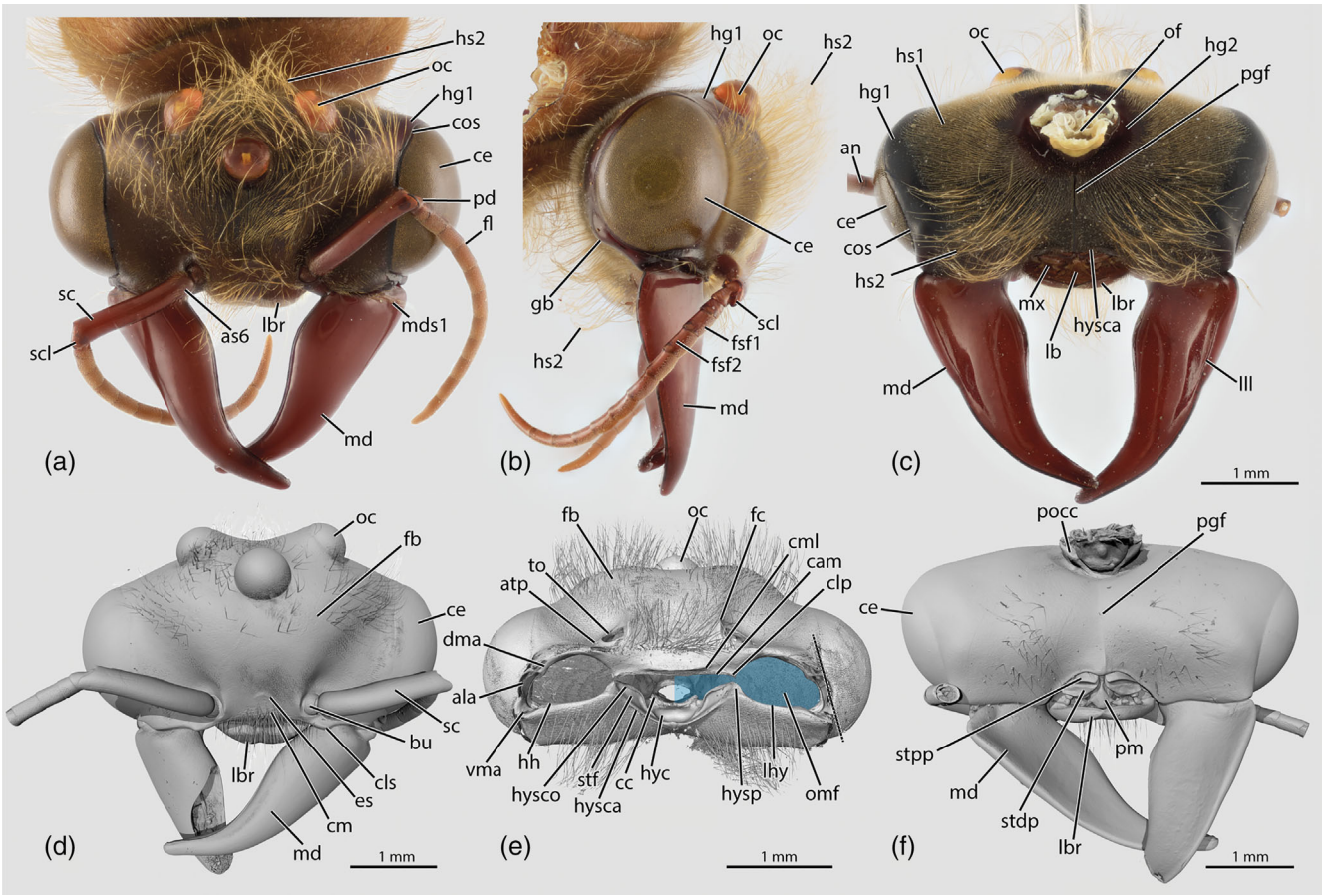

FIGURE 2 *Dorylus helvolus*, head of a male. (a–c) Photomicrographs. (d–f) 3D reconstructions. (a, d) Head in frontal (anterior) view. (b) Head in lateral view. (c, f) Head in postgenal (posterior) view. (e) Head in oral view. ala, atalar acetabulum; as6, setae of the sixth antennal class; atp, anterior tentorial pits; bu, bulbus; cam, true anterior clypeal margin; cc, cardinal condyle; ce, compound eye; cd, cardo; clp, lateral clypeal process; cm, medioclypeus; cml, anteromedial lobe of clypeus; cos, circumocular sulcus; dma, dorsal mandibular articulation; es, epistomal sulcus; fb, frontal bulge; fc, frontal carinae; fsf1, fsf2, primary and secondary seta fields of the flagellum; gb, genal bulge; hg1, hg2 first and second glabrous surfaces of head; hh, hypostomal hump; hs1, hs2, setae of the first and second head classes; hyc, hypostomal cavity; hysca, aboral hypostomal carina; hysco, oral hypostomal carina; hysp, hypostomal process; lb, labium; lbr, labrum; lhy, lateral hypostoma; lll, lateral longitudinal mandibular carina; md, mandible; mds1, first class of mandibular setae; mx, maxilla; oc, ocellus; of, foramen occipitale; omf, ocular-mandibular foramen; pgf, postgenal furrow; pm, prementum; pocc, postocciput; pt, prothorax; sc, scape shaft; scl, distal scapal lobe; stpd, distal stipital portion; stpp, proximal stipital portion; stf, stipital furrow; to, torulus; vma, ventral mandibular articulation

prostrate setae ***(3-as3)*** occur dilutely on the proximal contact surface of the pedicellar bell (in distinction to the primary scapal contact surface) (c′), and densely on the proximal primary contact surfaces of all flagellomeres (d) except apparently the proximalmost. The short hair-like and approximately decumbent setae ***(4-as4)*** are interspersed among the thick blade-like (*as7*) and long hair-like (*as4*) structures on the medial flagellomere surfaces (d) and extend dilutely onto the lateral flagellomere surfaces. The long hair-like and stiff setae ***(5-as5)*** occur dilutely on the primary sensilloid fields alongside the short hair-like (*as4*) and the short blade-like (*as7*) structures of the flagellomeres (d), but also occur sporadically on the more glabrous side, becoming denser toward the antennal apex. The long hair-like and flexuous setae ***(6-as6)*** occur on the proximal portion of the scape shaft (b). The short, thick, and blade-like structures ***(7-as7)*** form the primary sensilloid field of the flagellum (d); these structures are set in broad sockets that themselves are set in distally oriented micro-sulci; the base of the structure itself comprises a broad disc, from which the shaft of the blade arises in the proximal portion; the base of the shaft has a diameter that exceeds the diameter of the proximal disc; the shaft is lateromedially compressed, thus does not have a terete (circular) cross-section; the shaft curves slightly distad, and has an acute apex. ***(8-as8)*** the longer, blade-like structures were not observed in the male.

Musculature

The action of the scapus is caused by contraction of four extrinsic antennal muscles which originate on the lamellae of the tentorial arms; the tendons of **0an1** and **0an3**, and those of **0an2** and **0an4** are closely adjacent; **0an2** is the least voluminous extrinsic antennal muscle. The action of the pedicellus and distally attached flagellum is

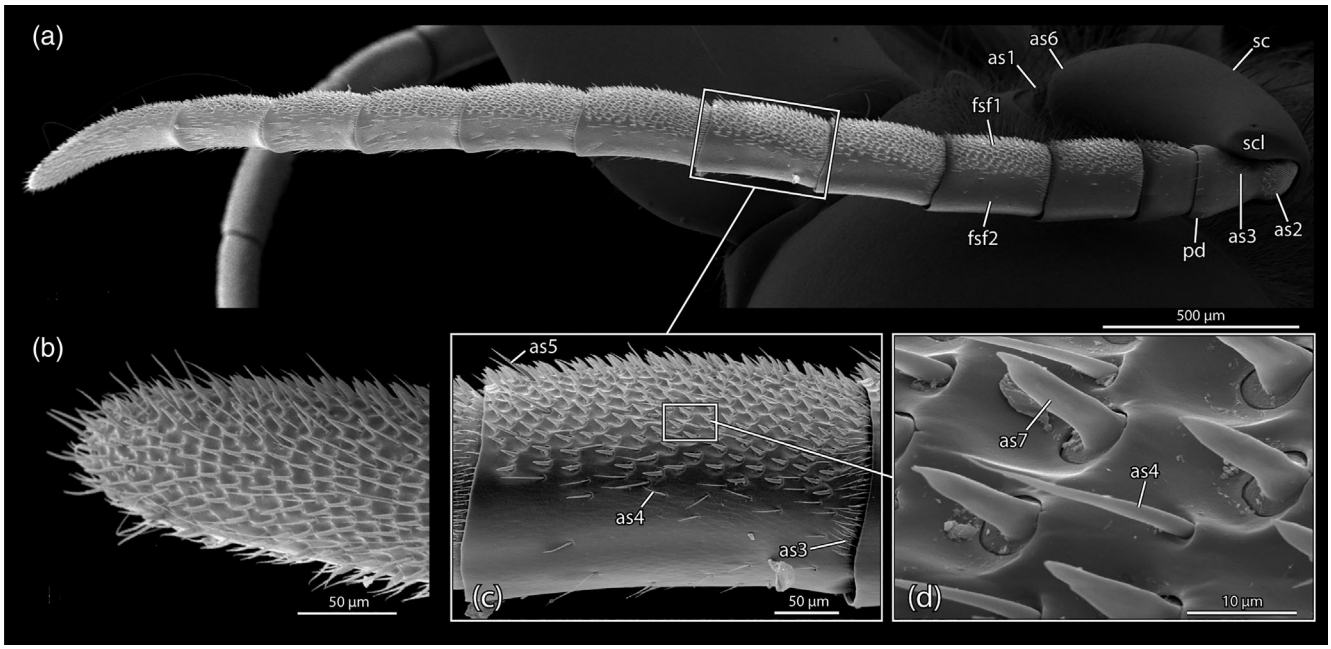

FIGURE 3 *Dorylus helvolus*, scanning electron micrographs of the antenna of a male. (a) Overview of the antenna in dorsal (apparent lateral) view. (b) Apical antennomere in medial (apparent frontal) view. (c) Seventh antennomere in dorsal (apparent lateral) view. (d) Detailed view of the sensilla of the seventh antennomere. as1–7, setae of the antennal classes 1–7; fsf1, fsf2, primary and secondary seta fields of the flagellum; pd, pedicellus; sc, scape shaft; scl, distal scapal lobe

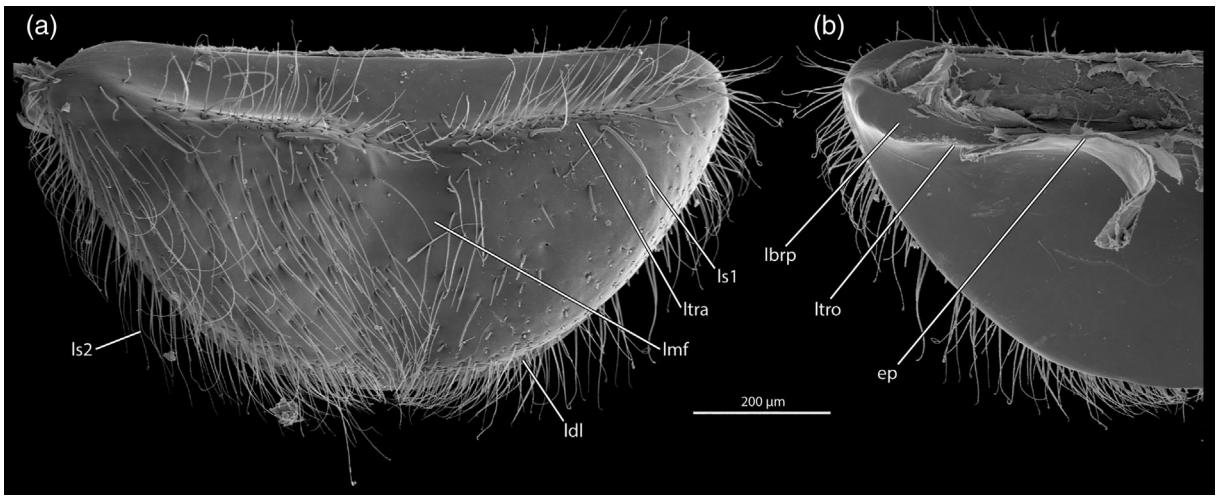

FIGURE 4 *Dorylus helvolus*, scanning electron micrographs of the labrum of a male. (a) Aboral (apparent anterior) view. (b) Oral (apparent posterior) view. ep, epistoma; lbrp, labral process; ldl, distal labral lamella; lmf, medial labral furrow; ls1, ls2, setae of the first and second labral classes; ltra, aboral labral transverse ridge; ltro, oral labral transverse ridge

caused by contraction of two muscles which originate within the scape shaft. The tendons of **0an6** and **0an7** are short but distinct. (1) ***M. tentorioscapalis anterior*** (**M. 1/0an1**; Figure 5a,c,e). *O* (= *origin*): On the cup-shaped surface of the anterior (dorsomedial) tentorial lamella. *I* (= *insertion*): The oral-lateral margin of the bulbus. (2) ***M. tentorioscapalis posterior*** (**M. 2/0an2**; Figure 5a,c,e). *O*: On the ventral surface of the anterior (dorsomedial) lamella of the anterior tentorial arm. *I*: On the aboral-medial (dorsomedial) margin of the bulbus. (3) ***M. tentorioscapalis lateralis*** (**M. 3/0an3**; Figure 5a,c,e). *O*: On the oral-ventral surface of the anterior (dorsomedial) lamella of the anterior tentorial arm. *I*: On the aboral-lateral (dorsolateral) margin of the bulbus. (4) ***M. tentorioscapalis medialis*** (**M. 4/0an4**; Figure 5a, c, e). *O*: On the surface between the anterior and posterior lamellae of the anterior tentorial arm, below 0an1. *I*: On the oral-medial margin of the

bulbus. (5) ***M. scapopedicellaris lateralis*** **(M. 5/0an6**;Figure 5b′). *O*: On the lateral surface of the scape shaft, extending from the base of the shaft to about 2/3 the total length of the shaft. *I*: On the lateral rim of the pedicellar base. (6) ***M. scapopedicellaris medialis*** **(M. 6/0an7**;-Figure 5b′). *O*: On the medial surface of the scape shaft, not quite reaching the shaft base. *I*: On the medial rim of the pedicellar base.

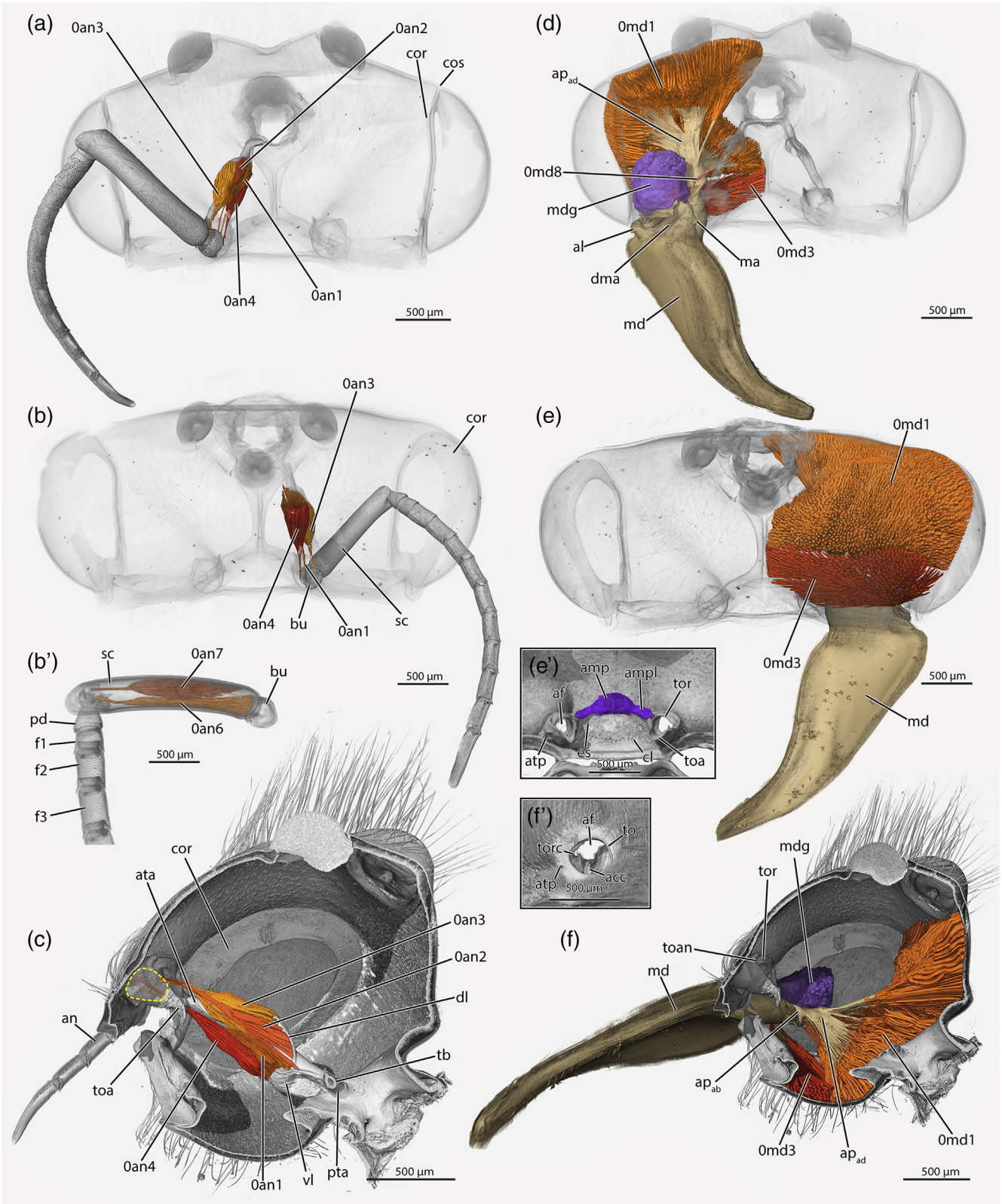

FIGURE 5 Legend on next page.

3.1.4 | Labrum

The **labrum** is arc-shaped and has a reddish-brown coloration (lbr, Figure 2a, c). The **aboral surface of the labrum** is smooth and shining. The **transverse labral ridge** occurs proximally on the aboral surface (ltra, Figure 4a) and is shallowly arcuate; it divides the **proximal clypeal contact surface** from the **distal seta-bearing surface**. The **median aboral region of the labrum** is shallowly and longitudinally (proximodistally) furrowed (lmf, Figure 4a). The **distal labral margin** is evenly rounded from the lateral bases to the apex and lacks a distal, median emargination; the **distal labral margin** bears a **distal lamella** that is produced as a thin and narrow rim where it meets the oral labral surface (ldl, Figure 4a); in distal view, it can be seen that the apex of the labrum is weakly pointed (lbr, Figure 2c). The **oral surface of the labrum** is sclerotized, nearly flat, and is entirely glabrous and smooth. The **transverse ridge of the oral labral surface** is located proximally (ltro, Figure 4b), and is weakly produced laterally, forming the underdeveloped **labral processes** (lbrp, Figure 4b). Proximad the aboral transverse ridge is **the labral articulation to the clypeus**, which is laterally and proximally connected to sclerite via conjunctiva, and on the oral surface is proximally continuous with the **medial portion of the epipharynx** (ep, Figure 4b). When closed over the oral foramen, the distal margin of the labrum fits into the transverse stipital sulcus, thus almost completely covering the maxillolabial complex.

Sensilloid structures

Patterning overview. The **sensilloid patterning of the labrum** comprises two classes distributed solely on the aboral surface, while the oral surface is glabrous; sensilloid structures do not occur proximad the aboral transverse ridge, nor do they occur in the longitudinal furrow.

Sensilloid structure classes. The labrum bears two distinct categories of sensilloid structures, all of which are flexuous and hair-like (thus "setae"): (1) short-to-long, thin, field-forming, and variable in stature (ls1, Figure 4a); and (2) long, thicker, location-specific, and more erect (ls2, Figure 4a).

Sensilloid pattern. The short, thin setae ***(1-ls1)*** form a field over most of the setose labral surface, being less dense in occurrence at the lateralmost regions of the transverse ridge; these setae appear denser toward the labral apex and along the transverse ridge, along the distal labral lamella. The long, thick setae ***(2-ls2)*** are four in count and are specifically located on the transverse ridge, with the laterally paired setae being closer to one another, and with the pairs distant from one another.

Musculature

Only one strongly developed extrinsic muscle is present. (1) ***M. frontoepipharyngalis*** (**M. 9/0lb2**; Figure 10a,d). *O*: On the frontal surface of the head capsule (cranium) ventrolaterad (oral-laterad) the median ocellus and laterad 0hy1 and 0bu3. *I*: On the proximolateral surfaces of the oral labral surface via a long tendon.

3.1.5 | Mandible

External structures

The **mandible** is shining and reddish-brown (md, Figure 2); in facial view it appears falcate (sickle-shaped), with a lateromedially broad proximal half that tapers through a concave curve to the rounded and ventromedially-directed tip (Figure 6a); the length in frontal view is about 3x the maximum width; in medial view, the mandible is fronto-abfrontally compressed, with the apex slightly downcurved (i.e., curved posteriorly); in medial view, the mandible is about 5 x as long as wide. The **mandalus** (ma, Figure 6a, inset) is present as a long, narrow median furrow on the proximomedial mandibular base, near the attachment of the **mandibular adductor apodem**e (ma, Figure 5d). The **atala** (al, Figure 6a, b) is present on the lateral mandibular base as a large bulge that is smaller than the **cranial condyle** and **mandibular acetabulum** of the **dorsal mandibular articulation** (dma, Figure 6a, b), but considerably larger than the **mandibular condyle** (vma, Figure 6b). The **ventral mandibular articulation** is largely reduced, with the mandibular condyle represented by a simple, small, triangular slope posterad the atala (vma, Figure 6b). The **basal and masticatory margins** are not differentiated. On the **medial mandibular surface** is a **longitudinal carina** that extends from the mandibular base to its apex (ll, Figure 6a); it is approximately aligned with the mandalus; the carina lacks teeth, but the apex is angular, where its direction changes posterad (aa, Figure 6a). The mandible also bears a **lateral longitudinal carina**, which continues along the posterolateral mandibular margin for slightly more than half the mandibular length (lll, Figure 2c).

FIGURE 5 *Dorylus helvolus*, 3D-reconstruction of the mandibular and antennal musculature of a male. (a, b′, c, e) Antennal muscles. (b, d, f) Mandibular muscles. (e′) antennal ampulla. Views: (a, b) frontal, (c, d) posterior, (e, f) sagittal, (e′) internal dorso-oral oblique, (f′) external oral-lateral oblique. Yellow dotted line in (c): Cutaway of cuticle to show muscular insertions. 0an1, *M. tentorioscapalis anterior*; 0an2, *M. tentorioscapalis posterior*; 0an3, *M. tentorioscapalis lateralis*; 0an4, *M. tentorioscapalis medialis*; 0an6, *M. scapopedicellaris lateralis*; 0an7, *M. scapopedicellaris medialis*. 0md1, *M. craniomandibularis internus*; 0md3, *M. craniomandibularis externus*; 0md8, *M. tentoriomandibularis medialis inferior*; acc, cranial antennal condyle af, antennal foramen; al, atala; amp, antennal ampulla; ampl, lateral vessel of antennal ampulla; an, antenna; apab, abductor apodeme; apad, adductor apodeme; ata, anterior tentorial arm; atp, anterior tentorial pit; bu, bulbus of scape; cl, clypeus; cos, circumocular sulcus; dl, anterior (dorsomedial) lamella of the anterior tentorium; dma, dorsal mandibular articulation; es, epistomal sulcus; f1–3, first through third flagellomeres; ma, mandalus; md, mandible; mdg, mandibular gland; mds1–3, first through third seta classes of the mandible; pd, pedicellus; sc, scape shape; tb, tentorial bridge; to, torulus; toa, torular apodeme; tor, torular ridge; torc, lateral curl of the torular ridge; trn, dorsomedial notch of the torular ridge; vl, posterior (ventromedial) lamella of the anterior tentorium

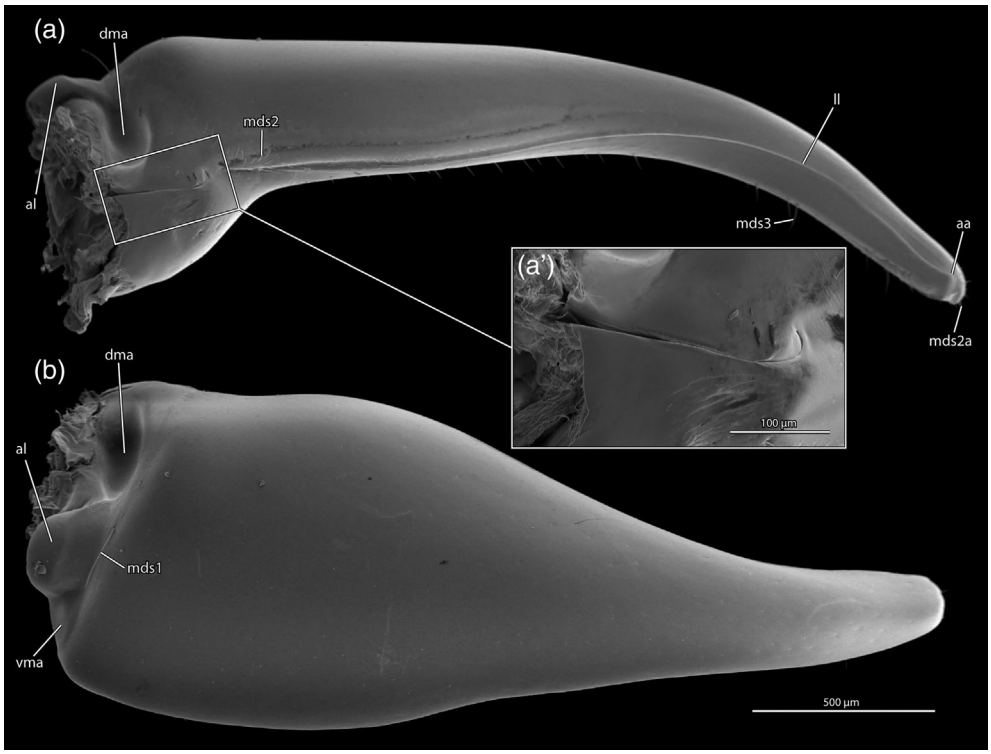

FIGURE 6 *Dorylus helvolus*, scanning electron micrographs of the mandible of a male. (a) Medial view. (a′) Detail of (a) showing mandalus. (b) Anterior view. aa, apical angle; at, atala; dma, dorsal mandibular articulation; ll, longitudinal line; vma, ventral mandibular articulation

Internal structures

The **massive tendon of the adductor muscle** (**0md1**) is medially attached to the mandibular base (ap_{ad}, Figure 5d,f); it is divided into two plate-like branches with different orientation; the individual fibers of the muscle bundles are attached on these structures via thin cuticular fibrillae; an additional branch is the attachment area of a separate bundle, which originates above the foramen occipitale. The **tendon of the abductor** (**0md3**) is distinctly less massive (ap_{ab}, Figure 5f). The **mandibular gland** is about 1/3 the length of the compound eye and is almost adjacent to it within the cephalic lumen, above the mandibular articulation (mdg, Figure 5d, f). A **tube-like channel of the mandibular gland** stretches through the anterior mandibular base and opens at the mandalus.

Sensilloid structures

Patterning overview. The **sensilloid patterning of the mandible** is inconspicuous but is represented by three distinct lines. Hair-like sensilloid structures occur as a tuft-like line anterodistad the atala; as a line near the dorsal mandibular acetabulum, continuing along the longitudinal carina; at the mandibular apex; and as in impressed longitudinal line on the posterior surface. There are minute evenly spaced divots across the dorsal mandibular surface that might individually bear extremely short setae (SEM resolution insufficient).

Sensilloid structure classes. The sensilloid structures of the mandible can be sorted into three classes, all of which are thin and hair-like (thus "setae"): (1) long, flexuous, forming a tuft-like line, and approximately decumbent (mds1, Figures 2a and 6a); (2) short, perhaps stiff, forming a line, and appressed (mds2, mds2a, Figure 6a); and (3) short, stiff in appearance, forming a line, and erect to subdecumbent (mds3, Figure 6a).

Sensilloid pattern. The long, villous setae ***(1-mds1)*** are restricted to the atalar tuft region and are arranged in an uneven row. The short, appressed setae ***(2-mds2)*** occur along the longitudinal carina. The short, standing setae **(*3-mds3*)** occur along an impressed line on the opposite side of the mandible from the second class of setae.

Musculature

Three muscles are present; two of them, **0md1** and **0md3**, are strongly developed, together occupying about 1/3 of the lumen of the head. (1) ***M. craniomandibularis internus*** (**M. 11/0md1**; Figure 5d–f). This is the largest intrinsic muscle of the head. *O*: On the posterior and dorsal internal surface of the head capsule, covering a large area. *I*: On the adductor apodeme via thin cuticular fibers. (2) ***M. craniomandibularis externus*** (**M. 12/0md3**; Figure 5d–f). This muscle is distinctly smaller than 0md1. *O*: On the entire ventral internal surface of the posterior head capsule and on the postgenal ridge. *I*: On the abductor apodeme via thin cuticular fibers. (3) ***M. hypopharyngomandibularis*** (**M. 13**)/ ***M. tentoriomandibularis*** (**0md8**; Figure 5d). This muscle is thin. *O*: On the ventrolateral surface of the middle part of the tentorium. *I*: On the anterior surface of mandibular base at attachment of the adductor apodeme.

3.1.6 | Maxilla

The **maxillae** are shiny, reddish-brown, and small compared to the head capsule and mandibles (mx, Figure 2c) and closely connected with the labium. The entire **maxillolabial complex** is almost completely covered by the labrum in its resting position (lbr, Figure 2a,c). The

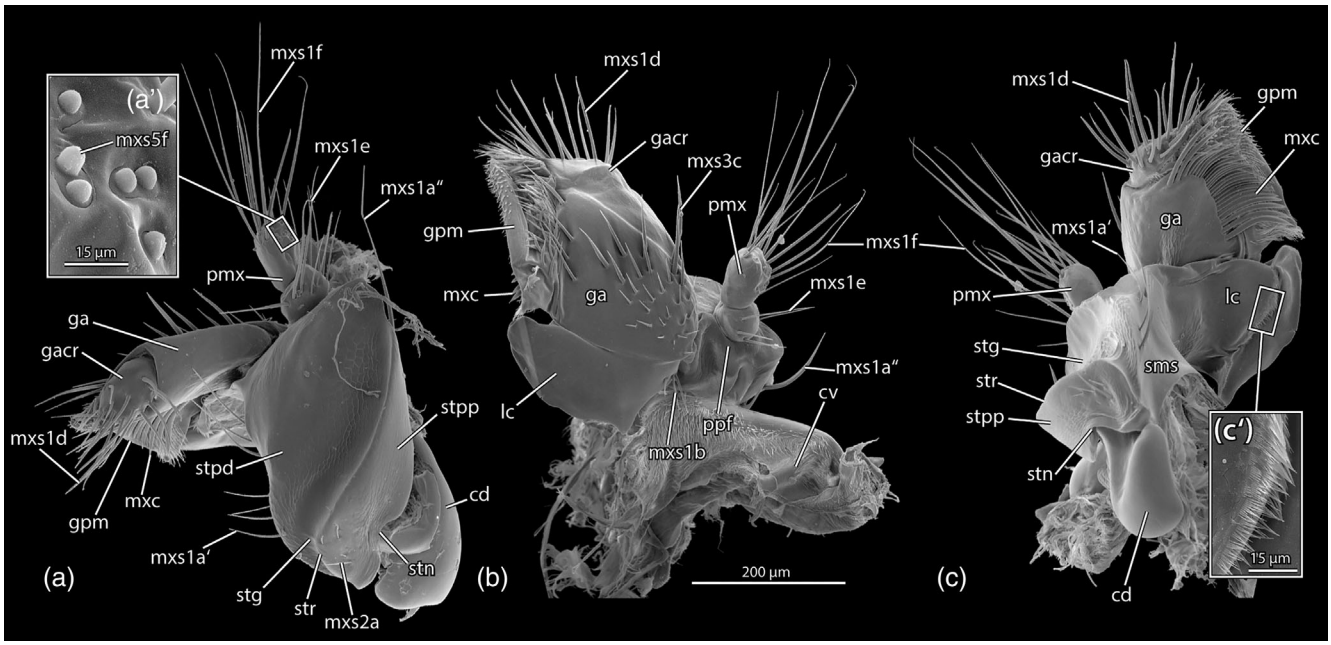

FIGURE 7 *Dorylus helvolus*, scanning electron micrographs of the maxilla of a male; note that (a–c) are to the same scale. (a) Aboral view; inset: Sensilla of palp; proximal downwards. (b) Distal view; Oral downwards. (c) Oral view; inset: Lacinial fimbriae; proximal downwards. cd, cardo; cv, conjunctiva closing the oral foramen, note dense microtrichia; ga, galea; gacr, galeal crown; gpm, medial part of galea; lc, lacinia; mxc, maxillary comb; mxs1a–f, setae of the six subgroups of the first maxillary class; mxs2–5, setae of the second through fifth maxillary classes; pmx, maxillary palp; ppf, palpifer; sms, medial stipital surface; sp, sensilla placodea; stg, transverse stipital groove; stn, stipital notch; str, stipital ridge; stpd, distal portion of stipes; stpp, proximal portion of stipes

cardo and a part of the stipes form the **base of the maxillolabial complex** which is inserted in the **hypostomal groove**. The **cardo** (cd, Figure 7a,c) is almost as long as the stipes and its broad base abuts the broad lateral stipital surface in resting position (Figures 2f and 7a); it articulates with the **cardinal process of the hypostoma** (cc, Figure 2e) and is also connected with the head capsule by an articulatory conjunctiva (cv, Figure 7b) which is densely covered with thin microtrichia. The roughly oval **stipes** is about 1.5 times as long as wide (stpd, stpp, Figure 7a,c); its aboral (external) surface is traversed by the **transverse stipital sulcus** (stg, Figures 2d and 7a), a line that divides the **proximal portion of the stipes** from the **distal portion of the stipes** (stpp, stpd, Figures 2f, and 7a,c); the transverse stipital sulcus is margined proximally by the **transverse stipital ridge** (str, Figure 7); the **medial stipital surface** (sms, Figure 7c) is largely continuous with the distal portion of the stipes, and is distally continuous with the galeolacinial complex; the **proximolateral notch of the stipes** corresponds to the cardinostipital articulation (stn, Figure 7a). The **endite lobes of the maxilla** (lacinia, galea) are attached to the stipes on the **medial stipital edge**, and form a single oval **galeolacinial complex** (ga, lc, Figure 7a–c); this structure is about as long as the whole stipes (Figure 7). The **galea** is about twice as large as the lacinia; it bears a complicated array of setae and microtrichia on both sides; the **medial part of the galea** (gpm, Figure 7b) is a differentiated region of the galea mediad the **maxillary comb** (mxc, Figure 7c) and of the **galeal crown (**gacr, Figure 7a–c), and is separated from the remaining endite by a distinct fold. The **maxillary palp** (pmx, Figure 7a–c) attaches to the distolateral region of the stipes, which itself is weakly differentiated as the **palpifer** (ppf, Figure 7b); the palp is two-segmented, comprising the **proximal and distal palpomeres**.

Sensilloid structures

Patterning overview. The **sensilloid patterning (SP) of the maxilla** occurs in five rough classes on six of the seven primary maxillary sclerites, except for the glabrous cardo; the **SP of the stipes** (a) is distributed in three zones (a, a′, a″) and includes two of the rough seta classes; the **SP of the lacinia** (b) occurs in one zone; the **SP of the galea** (c) occurs in one zone; the **SP of the galeal crown** (d) occurs in one zone; the **SP of the proximal palpomere** (e) occurs in one zone; and the **SP of the distal palpomere** (f) occurs in one zone and includes two seta classes.

Sensilloid structure classes. Five sensilloid structure classes are coarsely defined due to the complexity of maxillary setation patterning, and the considerable variation in form and length: (1) variably long, thin, hair-like, and standing (mxs1a′, a″, b, d, e, f, Figure 7a–c); (2) short, thin, hair-like, and appressed to decumbent (mxs2a, Figure 7a–c); (3) variably long, thick, spine-like, and appressed to decumbent (mxs3c, Figure 7a–c); (4) long, thick, hair-like, comb-like in arrangement, and appressed (mxc, Figure 7a–c); and (5) extremely short, hemispherical, papilla- or button-like, and situated on discs (mxs5f, Figure 7a′).

Sensilloid pattern. The variably long, thin, hair-like setae ***(1-mxs1)*** occur on the stipes (a), lacinia (b), galeal crown (d), and both palpomeres (e,f);

those hair-like setae on the stipes (a) are in two patches, the first on the medial surface of the stipes (a′), the second on the lateral surfaces of the stipes (a″); those hair-like setae on the medial surface of the stipes (a′) are arranged in a line orad the medial stipital surface, and they are intermediate in length relative to the setal fields of the two palpomeres; those hair-like setae on the lateral surface of the stipes (a″) are apparently paired and situated near the apicolateral corner of the stipes, opposite of the galeolacinial complex, and they are both long, thick, and curved, similar to those setae of the galeal crown; those hair-like setae on the lacinia (b) are arranged in a line on the lateral aboral surface, and they are shorter than those on the proximal labial palpomere and increase in length mediad; those hair-like setae on the galeal crown (d) are arranged in a field resembling a "crown of thorns" on the galeal cuticle, and they are thicker than those on either the stipes or palp; those hair-like setae on the palp (e,f) are arranged as a field on the apical and apicolateral palpal surfaces, and they are long to very long, with thinly tapered apices; those hair-like setae on the proximal palpomere (e) are distinctly shorter than those on the distal palpomere (f). The short, thin, hair-like setae ***(2-mxs2)*** occur on the proximal portion of the stipital disc (a) are between the cardinostipital articulation and the transverse stipital groove, and they are short relative to other thin, hair-like setae (1) of the maxilla. The variably long, thick, spine-like structures ***(3-mxs3)*** occur on the aboral cuticle of the galea (c), and are roughly arranged in lines, forming a field; the proximal setae are short, with the length of the setae increasing distad; a second line of similar structures is arranged along the medial part of the galea, and these structures taper strongly to a sharp point. The long, thick, comb-like setae ***(4-mxs4/mxc)*** occur on the oral-medial surface of the galea (c) proximad the galeal crown and laterad the medial part of the galea; these setae are of varying lengths, but their apices are uniform in their arrangement; these setae are also compressed or flattened, and the proximomedial-most setae have a strong curve. The extremely short, button-like sensilloid structures ***(5-mxs5)*** occur on the distal labial palpomere (f) on the distal aboral surface; these structures are arranged in an uneven field, and some of them are paired, apparently arising from the same disc-shaped base.

Musculature

Four weakly developed muscles are retained and four are lost relative to what was previously reported in ant workers. Those muscles that are retained are listed first. (1) ***M. tentoriocardinalis*** (**M. 17/0mx3**; Figure 9a–c). *O*: On the anterior tentorium near to the torular ridge. *I*:

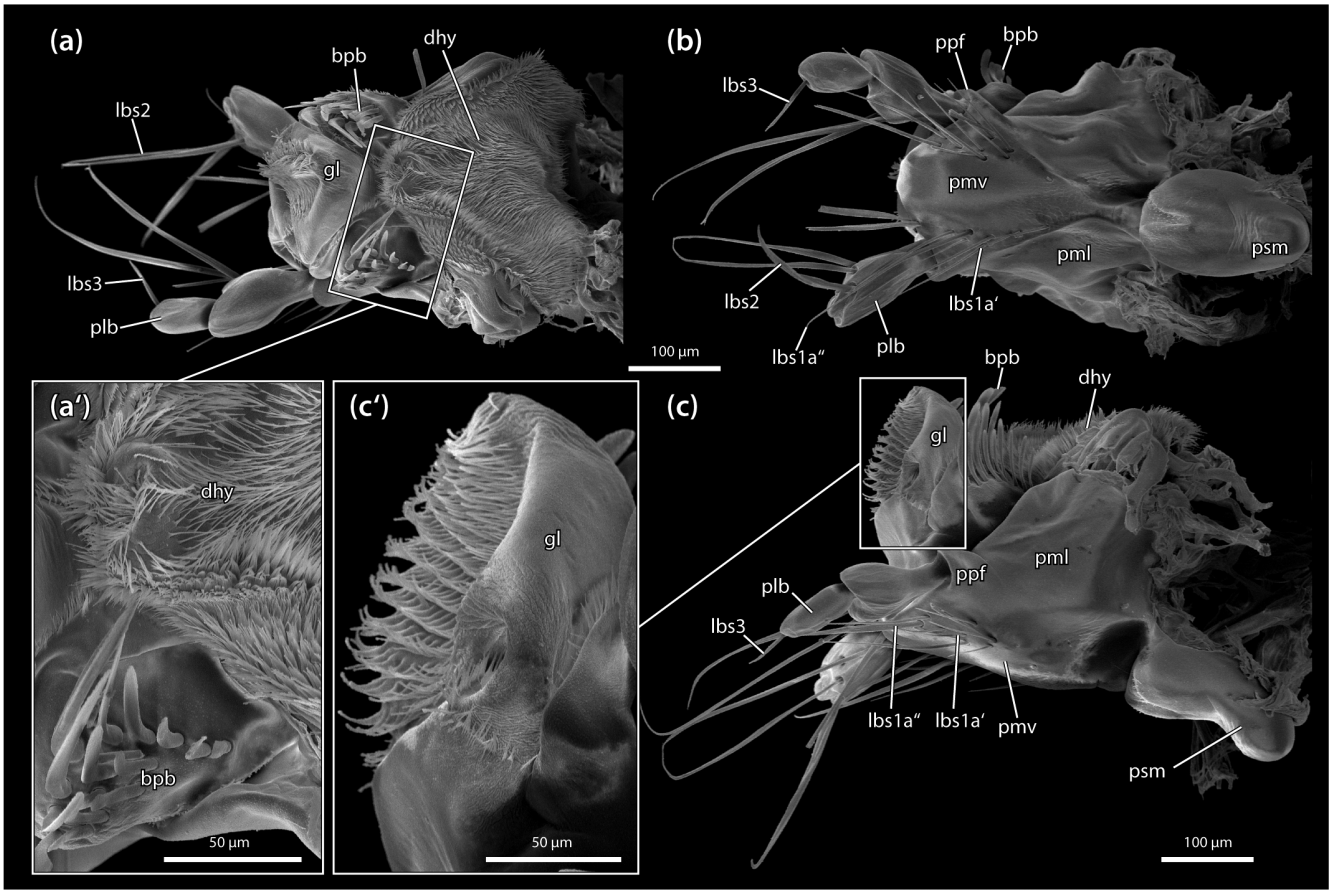

FIGURE 8 *Dorylus helvolus*, scanning electron micrographs of the labium of a male. (a) Oral view, oblique; proximal to the left. (a′) Detail view of hypopharynx and basiparaglossal brush. (b) Aboral view; proximal to the left. (c) Lateral view; proximal to the left. (c′) Detail view of glossa. bpb, basiparaglossal brush; dhy, distal hypopharynx; gl, glossa; lbs1a′, lbs1a″, proximal and distal clusters of the first labial seta class; lbs2, lbs3, setae of the second and third labial classes; plb, labial palp; pml, lateral prementum; pmv; medial prementum/ventral premental surface; ppf, palpifer; psm, postmentum

On a small internal process of the stipital base close to the cardinostipital hinge via a bent tendon. (2) ***M. tentoriostipitalis (anterior)*** (**M. 18/0mx4**; Figure 9a–c). *O*: On the margin of the posterior (medioventral) tentorial lamella. *I*: On the central surface of the stipes via a bent tendon. (3) ***M. stipitolacinialis*** (**M. 20/0mx6**; Figure 9a–c). *O*: On the external and lateral surface of the stipital sclerite. *I*: On the

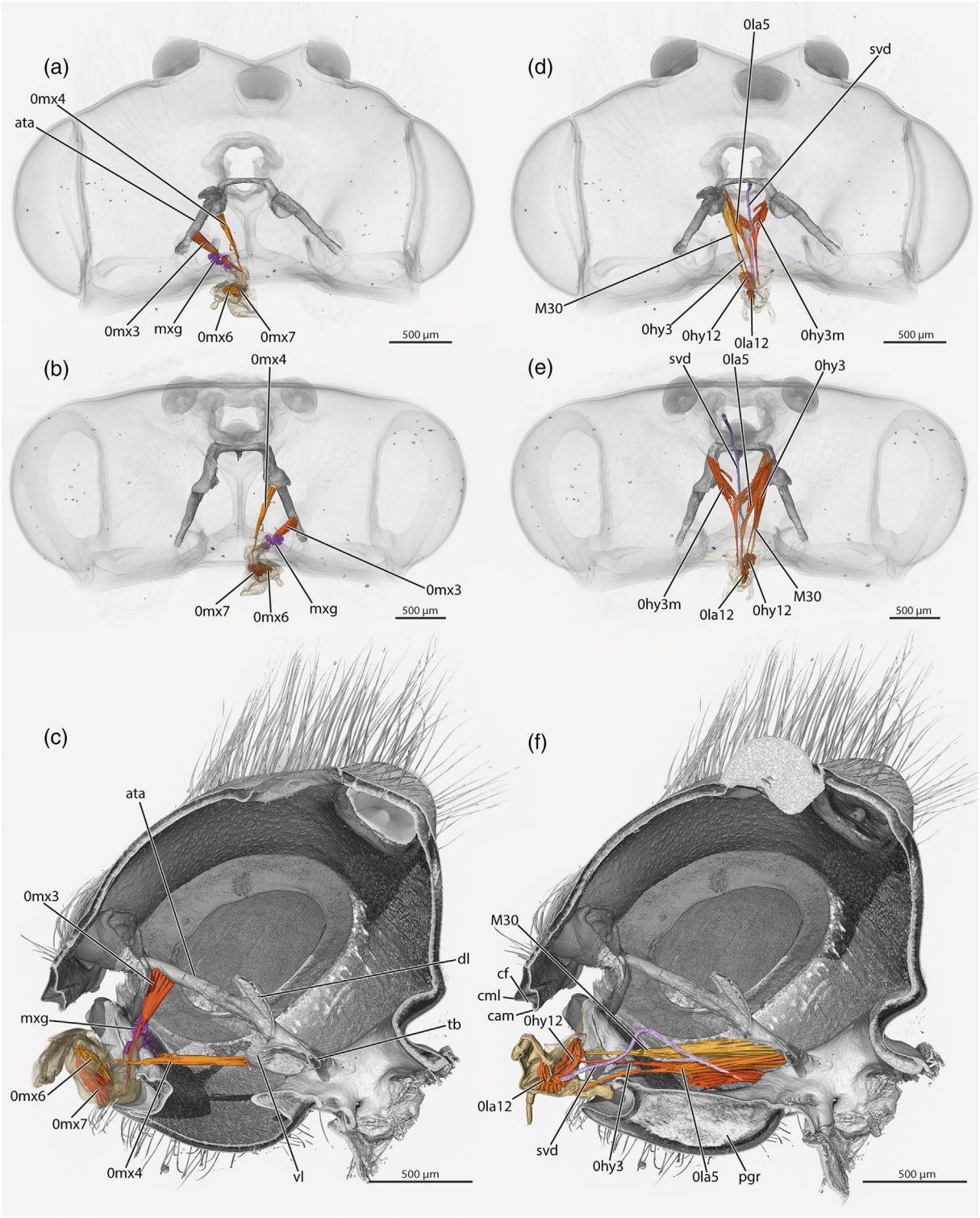

FIGURE 9 *Dorylus helvolus*, 3D-reconstruction of the maxillolabial musculature of a male. (a, c, e) Maxilla. (b, d, f) Labium. (a, d) Frontal view. (b, e) Posterior view. (e) Paramedian sagittal view, right. (f) Paramedian sagittal view, left. 0hy12, *M. hypopharyngosalivarialis*; 0hy3, *M. tentoriohypopharyngalis*; 0hy3m, mutant *M. tentoriohypopharyngalis*; 0la12, *M. praementoglossalis*; 0la5, *M. tentoriopraementalis inferior*; 0mx3, *M. tentoriocardinalis*; 0mx4, *M. tentoriostipitalis (anterior)*; 0mx6, *M. stipitolacinialis*; 0mx7, *M. stipitogalealis*; ata, anterior tentorium; dl, dorsal (anteromedial) lamella of the anterior tentorium; M30, M. tentorioparaglossalis; mxg, maxillary gland; pgr, postgenal ridge; svd, salivary duct; tb, tentorial bridge; vl, ventral (posteromedial) lamella of the anterior tentorium

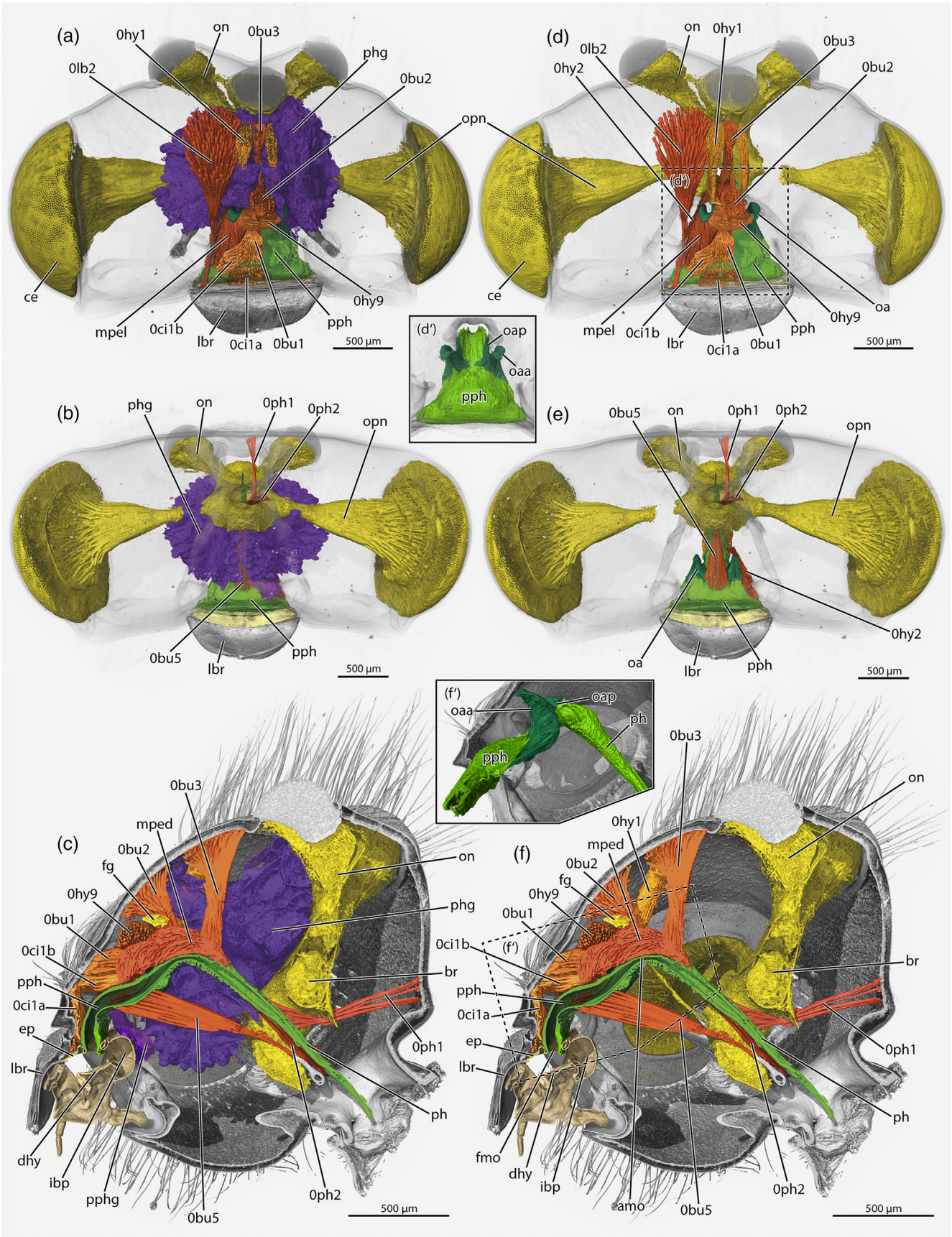

FIGURE 10 Legend on next page.

base of the lacinia, broadly. (4) ***M. stipitogalealis*** (**M. 21/0mx7**; Figure 9a–c). This muscle is slightly larger than 0mx6. *O*: On the proximal surface of the external stipital sclerite. *I*: On the base of the galea via a short tendon. (–) *Muscles that are absent*: ***M. craniocardinalis externus*** (**M. 15/0mx1**), ***M. stipitopalpalis externus*** (**M. 22/0mx8**), ***M. palpopalpalis maxillae primus*** (**M. 24/0mx12**), ***M. palpopalpalis maxillae secundus*** (**M. 25/0mx13**).

3.1.7 | Labium, distal hypopharynx, and salivarium

The **labium** is shiny, reddish-brown, and small; it forms the median part of the maxillolabial complex (lb, Figure 2c,f). The short **proximal postmentum** (psm, Figure 8b,e) is connected with the slightly longer **distal prementum**. The **ventral premental face** is diamond-shaped with a truncated distal margin (pmv, Figure 8b). The **endite lobes of the labium** (glossa, paraglossa) are attached to the prementum orally and distally (gl, Figure 8a,c,c′; bpb, Figure 8a,c). The **glossa** appears folded or sunken into itself in all investigated specimens (likely a drying artifact) (gl, Figure 8a,c′); its surface is covered in rows of long, thin, mostly J-shaped microtrichia. The paired **paraglossae** are not distinctly recognizable; the **basiparaglossal brush** (bpb, Figure 8a,c) consisting of long, thick, and apically rounded setae, is well developed. The **labial palps** are attached to the **palpifer** of the distolateral region of the prementum; the palps are two-segmented (plb, Figure 8a–c) and longer than the maxillary palps; the **proximal palpomere** is spatulate and is the distinctly wider and larger than the **distal palpomere**.

The **distal hypopharynx** is located above the **basal labial part** (dhy, Figure 8a,a′,c); its roughly triangular apex (**hypopharyngeal buttons**) reaches close to the glossa; the **lateral hypopharyngeal sclerites** (hypopharyngeal rods) are connected with **proximolateral premental arms**; the surface of the **distal hypopharynx** is completely covered in a dense array of thin microtrichia. The **salivary canal** opens medially between the basiparaglossal brushes and enters the **cephalic lumen** obliquely; it forms a bend approximately at the level of the AMO and then extends through the head parallel to the tentorium and through the foramen occipitale into the prothorax (svd, Figure 9d–f).

Sensilloid structures

Patterning overview. The **sensilloid patterning (SP) of the labium** is restricted to four zones, each of which is on one of the principal sclerites of the labium, including the **SP of the prementum** (a), the **SP of the paraglossa** (b), the **SP of the proximal labial palpomere** (c), and the **SP of the distal labial palpomere** (d).

Sensilloid structure classes. Three sensilloid structure classes are recognizable, all of which are approximately hair-like (thus "setae"): (1) variably long, terete (round in cross-section), tufted (lbs1a′, a″, Figure 8a–c); (2) long, compressed, tufted (lbs2, Figure 8a–c); (3) short, apparently terete, single (lbs3, Figure 8a–c); and (4) long, compressed, combed (bpg, Figure 8a–c).

Sensilloid pattern

The long, terete setae ***(1-lbs1)*** occur on the lateral surfaces of the prementum (a); these setae are arranged in paired triangular fields and are directed distally such that they cover the labial palps in aboral view (Figure 8b); the proximal setae (a′) are distinctly shorter than the distal seta or pair (a″), which are themselves about as long as those occurring on the proximal labial palpomere; the longer, compressed setae ***(2-lbs2)*** occur on the proximal labial palpomere (c); these setae appear to be arranged as a tufted field on the apicomedial surface of the palpomere; their length exceeds that of the proximal but not the distal premental setae. The short, apparently compressed seta ***(3-lbs3)*** occurs singly at the apex of the distal labial palpomere (d); this seta is about as long as the proximal premental setae. The long, compressed, and combed setae ***(4-lbs4/bpg)*** occur on the paraglossa (b); these setae are arranged in a triangular field, and their apices are curved mediad toward the distal hypopharynx; their lengths are variable.

Musculature

Five weakly developed muscles are retained and four are missing relative to what was previously reported in ant workers. Those muscles that are retained are listed first. (1) ***M. tentoriopraementalis inferior*** (**M. 29/0la5**; Figure 9d–f). *O*: On the ventral surface of the tentorium at the level of the tentorial bridge. *I*: On the proximal margin of the prementum via a thick tendon; the muscle bundles of both sides insert together on one tendon. (2) ***M. tentorioparaglossalis*** (**M. 30**; identity uncertain but possible; Figure 9d–f). *O*: On the ventral surface of the posterolateral tentorial lamella. *I*: On the premental arm via a tendon. (3) ***M. praementoglossalis*** (**M. 32/0la12**; Figure 9d, e, f). *O*: On the main portion of the prementum, covering a large area. *I*: On the dorsal base of glossa. (4) ***M. tentoriohypopharyngalis*** (**M. 42/0hy3**; Figure 9d–f). *O*: On the anterior tentorial arm, anterad 0la5. *I*: On the hypopharyngeal buttons via a long tendon; these muscles are asymmetrical in the examined specimen, where the muscle fibers from both sides of the head converge on the left side tendon, while only fibers from the right side of the head connect to the right tendon. (5) ***M. hypopharyngosalivarialis*** (**M. 37/0hy12**; Figure 9d–f). *O*: On the dorsolateral surface of the distal hypopharynx. *I*: On the dorsal

FIGURE 10 *Dorylus helvolus*, 3D-reconstruction of the labral and pharyngeal musculature of a male. (a, c, e) with glands. (b, d, d′, f) Without glands. (a, d) Frontal view. (b, e) Posterior view. (e, f) Sagittal view at body midline. (f′) Paramedian sagittal view. 0bu1, *M. clypeobuccalis*; 0bu2, *M. frontobuccalis anterior*; 0bu3, *M. frontobuccalis posterior*; 0bu5, *M. tentoriobuccalis*; 0ci1a, *M. clypeopalatalis a*; 0ci1b, *M. clypeopalatalis b*; 0hy1, *M. frontooralis*; 0hy2, *M. tentoriooralis*; 0hy9, *M. oralis transversalis (transversalis buccae)*; 0lb2, *M. frontoepipharyngalis*; 0ph1, *M. verticopharyngalis*; 0ph2, *M. tentoriopharyngalis*; amo, anatomical mouth opening; br, brain; ce, compound eye; ep, epipharynx; fg, frontal ganglion; fmo, functional mouth opening; lbr, labrum; mpel, *M. pharyngoepipharyngealis lateralis*; mped, *M. pharyngoepipharyngealis dorsalis*; mut, mutated muscle; oa, oral arm; oaa, anterior lamella of the oral arm; oap, posteromedial lamella of the oral arm; on, ocellar nerve; opn, optical neuropil; ph, pharynx; phg, pharyngeal gland; pph, prepharynx; pphg, prepharyngeal gland

TABLE 2 Summary matrix for those states observed to be shared between two or more phenogroups of *Dorylus*

No.	Character or property	State 0	State 1	M	Q	W
4.1.1	Facial antenna contact-surface	Not developed	Developed	1	1	1
4.1.2	Face seta orientation	Dissimilar	Similar	1	1	1
4.1.3	Torulus	High rim	Low rim	1	1	1
4.1.4	Anteromedian clypeal lobe	Not developed	Developed	1	1	1
4.1.5	Lateral clypeal shelves	Not developed	Developed	1	1	1
4.1.6	Scape	Terete, straight	Flattened, arched	1	1	1
4.1.7	Flagellum sulcate punctae	Not developed	Developed	1	?	1
4.1.8	Flagellum as7	Not developed	Developed	1	?	1
4.1.9a	Flagellomere contact field setae	Not developed	Developed	1	?	1
4.1.9b	Flagellum thin appressed setae	Not developed	Developed	1	?	1
4.1.9c	Flagellum thin erect setae	Not developed	Developed	1	?	1
4.1.10	Flagellum seta density, base–apex	Not increasing	Developed	1	?	1
4.1.11	Longitudinal mandibular line	Not developed	Developed	1	?	1
4.1.12	Labrum, four long setae	Not developed	Developed	1	?	1
4.1.13	Maxillolabial complex (MLC) parts	Not matching	Matching	1	?	1
4.1.14	MLC setation zone patterning	Not matching	Matching	1	?	1
4.2.1	Cranium orientation	Hypognathous	Prognathous	0	1	1
4.2.2	Head form	Not transverse	Transverse	1	0	0
4.2.3	Facial medial bulge	Not developed	Developed	1	0	0
4.2.4	Postgenal surfaces	Not concave	Concave	1	0	0
4.2.5	Facial, postgenal setation	Short, appressed	Long, standing	1	0	0
4.2.6	Posterodorsal head margin	Concave	Convex	1	0	0
4.2.7	Compound eyes, ocelli	Not developed	Developed	1	0	0
4.2.8	Lateral clypeal shelves	Linear to convex	Subtriangular	1	0	0
4.2.9	Oral clypeal margin	Unevenly convex	Strongly concave	1	0	0
4.2.10	Anteromedian clypeal lobe	Poorly developed	Well-developed	0	1	1
4.2.11	Ventral mandibular articulation	Poorly developed	Well-developed	0	1	1
4.2.12	Genal lobe near mandible	Not developed	Developed	1	0	0
4.2.13	Antennomere count	13	11	1	0	0
4.2.14	Scape, main portion	Short	Long	1	0	0
4.2.15	Scape, main portion	Thin	Thick, subclavate	1	0	0
4.2.16	Scape, setiferous punctae	Not developed	Developed	0	1	1
4.2.17	Flagellum	Thick, thickening	Thin, thinning	1	0	0
4.2.18	Flagellomere dense sensilla field	On entire surface	Only on med. face	1	0	0
4.2.19	Mandible	Short	Long	1	0	0
4.2.20	Mandible microsetae	Not developed	Developed	0	1	1
4.2.21	Mandible proximal seta tuft	Not developed	Developed	1	0	0
4.3.1	Head, lateral view	Bulbous	Linear	0	0	1
4.3.2	Frontal carinae	Poorly developed	Well-developed	0	0	1
4.3.3	Antennal toruli	Distant	Close-set	0	0	1
4.3.4	Medioclypeal region	Broad, flat	Narrow, bulging	0	0	1
4.3.5	Ocular area cuticular invagination	Not developed	Developed	1	1	0
4.3.6	Scape	Rough	Shining	1	1	0
4.3.7	Mandibles	Subtriangular	Falcate	1	1	0
4.3.8	Mandible dorsal macrosetae	Not developed	Developed	0	0	1
4.3.9	Mandible dorsal grooving	Not developed	Developed	0	0	1

Note: Each character is numbered for the longer specific description in the main text. Note that word choice differs here for the purpose of concision. Phenotypes: "M" = male, "Q" = queen, and "W" = worker; states: 1 = observed; 0 = unobserved; "?" = uncertain.

surface of the salivary canal. (–) *Muscles that are absent*: ***M. praementoparaglossalis*** (**M. 31/0la11**), ***M. praementopalpalis externus*** (**M. 34/0la14**), ***M. praementopalpalis labii primus/secundus*** (**M. 35/36/0la16/17**), ***M. praementosalivarialis anterior*** and/or ***posterior*** (**M. 38, 39/0hy7**).

3.1.8 | Digestive tract

The **preoral membrane** comprises the medial portions of the epipharynx and hypopharynx; the **medial portion of the epipharynx** is the unsclerotized internal wall of the preoral cavity that is proximad the labrum (ep, Figure 10e,f); the **medial portion of the hypopharynx** is pouch-like, forming the **infrabuccal pocket** (ibp, Figure 10c,f). The **prepharynx** is materially differentiated from the preoral membrane and comprises the laterally fused proximal epipharyngeal and hypopharyngeal portions (pph, Figure 10); it is broad and roughly crescent shaped in cross section. The **functional mouth opening** is the juncture between the preoral membrane and the prepharynx (fmo, Figure 10f). The **sitophore plate** is the sclerite of the ventral surface of the prepharynx; it stabilizes the prepharynx and extends beyond it laterally and anteriorly, close to the AMO; laterally, the sitophore plate bears a pair of processes, the **oral arms** (oa, Figure 10d,e); these dorsally directed processes are laminar in appearance, and approximately S-shaped in dorsal view, with two curves that define the horn-shaped **anterior oral arm lamella** (oaa, Figure 10d′,f′) which is anterior to the wall-shaped **posteromedial oral arm lamella** (oap, Figure 10d′,f′); in lateral view, the anterior lamella is crescent-shaped. The **pharynx**, beginning at the AMO (marked by the frontal ganglion and muscle 0bu2; amo, Figure 10f), is bent at an almost 90° angle relative to the prepharynx; it extends posterad through a wide passage between the brain and suboesophageal ganglion and directly above the tentorial bridge toward the foramen occipitale (ph, Figure 10e,f). The **lumen of the pharynx** is distinctly narrowed relative to the prepharynx and roughly circular in cross section; while its shape is slightly irregular, no distinct longitudinal folds are developed. The **pharyngeal gland** is by far the largest gland in the head and fills out a large part of the cephalic lumen (phg, Figure 10a,c,e); its main portion lies ventrad the brain, both anterior and posterior the pharynx; its glandular epithelium surrounding the reservoir space is shaped in many interconnected lobes and bubbles. The **prepharyngeal gland** is small and located below the pharyngeal gland and the pharynx, opening laterally into the prepharynx (pphg, Figure 10c).

Musculature

The prepharyngeal musculature is strongly developed, totaling 12 muscles that vary in pairing. Three muscles (0bu2, 0bu3, 0hy1) are *transneural*, that is, completely encircled by the frontal ganglion. Three muscles (Mped, Mpel, 0hy9) are intrinsic to the cephalic digestive tract, that is, not connected to cranial surfaces. (1) ***M. clypeopalatalis a*** (**M. 43a/0ci1a**; Figure 10a,c,d,f). This muscle is unpaired. *O*: On the distal surface of the median clypeal area. *I*: On the epipharyngeal (dorsal) surface of the prepharynx directly above the functional mouth opening; some fibers (only one fiber in the specimen scanned in ethanol) insert on the proximal wall of the labrum. Note: As no muscle connecting from the anterior clypeus to the proximal labral wall is described in insects, we interpret these as aberrant fibers of 0ci1a, similar to the aberrant condition of 0hy3. (2) ***M. clypeopalatalis b*** (**M. 43b/0ci1b**; Figure 10a,c,d,f). This muscle is paired. *O*: On the median surface of the median clypeal portion dorsad 0ci1a. *I*: On the epipharyngeal surface of the prepharynx, immediately ventrad 0bu1, that is, closer to the FMO. (3) ***M. clypeobuccalis*** (**M. 44/0bu1**; Figure 10a,c,d,f). This muscle is paired, but with a combined region of origin. *O*: On the median surface of the medial clypeal area dorsal 0ci1b. *I*: On the epipharyngeal surface of the prepharynx shortly anterad the AMO. (4) ***M. frontobuccalis anterior*** (**M. 45/0bu2**; Figure 10a,c,d,f). This muscle is paired, but with closely adjacent regions of origin; it is also *transneural*. *O*: On the central surface of the cranial frontal region. *I*: On the epipharyngeal surface of the pharynx, directly at the AMO, bending around the frontal ganglion. (5) ***M. frontobuccalis posterior*** (**M. 46/0bu3**; Figure 10a,c,d,f). This muscle is paired, but with closely adjacent regions of origin; it is also *transneural*. *O*: On the cranial frontal region immediately ventrad the median ocellus. I: On the dorsal surface of the pharynx, posterad 0bu2. (6) ***M. tentoriobuccalis anterior*** (**M. 48/0bu5**; Figure 10b,c,e,f). This muscle is unpaired. *O*: On the anteromedian process of the tentorial bridge. *I*: On the hypostomal (ventral) surface of the prepharynx, and distinctly orad (anterad) the AMO. (7) ***M. verticopharyngalis*** (**M. 51/0ph1**; Figure 10b,c,e,f). This muscle is paired. *O*: On the posterior head surface, dorsad the foramen occipitale. *I*: On the dorsal surface of the pharynx at the level of the brain. (8) ***M. tentoriopharyngalis*** (**M. 52/0ph2**; Figure 10b,c,e,f). This muscle is paired. *O*: On the dorsal surface of the tentorium at the juncture of the anterior tentorial arm and tentorial bridge. *I*: On the ventral surface of the pharynx at the level of the brain. (9) ***M. pharyngoepipharyngalis dorsalis*** and ***lateralis*** (**mpe d/l**). This intrinsic longitudinal muscle of the cranial digestive tract is strongly developed, is divided into dorsal and lateral fascicles, and is dorsally situated on the digestive tract (**mped**; Figure 10c,f): This fascicle is unpaired; its anterior attachment site is on the epipharyngeal surface of the prepharynx at the level of the 0ci1b insertion, and its posterior attachment site is on the pharynx at the level of the 0bu3 insertion (**mpel**; Figure 10a,d): These fascicles are paired; their origin is on the anterior surface of the anterior oral arm lamella, and their insertion is on the prepharynx slightly orad (distad) that of 0ci1b. (10) ***M. frontooralis*** (**M. 41/0hy1**; Figure 10a,d,f). This muscle is paired and *transneural*. *O*: On the frontal area of the cranium, directly laterad 0bu3. *I*: On the posterodorsal surface of the posteromedial oral arm lamella, shortly posterad the AMO. (11) ***M. tentoriooralis*** (**M. 47/0hy2**; Figure 10d). This muscle is paired. *O*: On the torular apodeme. *I*: On the lateral surface of the posteromedial lamella of the oral arm, in the region of the AMO and ventrolaterad 0hy1. (12) ***M. oralis transversalis*** (***M. transversalis buccae***; **M. 64/0hy9**; Figure 10a,c,d,f). This transverse intrinsic muscle is unpaired and connects the oral arms of both sides.

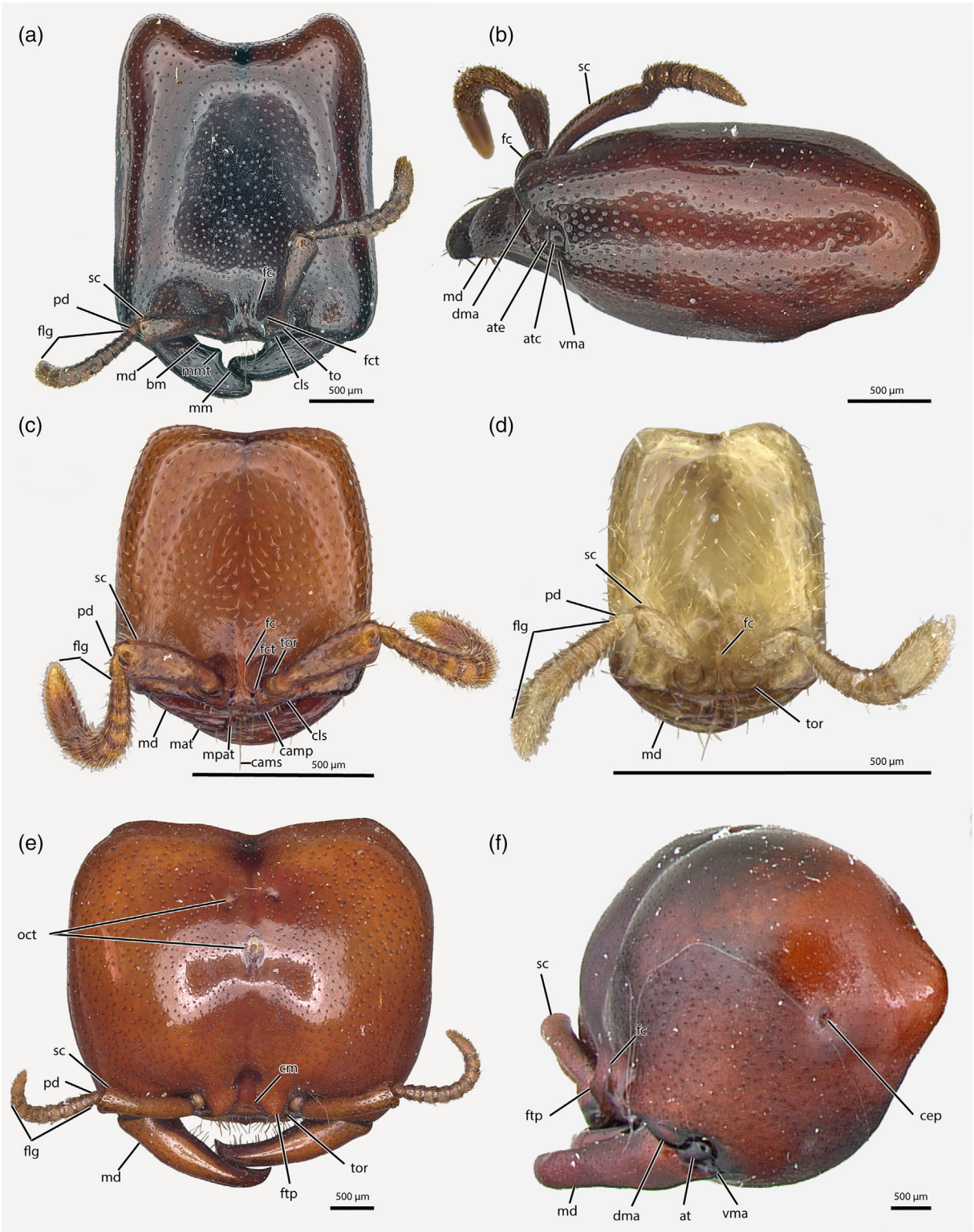

FIGURE 11 Photomicrographs documenting cranial phenotypic variation of the female castes of *Dorylus*. (a–d) *Dorylus helvolus* workers (a, b: CASENT0256791; c = CASENT0235177; d = CASENT0235883). (e) *Dorylus affinis pulliceps* queen (CASENT911328). (f) *Dorylus nigricans molestus* queen (CASENT0172663). (a, c–e) Frontal (dorsal) view. (b, f) Lateral view. at, atala; atc, atalar contact surface; ate, atalar external surface; bm, basal margin; cep, compound eye pit; cm, medioclypeus; dma, dorsal mandibular articulation; fc, frontal carina; fct, tooth of frontal carina; flg, flagellum; md, mandible; mpat, preapical mandibular tooth; mm, masticatory margin; oct, ocellar triangle; pd, pedicellus; sc, scapus; to, antennal torulus; vma, ventral mandibular articulation. (Images from AntWeb. Photographers: a, b = Bradley Reynolds; c = Shannon Hartman; d, e = William Ericson; f = April Nobile.)

3.1.9 | Brain and suboesophageal ganglion

The dumbbell-shaped **brain**, with well-developed optic lobes, appears small in relation to the size of the head (Figure 10d); it forms a compact structural unit with the **suboesophageal ganglion**, with a central passage for the pharynx between them (Figure 10d); in sagittal section, the brain is located anterior to the foramen occipitale at the level of the lateral ocelli (Figure 10f). The **optic lobes**, which widen distinctly toward the **lamina ganglionaris** and compound eyes, and the **ocellar nerves** are both larger than the remaining cerebral areas. The **frontal ganglion** lies above *M. pharyngoepipharyngealis* (Mpe) and is pinched in between the two bundles of *M. tentoriobuccalis anterior* (0bu5) and *M. oralis transversalis* (0hy9) (fg, Figure 10e,f); it is connected by long frontal connectives to the ventral side of the brain/tritocerebrum. The **ventral connectives** linking the suboesophageal and prothoracic ganglia form one thick nerve cord.

3.2 | Comparative morphology

This section of the results is divided into seven subsections: (i) specific features shared among all adults; (ii) features shared between the female castes; (iii) features shared between the queen and male; (iv) features shared between workers and males; (v) a specific description of the worker forms; (vi) a specific description of the queen; and (vii) a specific comparison of the internal sclerotized elements of the male to *Protanilla*, *Brachyponera*, *Formica*, and *Wasmannia* (Richter et al., 2019, 2020, 2021). The lattermost comparisons are made as they represent the first effort to diagnose structural differences between males and workers, in accord with the third objective of our manuscript as stated in the introduction. These workers represent a phylogenetically diverse sample of taxa (sensu Höhna et al., 2011), spanning the major nodes of the ant tree of life. As noted in the Material and Methods section, queen *D. helvolus* were unavailable for comparison, thus we rely primarily on the closely related species *D. affinis*. We use the term "features" here to include both developmental characters and states. Comparative results from subsections (i)–(iii) are summarized in Table 2. Anatomical characters which are generally developed across the Hexapoda (e.g., development of mandibles, antennae, etc.) are not addressed. Because μ-CT data are not available for either female caste, we are unable to address features of the postocciput or internal anatomy; additionally, the antennae, labrum, and maxillolabial complex could not be studied for queens. We use asterisks (*) to highlight features which are subject to focus in the

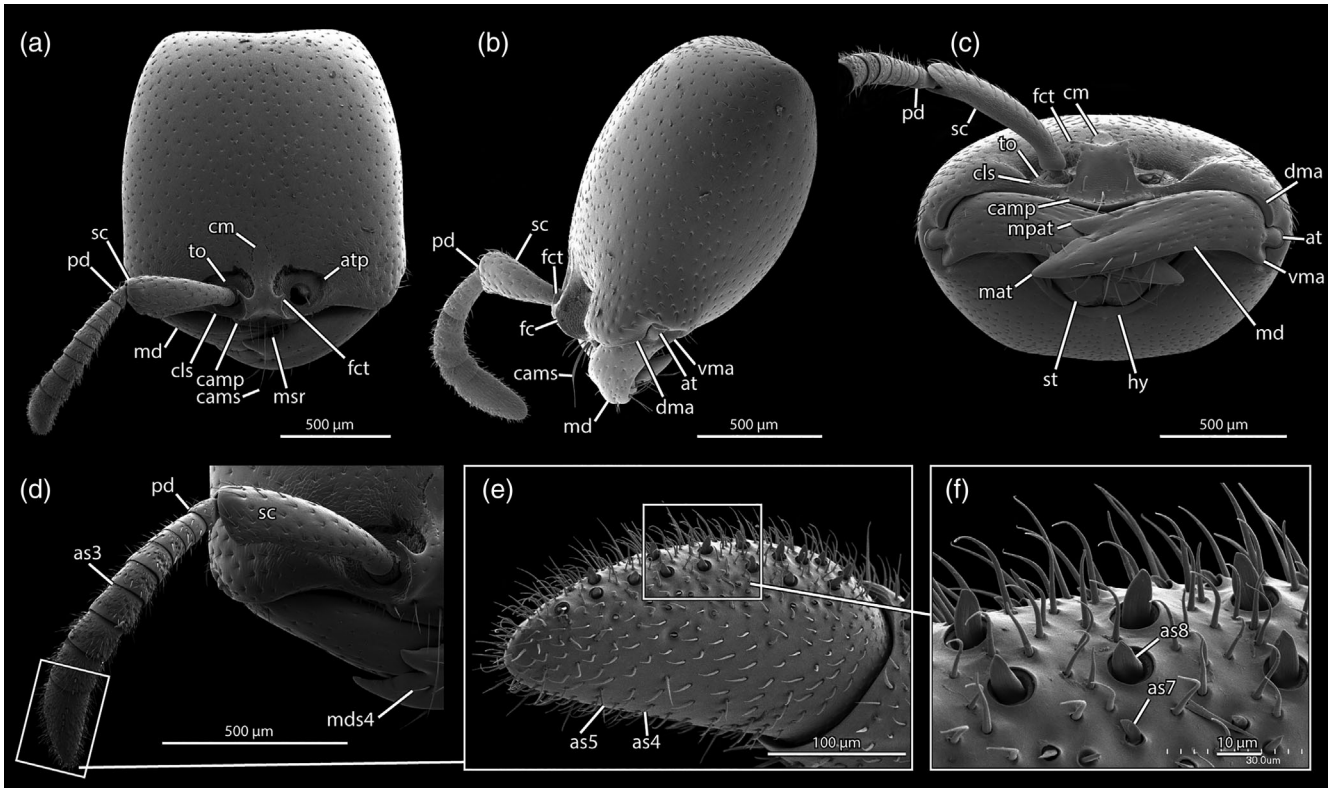

FIGURE 12 *Dorylus helvolus*, scanning electron micrographs of a worker (ANTWEB1008522). (a) Full-face (dorsal) view. (b) Lateral view. (c) Oral view. (d) Full-face antennal detail. (e) Detail of apical antennomere. (f) Detail of sensilla of apical antennomere. at, atala; atp, anterior tentorial pit; camp, anteromedial process of clypeus; cams, anteromedian differentiated seta of clypeus; cls, lateroclypeal shelf; cm, medioclypeus; dma, dorsal mandibular articulation; fc, frontal carina; fct, tooth of frontal carina; hy, hypostoma; mat, apical mandibular tooth; md, mandible; mds4, setae of the fourth mandibular clasee; mpat, preapical mandibular tooth; msr, mandibular serrations between medial and preapical teeth; pd, pedicel; sc, scape; to, torulus. Images by R. Keller; modified from AntWeb

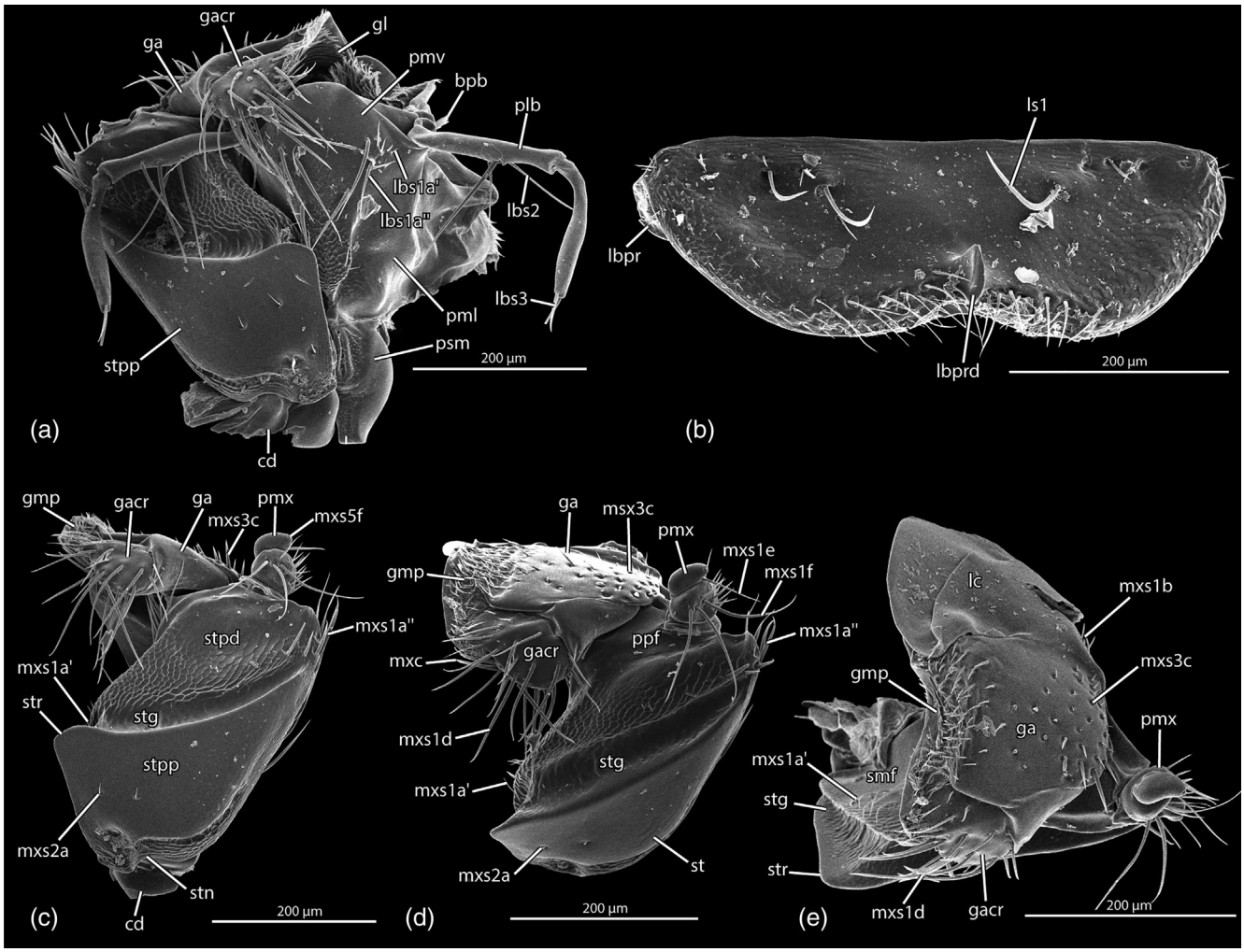

FIGURE 13 *Dorylus helvolus*, scanning electron micrographs of the labrum and maxillolabial complex of a worker (ANTWEB1008522). (a) Maxillolabial complex, aboral view, with one maxilla removed; proximal is downward (note that the maxillary palp is broken off). (b) Labrum, aboral view; distal is downward. (c) Left maxilla, aboral view; proximal is downward. (d) Maxilla, aborally oblique distal view; aboral is approximately downward. (e) Maxilla, distally oblique oral view; aboral is approximately downward. bpb, basiparaglossal brush; cd, cardo; ga, galea; gacr, galeal crown; gl, glossa; gpm, medial galeal part; lbpr, labral process; lbprd, distal process of labral aboral face; lbs1–3, labial seta zones 1–3 (4 is pgb); ls1, differentiated sensilla of labral transverse ridge; mxc, maxillary comb; mxs1–3, maxillary seta zones 1–3 and 5 (4 is mxc); plb, labial palp; pml, lateral prementum; pmv, ventral prementum; pmx, maxillary palp; psm, postmentum; smf, medial face of stipes; st, stipes; stg, stipital groove; stn, proximolateral stipital notch; stpd, distal portion of stipes; stpp, proximal portion of stipes; str, stipital ridge

discussion, a hyphen (–) is used to indicate state descriptions that are negative, that is, that the shared condition is an absence of a specific feature, rather than expression of one, and a hyphen q (–q) to indicate that no data are available for the queen.

3.2.1 | Traits shared among all sexes and castes

Both males and females, including all worker variants, share the following specific conditions that are not known to be conserved across the Formicidae: (**1**) Face impressed caudad and laterad antennal toruli, forming facial antennal contact surface (Figures 2a,d,e and 11a,f,b,c); (**2**) setal orientation on face similar, being aborally directed in the middle of the face and directed toward the mandibular base in the region around the articulation (Figures 2a and 12a); (**3**) antennal torulus weakly developed as low rim (to: Figures 2e and 12c); (**4**) apparent distal clypeal margin with an anteromedian lobate process (cml: Figure 2e); (**5**) lateral clypeal shelves present between the torulus and anterolateral clypeal margins (cls: Figures 2d; 11c, and 12a,c); (**6**) scape lateromedially flattened and arched medially, such that concave surface contacts the cranium when the antenna is flexed (sc: Figures 2a, b and 12c); (**7-q**) at least some flagellar sensilloid structures set in distally-directed sulcate punctures (Figure 3c,d; flagellomeres III–VII in Figure 12d); (**8-q**) flagellum with short, thick, blade-like, and curved setae set in broad pits, with the blade arising from a proximal disc (as7: Figures 3d and 12f); (**9-q**) flagellum with at least three forms of thin, hair-like setae: (a) short, fine setae on the proximal contact surface of each flagellomere (as3: Figures 3a,c and 12d), (b) short, thin,

appressed to subdecumbent setae (as4: Figures 3 and 12), and (c) longer, thin, subdecumbent to erect setae (as5: Figures 3 and 12) (*note*: "bristles" of Hashimoto, 1990, 1991; no data for queen); (**10**) hair-like setae on flagellum becoming denser toward antennal apex (Figures 3a and 12d); (**11*-q**) mandible with longitudinal carinate line on the anteromedial (male) or dorsomedial (female) surface (ll, Figures 6a and 12a,c,d); (**12-q**) aboral face of labrum with about four distinct and long setae near the proximal transverse labral ridge (ls1: Figures 4a and 13b); (**13-q**) main elements of maxillolabial complex recorded as present in male also occurring in worker, including the proximolateral stipital notch present (stn), the division of the stipes into proximal and distal portions by a ridged sulcus (stpp, stpd, stg, str), separation of the galeal crown from the galea by a distinct fold, presence of a differentiated medial galeal part (gpm), and the two-merous maxillary and labial palps, among others (pmx, plb; Figure 13a, c–e); and (**14-q**) zone patterning of maxillolabial setation similar (mxs1a′, mxs1a″, mxs2a, mxs3c, mxc, lbs1a′, lbs1a″ lbs2, lbs3, bpb: Figures 7, 8, and 13a,c–e; note: mcxs5 was not observable for the worker but may be present).

3.2.2 | Female-limited traits

Both queen and worker castes share the following conditions which differ from the male: (−**1***) head not transverse, that is, not subrectangular in facial view and without the lateromedial width as measured including the eyes being greater than the oral-aboral length (Figure 11a,c–e; vs. head transverse Figure 2a); (**2***) face, as seen in oral or lateral oblique view, without a broad convex median bulge (Figures 11f and 12c; vs. face with such a median bulge, Figure 2e); (**3**) lateral postgenal surfaces of cranium not concave (Figure 11b,f; vs. these surfaces shallowly and broadly concave, Figure 2c,f); (**4**) facial and postgenal cranial sensilloid pattern short, mostly appressed (Figure 11 [*note*: sensilloid structures of 10d appear longer due to scaling]; vs. long, standing, Figure 2a–c); (**5**) posterior margin of cranium concave (Figure 11a,c–e; vs. unevenly convex posterad compound eyes, Figure 2a,c); (**6**) compound eyes and ocelli not developed, underdeveloped or otherwise not visible externally (Figure 11; vs. eyes and ocelli well-developed, Figure 2); (**7**) lateral clypeal shelves not in the form of triangular processes, rather these are thin, somewhat dorsally produced, and with a linear to weakly convex margin (Figure 11a,c,d [*note*: difficult to evaluate in queen, but observed in queens of other species]; vs. clypeus anterad toruli not thin, shelf-like, produced, Figure 2d); (**8**) anterior clypeal margin not broadly concave between mandibles (Figure 11a,c–e; vs. concave, Figure 2d); (**9**) anteromedial process of anterior clypeal margin well-developed (Figures 11a,e, and 12a,c,d; vs. reduced, Figures 2e and 9f); (**10**) ventral mandibular articulation well-developed (Figures 11b,f, and 12b,c; vs. strongly reduced, Figures 2b and 6b); (**11**) gena, posterad ventral mandibular articulation, without bulge (Figures 11b,f, and 12b,c; vs. with bulge, Figure 2b); (**12**) antennae 11-merous (Figures 11 and 12; vs. 13-merous, Figures 2b, 3a, and 5a,b); (**13**) scape relatively short, barely extending beyond anterolateral head margins (Figure 11; vs. scape relatively long, distinctly extending beyond anterolateral head margins, Figure 2a); (**14**) scape thick, distinctly subclavate (Figures 11a–e and 12a,b,d; vs. thin, weakly subclavate, Figure 2a); (**15**) scape with setae set in pit-like impressions (punctures, punctae) (Figures 11 and 12a–d; vs. without such setigerous/setiferous impressions, Figure 3a); (**16**) flagellum thick, with each flagellomere proportionally stouter (Figures 11 and 12a–d; vs. thin, with flagellomeres increasing in length apically, Figures 2a,b and 3); (**17**) flagellar surface with an even distribution of sensilloid structures (Figure 12a,b,d; vs. most sensilloid structures restricted to medial surface, Figures 2a,b and 3); (**18**) mandible short, proximodistal length < 1/2 lateromedial width of head (Figures 11 and 12a,c; vs. mandible long, length > 1/2 head width, even including compound eyes, Figure 2a–d,f); (**19**) dorsal surface of mandible with more-or-less evenly distributed field of short microsetae set in distinct punctae (Figures 11 and 12b,c; vs. mandible without such microsetae, Figure 6); (**20**) dorsal mandibular base, along ventral mandibular articulation and atala, without tuft of long, wispy setae (Figures 11b,f, and 12c; vs. with such a setal tuft, Figure 2a–c).

3.2.3 | Reproductive-limited traits

Both the queen and male share the following conditions, to the exclusion of workers: (**1***) Head bulbous in lateral view, with anteroposterior length and dorsoventral height subequal (Figures 2b and 11f; vs. head elongate, with length considerably greater than height, Figures 11b and 12b); (**2**) frontal carinae indistinctly developed (Figures 2e and 11e, f; vs. frontal carinae developed, distinct, Figures 11a–d and 12a–c); (**3**) antennal toruli wide-set, being separated by more than twice their lateromedial diameters (Figures 2a,d,e, and 11e; vs. toruli separated by about one diameter, Figures 11a,c,d, and 12a,c); (**4***) median portion of clypeus lateromedially broad, not constricted by close-set frontal carinae (cm, Figures 2d and 11d; vs. medioclypeus narrow, anteroposteriorly longer than broad, constricted by frontal carinae, Figure 12a); (**5**) ocular region of cranium with cuticular invagination (cor, Figure 5a–e; cep, Figure 11f); (**6***) mandibles falcate, without distinct basal and masticatory margins, serrations, or median tooth (md, Figures 2a–d,f, 6, and 11e; vs. mandibles triangular, with distinct basal and masticatory margins, serrations, and a large median tooth, Figures 11a and 12a,c,d); (**7**) dorsal mandibular surface, excluding base, without macrosetae (Figures 6 and 11e; vs. dorsal mandibular surface with macrosetae proximad teeth and near ventral margin, mds4, Figures 11a,c,d and 12a–c); (**8**) dorsal mandibular surface without longitudinal grooves (Figures 2a–d,f, 5,and 11e; vs. mandible with longitudinal grooves, Figures 11a,c,d, and 12a–c). *Note*: We were unable to measure the IHW and OFW the queen; the male's MWR is 0.66 x that of the worker.

3.2.4 | Traits limited to the worker and male castes

No specific anatomical entities or states were detected that are shared between the male and worker to the exclusion of the queen,

with the caveat that SEM was not possible for the female reproductive caste.

3.2.5 | Worker-limited traits

Head, broadly

Worker *Dorylus* are continuously polyphenic, that is, with continuous size variation and without a discrete soldier caste (Figure 1); workers of the largest size form the major range (Figures 1c and 11a,b); the smaller, less extreme workers form the medium (Figures 1d and 11c) and minor (Figures 1d and 11d) ranges; in some cases, medium to minor workers of *Dorylus* will have convex anteromedian clypeal lobes and finely denticulate mandibles (e.g., Eguchi et al., 2014; Hollingsworth, 1960). The cranium of the major range is rectangular, about twice as long as broad, with subparallel, weakly anteriorly divergent and sublinear lateral margins, and a deeply concave posterior margin; that of the medium is distinctly longer than broad, with convex, anteriorly diverging, and strongly posteriorly converging lateral margins, and a shallow posterior margin; that of the minor is subrectangular, about twice as long as broad, with weakly convex, anteriorly diverging, and posteriorly converging lateral margins, and a shallowly concave posterior margin. The compound eyes and ocelli are not expressed in the worker caste; no external indication of eyes is visible. The frontal carinae are developed and distinct; the antennal contact surface immediately ventrad the carinae is vertical, thus the carinae are "dorsally directed"; at least in larger individuals (Figures 11a–d and 12a–c), the carinae are wide-set anteriorly and close-set posteriorly; anteriorly, the carinae are produced laterally, lamellate, concave along their anteroposterior length, and posterolaterally toothed, although the tooth is apparently not developed in the smallest workers (fct, Figures 11a,c, and 12a–c); from the frontal carina teeth, the carinae curve anteromedially then posteriorly; posteriorly, the frontal carinae are weakly divergent; in majors, the posterior portion of the carinae are wide-set compared to media, while media are wide-set compared with minors. The mediоclypeus between antennal toruli is narrow and virtually absent in the smallest workers. The clypeus has an anteromedian lobe; the lobe has a median, differentiated seta projecting anteriorly over mandibles (cams, Figure 12a–c).

Antenna

The scape shaft surface is alutaceous, with reticulated ridges matching epidermal cell patterning (sc, Figure 12d). The second flagellomere is apparently the shortest (Figure 12a,d). The antennal sensilloid pattern shares several sensilloid structure classes (*as1*, *as3*, *as4*, *as5*, and *as7* [*note*: *as2* unobservable due to specimen orientation]), and includes a distinct class not observed in males (as8, Figure 12f). This eighth class occurs on flagellomeres VI–IX, and the sensilloid structures are superficially similar to those of the seventh class but are several times larger; the structures are set in wide sockets and may have a distinct disc-like base; the blade of the structure is approximately scale-shaped and bears several proximodistally longitudinal microscopic grooves; the apex of the structure appears to be sulcate. The sensilloid pattern of those setae which are shared is distinct, without differentiation of primary and secondary sensilloid fields as in the male; the blade-like *as7* are absent on flagellomeres I and II and are considerably more dilute where they do occur; the scape is covered with thin, hair-like setae that are appressed and of variable length; these hair-like setae are absent on the male and are of the same class as that observed on the face and have similar spatial dispersion.

Labrum

The aboral surface of labrum is largely glabrous (Figure 13b); in addition to the differentiated setae near the transverse labral ridge (ls1, Figure 13b), the labrum bears (i) short, erect setae at the proximolateral labral corners, (ii) short, appressed setae on the lateral surface of the labral disc, and (iii) an uneven row of longer, appressed to decumbent setae near and projecting over the apical labral margin. The distal margin of the labrum is broadly emarginate. A toothed, proximodistally-oriented flange is present distally on the aboral labral surface, near the distal emargination (lbrpd, Figure 13b). No data are available for oral labral surface for castes other than males.

Mandible

The mandibles of all worker variants are capable of full closure against the clypeus (md, Figure 11a,c,d). The basal and masticatory margins are distinct and weakly oblique (Figure 11a). The mandible is tridentate, with a large median tooth delimiting the basal and masticatory margins (mmt, Figure 11a), two large apical teeth (mpat, mat, Figure 12c), and a series of sharp to rounded serrations between the basal and subapical teeth (msr, Figure 12a); serrations are sometimes also present on the basal margin. The dorsal mandibular surface is irregularly and longitudinally grooved (Figures 11a,c,d and 12a,c). In addition to a field of microsetae set in punctures, the dorsal surface bears much longer, stouter, subdecumbent to suberect setae subtending subapical and apical teeth, as well as along the lateral mandibular surface (Figure 12c).

Maxillolabial complex

The maxillolabial complex is relatively large, with an MWR (see "morphometrics" above) of 0.56 ($n = 1$). The parts of the complex are similar to that of the male, with the main distinction being labial palp shape, specifics of setation pattern, and apparently some other structural proportions, but the latter is difficult to evaluate due to noncomparable specimen positioning. The labial palpomeres are relatively long and thin, being nearly rod-like (plb, Figure 13a), rather than short and stout (Figure 7); the distal labial palpomere is proximally bent. Notable setational distinctions include the occurrence of long, thin, hair-like setae on the proximal palpomere and fewer of such setae on the distal palpomere (mxs1e, mxs1f, Figure 13d); more distolateral hair-like setae (mxs1a″, Figure 13d); and two, rather than one distal labial palpomere setae (lbs3, Figure 13a).

No.	Muscle	D	W	F	B	P
10	*M. verticopharyngalis* (0ph1, Figure 10b, e)	1	0	0	0	0
11	*M. tentorioparaglossalis* (M. 30, Figure 9d–f)	1	0	0	0	0
12	*M. craniocardinalis externus* (M. 15/0mx1)	0	1	1	1	1
13	*M. stipitopalpalis externus* (M. 22/0mx8)	0	1	1	1	1
14	*M. palpopalpalis maxillae primus* (M. 24/0mx12)	0	1	1	1	1
15	*M. palpopalpalis maxillae secundus* (M. 25/0mx13)	0	?	1	?	0
16	*M. praementoparaglossalis* (M. 31/0la11)	0	1	1	1	1
17	*M. praementopalpalis externus* (M. 34/0la14)	0	1	1	1	1
18	*M. praementopalpalis labii primus/secundus* (M. 35/36/0la16/17)	0	1	1	1	0
19	*M. praementosalivarialis anterior* and/or *posterior* (M. 38,39/0hy7)	0	1	1	?	1

Note: States: 1 = observed, 0 = not observed, "?" = uncertain.

TABLE 3 Observed muscle presence/absence comparing the male of *Dorylus* (*D*) to workers of *Wasmannia* (*W*, Richter et al., 2019), *Formica* and *Brachyponera* (*F*, *B*, Richter et al., 2020), and *Protanilla* (*P*, Richter et al., 2021)

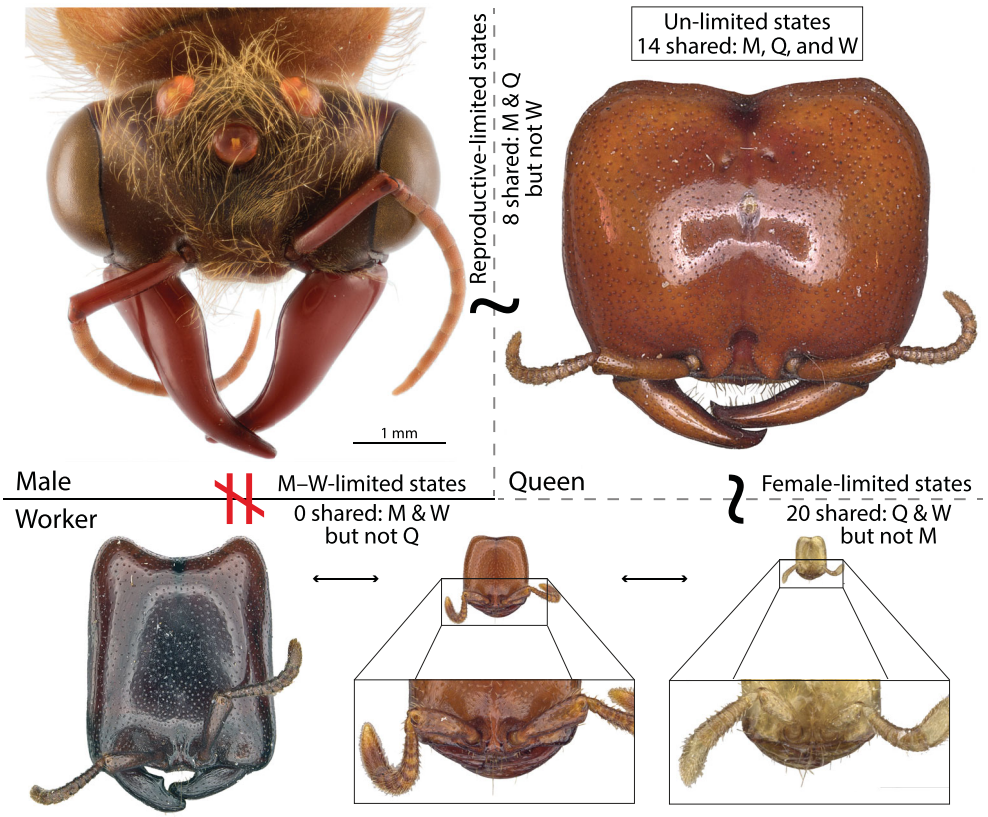

FIGURE 14 Visual summary of intercaste comparisons and trait limitation in *Dorylus*. Male and worker: *Dorylus helvolus*; queen: *D. affinis*. All images are to the same scale. The insets in the bottom frame are arbitrarily upscaled. Female image attributions are as in Figure 11

3.2.6 | Queen-limited traits

Head

Queens of *Dorylus* are dichthadiiform, that is, lacking wings and being massive, cylindrical, and almost teratological in appearance (Figures 1 and 11e,f). The cranium is subovoid, distinctly broader lateromedially than long anteroposteriorly, with broadly convex lateral margins which curve anteriorly through the rounded anterolateral cranial margin, and which evenly curve posteriorly through the posterolateral cranial margins to the convex posterior margin which is medially emarginate. The compound eyes are always absent, while the ocelli may be absent externally or imperfectly developed; distinct pits are present on the lateral (ocular) surfaces of the cranium (Figure 11f), possibly corresponding to development of at least the invagination of the internal ocular ridge; the ocellar triangle is variable, with each ocellus either in the form of pits or poorly developed lenses or facets (Figure 11e). The frontal carinae are apparently developed, but indistinct; they are present as short and rounded processes mediad the

antennal toruli; these processes margin a pair of triangular regions laterad the distinct medioclypeus. The medioclypeus between the antennal toruli is narrow, but relatively broader relative to the workers. The clypeus lacks a median, differentiated seta.

Mandible

The mandibles are incapable of complete closure against the clypeus (Figure 11e). Each mandible is falcate in form, and small relative to that of the male; only one apical tooth is present. The basal and masticatory margins are not developed, although the mandible has a medial bulge in basal half; the bulge is similar to that of the male, although much less well-developed. The dorsal mandibular surface lacks longitudinal grooves and macrosetae.

Labrum, antenna, maxillolabial complex

No data available.

3.2.7 | States differing between the male and workers of other taxa

In this subsection, *P* = *Protanilla*, *B* = *Brachyponera*, *F* = *Formica*, *W* = *Wasmannia*. Also note that external features are excluded from consideration.

Cranial skeleton. (**1**) The tentorium is almost perpendicular to the oral-aboral cranial axis (Figure 9c,f; vs. parallel to the oral-aboral axis in *P*, *B*, *F*, *W*); (**2**) the tentorium has a dorsomedially-directed anterior lamella and ventromedially-directed posterior lamella (dl, vl, Figure 9c, f; vs. medially- and frontally-directed lamellae in frontal plane in *P*, *B*, *F*, *W*, although in *P*, medial lamella directed anterodorsad); (**3**) the tentorial lamellae are short (Figure 9c,f; also short in *P*; long in *B*, *F*, *W*); (**4**) the oral margin of the torular apodeme, in sagittal view, is linear and directed toward the foramen occipitale (toa, Figure 5c; similar in *B*; bent postgenad in *W*; bent orad in *F*; absent in *P*); (**5**) the epistomal ridge is indistinctly developed (apparently not developed in *W*; developed in *P*, *B*, *F*); (**6**) the clypeus in sagittal view has two carinae, one margining the oral cavity (cam, Figure 9f) and the other forming the apparent distal clypeal margin (cml, Figure 9f; similar in *P*, *B*, *W*; distinct aboral carina not developed in *F*); (**7**) the oral cavity is subequal in size to the mandibular cavities in oral view (Figure 2e; vs. oral cavity much larger than mandibular cavities in *P*, *B*, *F* [*W* uncertain]); (**8**) in oral view, lines drawn connecting the lateral apices of the ventral mandibular and atalar articulations of both sides converge toward the face (dotted line, Figure 2e; vs. converging toward the postgena in *P*, *B*, *F* [*W* uncertain]); (**9**) in oral view, the toruli only are slightly above the oral margin of the clypeus (to, Figure 2e; vs. raised distinctly above the oral clypeal margin in *P*, *B*, *F*, *W*).

Musculature

(**10–19**) Ten discrete muscular differences are observed, two of which are presences in the male *Dorylus* that are not observed in the other workers, and eight of which are absences in the male *Dorylus* (Table 3).

4 | DISCUSSION

4.1 | Observations in overview

Overall, we observe numerous, highly specific anatomical entities and states of the male phenotype (Sections 3.1.1–3.1.9; Figures 14, Supplementary material, Figure S1). After comparison with the female phenogroups, we were surprised to observe that no specific entities or states are shared between the male and worker to the exclusion of the queen (Section 3.2.4), while the queens and males share several unique features to the exclusion of workers (Section 3.2.3; Figure 14). In other words, while there were traits limited by sex, caste, and to the reproductives, no traits were specifically limited to workers and males. To the best of our knowledge, this observation has not been recorded in the literature before and should be evaluated across the Formicidae to determine its generality. Unexpectedly, we did observe conservation of maxillolabial setation zoning patterns (Section 3.2.1), despite sex-specific sclerite and seta development (Section 3.2.5). We do confirm certain previous generalizations about sexual dimorphism in ants, such as a sex-limited pattern of eye expression and the differential count of the antennomeres, and we also found numerous female-limited anatomical entities and states (Section 3.2.2). Completely unexpected, however, was the observation that two discrete muscles are expressed in the male phenotype, the postcerebral *M. verticopharyngalis* (0ph1) and what could be the *M. tentorioparaglossalis* (M. 30), as well as absence of eight muscles known to be conserved among workers of the Formicidae (Table 3; Supplementary material, Table S2).

These and other observations spur our consideration of several topics, including the muscular patterns of ant heads (Section 4.2), the developmental patterning of mandibles and their evolution (Section 4.3), the evolution of the cranium itself (Section 4.4), and the classification of sensilla (Section 4.5). Arching through these separate discussions are the observations that while males and workers do share some features, no feature to our knowledge is specifically and uniquely developed in males and workers that is not developed in the queen. Modulated by the observation that the male and queen share a number of specific and unique states to the exclusion of workers (Figure 14), these patterns suggest that worker development is dependent on female-specific regulation and independent from male-specific regulation, and that, in *Dorylus*, there is an independent factor, cue, or regulatory system which determines reproductive-specific phenotypes and phenotypic variation.

4.2 | Muscular peculiarities

We observed two muscles that have not been previously recorded in Formicidae, **0ph1** and **M. 30** (10, 11 in Table 3), which insert on the pharynx and premental arms, respectively. The muscle which we have labeled **0ph1** is known from other aculeates and is thus a presumptive plesiomorphy (Zimmermann & Vilhelmsen, 2016). On the other hand, the muscle which we have labeled "M. 30" is perplexing. This muscle originates on the tentorial bridge base and extends dorsolaterally on

the proximal premental arms. In addition to not being observed in worker ants to date (Richter et al., 2019, 2020, 2021), no similar muscle has been described for any member of the Aculeata so far (Zimmermann & Vilhelmsen, 2016). "M. 30" does, however, correspond to the *M. tentoriopraementalis superior*, which is known to occur in Xyelidae and other insects (Beutel & Vilhelmsen, 2007). The character polarity of this muscle remains ambiguous because the anatomical sampling of aculeate cranial skeletomusculature is limited.

We also observed the absence of muscles in the male that are otherwise largely conserved across the crown ants. Notably, these apparent muscle losses are restricted to the maxillolabial complex (12–19 in Table 3). Absence of the palpal muscles (13–15, 17–19 in Table 3) is unsurprising, as both the labial and maxillary palps are only two-segmented and short, so their independent movement may perhaps be neither useful nor necessary. However, absence of the craniocardinal and prementoparaglossal muscles (12, 16 in Table 3) is unexpected; their absence indicates reduced mobility for the maxilla and glossa, respectively. A possible explanation is the worker-dependent role of the male within the colony. In other words, males are fed by workers and neither interact with brood nor potential, unprocessed, food substances, thus the range of maxillolabial motion may be less relevant for them compared with workers. Alternatively, this could be a condition general among doryline or perhaps other poneroformican clades. Preliminary data of a worker of *Dorylus orientalis* Westwood, 1835 reveals presence of the craniocardinal muscle, indicating that these absences are indeed specific to males. Further evaluation of male head anatomy across the Dorylinae and the Formicidae more broadly is necessary to resolve this question.

Finally, with respect to musculature, we observed two aberrant muscles, belonging to the clypeopalatial (**0ci1a**) and tentoriohypopharyngeal (**0hy3**) groups. In both of the scanned specimens, fibers of 0ci1a connected to the labrum, whereas in workers of other species, this muscle originates solely on the clypeus. In contrast, 0hy3 was asymmetrical in

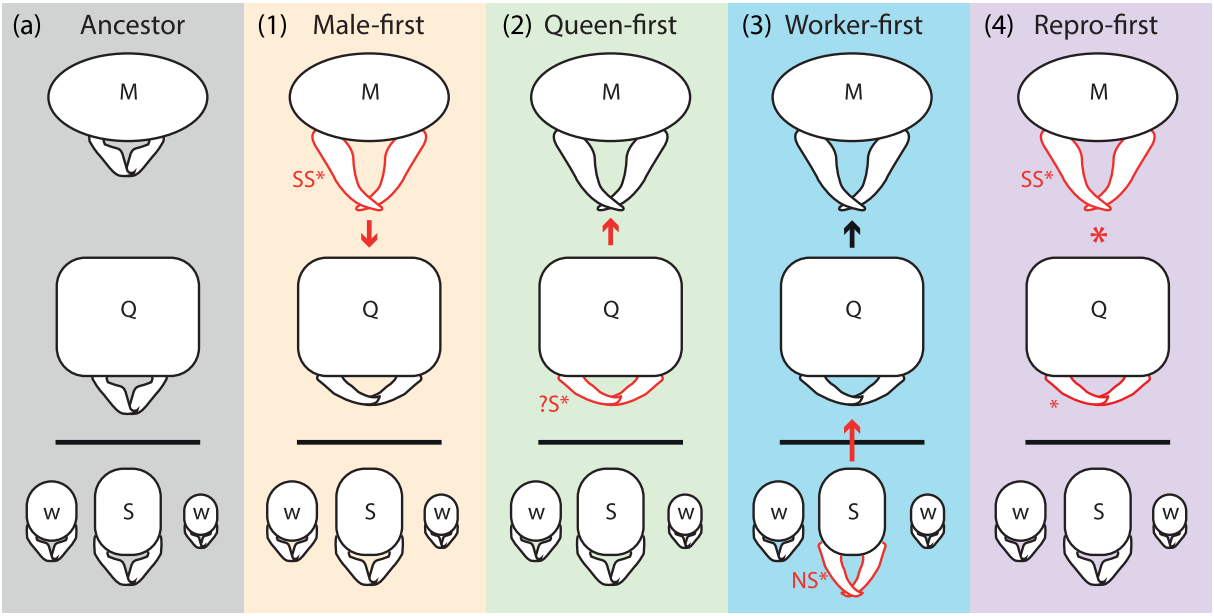

FIGURE 15 Alternative hypotheses for the origin of the derived and reproductive-limited falcate-mandibular phenotype in *Dorylus*. (a) Schematic outline of the ancestral condition of Dorylinae where all castes have triangular mandibles, plus four alternative evolutionary pathways (1–4) for the derivation of a reproductive-specific mandible phenotype, with arrows indicating phenotype transfer from one caste-specific developmental pathway to another. (1) In the first scenario (male-limited origin), the male (**M**) derives a falcate phenotype (red mandibles) as a response to sexual selection on the known copulatory clamping function (**SS***); due to the strength of the selective force, the falcate mandibular program is coincidentally expressed in the queen-specific developmental pathway (red arrow); however, the program is not expressed in the worker-specific pathway due to a hypothetical mechanism that is unique to the development of the reproductive castes (black bar). (2) In the second scenario (queen-limited origin), the queen-specific developmental pathway (**Q**) derives the falcate mandibular program in response to an unknown selection pressure (**?S***); the falcate program is then "co-opted" by the male for sexual purposes, and is not expressed in the worker-specific developmental pathway. (3) In the third scenario (worker-limited origin), the largest workers (presumptive soldiers, **S**) derive falcate mandibles as a response to natural selection (**NS***) on ergonomic efficiency; the falcate phenotype is then expressed in the queen via a sex-specific mechanism and is eventually expressed in the male pathway resulting in sexual advantage and is repressed in the worker pathway for unknown reason. (4) In the fourth scenario (reproductive-limited origin), the reproductive castes simultaneously derive the falcate-mandible developmental program (red asterisk) due to strong sexual selection pressure on the male and possible developmental constraint on the queen. Three additional scenarios are as follows: (5) simultaneous origin of falcate mandibles in all castes, that is, workers, queens, and males, with suppression of the falcate phenotype restricted to workers; (6) simultaneous origin of the falcate phenotype in females, with subsequent repression in workers and expression in males; and (7) origin of the falcate phenotype in the worker caste with subsequent transfer to the queen via the male. Given the total absence of male-to-worker-limited states, we do not consider scenario 7 further

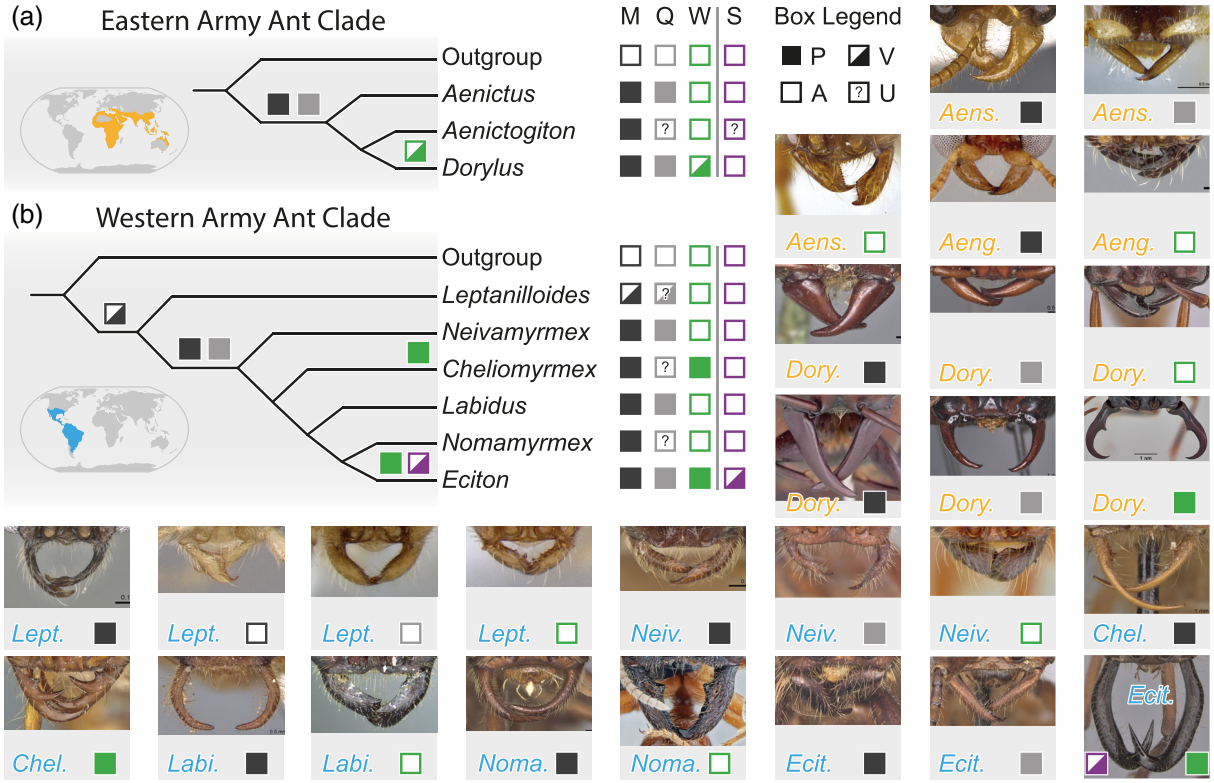

FIGURE 16 Summary of the phylogenetic pattern of falcate-mandible phenotype occurrence in the male (M), queen (Q), and worker (W) castes and of the occurrence of a discrete soldier caste (S) in the Eastern (a) and Western (b) doryline army-ant clades. The present (P) states are parsimoniously mapped onto the preferred topology of Borowiec et al. (2019); variability (V), absence (A), and uncertainty (U) are recorded in the center-right column (see "box legend" to the upper right). The phylogenetic distribution of mandible states supports the male- or reproductive-first hypotheses, while at least three independent origins of worker falcate phenotypes are indicated (*Dorylus*, *Cheliomyrmex*, and *Eciton*). The sparse data on allometry in worker caste(s) of doryline army ants support a pattern of continuous variation in worker size for most polyphenic genera (e.g., Gotwald Jr. & Kupiec, 1975; Hollingsworth, 1960; Topoff, 1971), except for some species of *Eciton* that develop a discrete soldier caste (Powell & Franks, 2006). Information on the mandible form of males, queens, and workers of large size is also available from Borgmeier (1955). Fine-scale and quantitative evaluation of doryline army ant mandibles is a high priority. The geographical distributions represented in (a) and (b) are records for *Aenictus* and *Neivamyrmex*, respectively, after projections from AntMaps (Guénard et al., 2017; Janicki et al., 2016) and Kronauer (2009). The queen of *Labidus* is not pictured but has been recorded as having falcate mandibles by Weber (1941). Inset species, specimens, and AntWeb imagers are as follows, starting from the *Aenictus* male to the right of the box legend, and proceeding left-to-right, top-to-bottom (C-# = CASENT): *Aens. clavatus atripennis* (C-0901982, Ziv Lieberman); *Aens. nuchiti* (THNHM-I-02613, THNHM-I-02612, Jaitrong Weeyawat); *Aenictogiton* zm02 (C-0106126, Michael Branstetter); *Aeng.* ug01 (C-0906052, Estella Ortega); *Dorylus affinis* (C-0901948, Ryan Perry; C-0911328, Will Ericson; C-0249445, WE); *D. nigricans* (C-0172641, April Nobile; C-0915346, ZL; C-0172642, AN); *Leptanilloides* indet. (C-0374401, Michele Esposito); *L. mckennae* (C-0010699, AN); *L. Erinys* (C-0234616, Marek Borowiec); *L. gracilis* (C-0106179, MBr); *Neivamyrmex nigrescens* (C-0862452, ME; C-0104061, AN; C-0106080, MBr); *Cheliomyrmex megalonyx* (C-0902670, WE; C-0911369, ZL); *Nomamyrmex hartigii* (JTLC000009350, WE; C-0915866, Anna Pal); *Eciton hamatum* (INB0003692970, INBIOCRI001283500, C-0612205 WE)

only one of the scanned specimens, with fibers of the right head side connecting to the tendon of the left. Previously, the only other aberrant muscle observed was functionless fibers of 0md1 in a *Formica rufa* Linnaeus, 1761 worker that attached to the dorsal and ventral surfaces of the cranium (Richter et al., 2020). Because muscular teratology in ants has not yet been a focal point of study, in contrast to external anatomy (e.g., Laciny, 2021; Sokolowski & Wisniewski, 1975), we suggest three alternative hypotheses to investigate at finer scale: (null) aberrant muscles occur purely by chance developmental misspecification (i.e., by pure "mistake"); (1) parasites or larval trauma; or (2) relaxed ecological selection on males may allow for accumulation of loss of function mutations. High throughput scanning and reconstruction of ants may be the best way to quantify these occurrences.

4.2.1 | Note on the galea

The medial differentiated region of the galea has yet to be observed in other ants. Because it is shared between the male and worker, it is probably developmentally specified, and thus its phylogenetic distribution is worth evaluating. Gotwald Jr. and Schaefer Jr. (1982) note that the conical form of the galeal crown, as observed here,

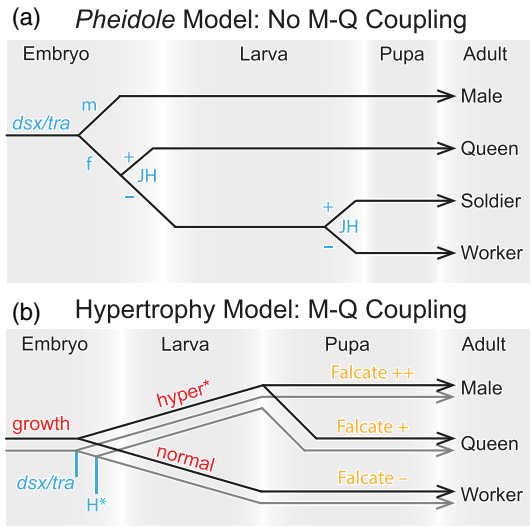

FIGURE 17 Extended "standard" or developmental switch models, accounting for the male phenotypic caste. (a) The *Pheidole* switch model of Wheeler (1986), with the addition of sex determination via the *doublesex/transformer* axis (*dsx/tra*; e.g., Nipitwattanaphon et al., 2014; Klein et al., 2016). In *Pheidole*, JH exposure at two critical periods determines the fate of female larvae (Lillico-Ouachour & Abouheif, 2017; also, e.g., Passera & Suzzoni, 1979 and Wheeler & Nijhout, 1983); the first period, during embryogenesis, splits queens and nonreproductive larvae, while the second, around the time of pupation, determines soldier versus worker fate for larvae of the bipotential neuter caste. (b) A hypothetical model proposed for *Dorylus* to explain the expression of derived reproductive-limited traits, that is, apomorphic features unique to the queens and males of *Dorylus* to the exclusion of their workers. This model assumes embryonic regulation of queen versus worker fate due to some signal or cue (H*), similar to *Pheidole*. The key observation is that the reproductive-fated larvae of *Dorylus* are hypertrophied (hyper*) relative to worker-fated larvae, such that queens and males are an order of magnitude larger than workers, without any overlap in size range (e.g., Berghoff, 2002; Schöning et al., 2008; also, e.g., Arnold, 1915; Santschi, 1939). The excessive growth of the reproductive castes was likely derived due to selection for hyper-fecundity, as a single queen of *Dorylus* may lay more than a hundred million fertilized eggs in her lifetime (e.g., Kronauer, 2009). We hypothesize that queen and male larval hypertrophy is the cause for the apparent developmental coupling of the reproductive castes, as such feeding presumably frees male and queen larvae to differentially invest accumulated nutrients among body structures, relative to workers (e.g., Nijhout & Emlen, 1998). Mapped in the pupal phase is mandible form, which is highly specialized and falcate in males (++), falcate but poorly developed in queens (+), and is not falcate in workers (−). The proximal genetic, hormonal, or other signals or cues for reproductive larva hypertrophy are unknown. Non-overlap of size between doryline army ant reproductives and workers has also been observed for *Aenictus* (e.g., Jaitrong & Ruangsittichai, 2018; Jaitrong & Yamane, 2013; Wilson, 1964), *Eciton* (e.g., Borgmeier, 1955; Reichensperger, 1924; Wheeler, 1921, 1925), *Labidus* (Bruch, 1934), and *Neivamyrmex* (e.g., Snelling & Snelling, 2007). The males of the former taxa are especially large, while the male is unknown for the only *Leptanilloides* species for which a queen is described (Borowiec & Longino, 2011)

distinguishes *Dorylus* from *Aenictus* and the "ecitoninae" (i.e., the Western army ant clade).

4.3 | Mandible development and evolution

4.3.1 | Mandibles and male nipples

Two observations are worthy of particular scrutiny: (I) the mandibles of males and queens are discretely different in form relative to the worker phenotypes, being both falcate (sickle-shaped) and edentate, that is, they are of a reproductive-limited form (state 7, Section 3.2.3; Figure 14); and (II) the mandibles of the male are massive and highly specialized, whereas those of the queen are comparatively underdeveloped (Section 3.2.6; Figure 14). Both of these states contrast with the general condition in Formicidae, where there is no discrete reproductive mandibular phenotype, and where it is in males that the mandibles are underdeveloped, sometimes to the point of near total loss. To explain this inversion of the general pattern of mandible development for ants, we hypothesize that the reproductive-limited mandibular phenotype of *Dorylus* is canalized and derived via male-specific selection. In other words, that the queen mandibular phenotype in this genus is at least partially: (a) developmentally decoupled from that of the worker; (b) developmentally coupled with that of the male; and (c) constrained by selection on the male-specific phenotype.

Because of this exceptional situation in *Dorylus*, we ask: Did the developmental feature or program that causes the development of the falcate mandibular phenotype originate in the male-fated pathway before expression in the queen-fated pathway, did it originate in both reproductive castes simultaneously, or was it a worker-limited phenotype that became expressed ("co-opted") in the reproductive pathways (Figure 15)? Relative to the sexual dimorphism in vertebrates and other arthropods (e.g., Coyne et al., 2007; Oliver & Monteiro, 2011; Owens & Hartley, 1998; Williams & Carrol, 2009), where a trait may arise in one sex and remain limited or may arise in both and be repressed or promoted, the question for *Dorylus* is complicated by the possible origin of a trait in the worker caste or in a worker subcaste, and by the limitation of certain derived traits solely to the reproductive or dispersing caste (Figure 14). Further, *Dorylus* and other doryline army ants represent extreme cases of obligate eusociality (Boomsma & Gawne, 2018), having highly polyphenic workers and discrete, thus certainly canalized male, queen, and worker castes (Sections 3.1.1–3.1.9, 3.2.5, 3.2.6).

Comparison with other genera reveals that both the male and female reproductive castes of doryline army ants develop an edentate-falcate mandibular phenotype, as observed in *Dorylus* (Q, Figure 16), in contrast to the more-or-less triangular form of most workers. Contrary to the expectation of the worker-, female-, or all-caste-first hypotheses (3, 5, 6, 7, Figure 15), the falcate phenotype is only developed among the largest workers of some *Dorylus* species and in the genera *Cheliomyrmex* and *Eciton* (W, Figure 16), indicating that non-reproductive females evolved such mandibles independently

at least three times. Moreover, the falcate forms of these genera are highly distinct in appearance, further supporting the scenario of independent origins for worker-specific falcate phenotypes (photo insets, Figure 16). The Western genus *Leptanilloides* provides ambiguous support for the male-first hypothesis (Figure 15b). The known queen of this genus has mandibles that are similar in form to the conspecific worker (Borowiec & Longino, 2011), while the males of various species display transitional states with some having distinctly falcate mandibles and others having more triangular forms (Figure 16). The phylogenetic distribution of these states indicates that the distinct falcate phenotypes, or expressions thereof, have evolved independently in both the reproductive and worker castes and in the Eastern and Western army ant clades.

Partial developmental coupling of the highly specialized "dichthadiiform" males and queens of *Dorylus* and other doryline army ants may explain the discrete reproductive mandible phenotype observed in these taxa. Such coupling may plausibly be due to larval hypertrophy (Figure 17b), which results in massive reproductives that do not overlap in body size with workers (e.g., Figure 1). The causes of the observed hypertrophy of male- and queen-fated larvae in *Dorylus* are uncertain. Two potential signals may be juvenile hormone (JH) or alternative splicing of *doublesex* (*dsx*). Juvenile hormone pulses at critical periods in development (e.g., Figure 17a) are known, for example, to cause diphenic expression of dung beetle horns (Emlen et al., 2005), enlarged mandibles of termite soldiers and stag beetles (Cornette et al., 2008; Gotoh et al., 2011, 2014, 2017; Kajimoto et al., 2012), and development of the soldier caste in *Pheidole* (Abouheif & Wray, 2002; Koch et al., 2021; Rajakumar et al., 2018). Alternatively, an embryonic signal such as alternative splicing of *dsx* may cause differentiation toward the reproductive-fated pathway with its associated states not shared with workers. For example, *dsx* has been found to also coordinate female caste diphenism of *Cardiocondyla* in addition to specifying sex (Klein et al., 2016). These alternatives may be complementary, and other factors should definitely be accounted for.

One approach would be to test the hypothesis of developmental coupling itself through artificial selection on the army ants under question, although this will be exceptionally difficult due to their life histories. Given the available evidence, however, we consider developmental constraint of the male and queen mandibles for most doryline army ants to be a plausible explanation, in particular because of the following points: (1) male mandibles have a specific and sexually critical function (thus favoring the male-first hypothesis, 1 in Figure 16; see also next paragraph); (2) falcate male mandibles have likely evolved at least twice in the doryline phylogeny (Figure 16), with similar function in both army ant instances; (3) falcate queen mandibles have no known special function (thus disfavoring the queen-first hypothesis, 2 in Figure 15); and (4) male and queen *Dorylus* are absolutely discrete in body size relative to their offspring workers (Figures 1 and 17). The situation of *Leptanilloides* is especially important in this context (Figure 16), as males are small to miniscule and are known to have falcate to triangular mandibles, while the only reported queen of that genus is a singleton with worker-like mandibles (Borowiec & Longino, 2011). If males derived the falcate form first, perhaps in small-bodied species, then queens would not be coupled and coupling in other doryline army ants, possibly via hypertrophy, would have been a subsequent derivation.

Whether the falcate phenotype was derived in males first (1, Figure 15) or simultaneously in the reproductive castes (4, Figure 15), natural history observations provide evidence that sexual selection on the male is likely to have been the driving evolutionary force. While falcate queen mandibles have not been observed to have any special use in the doryline army ants, males of *Dorylus*, *Eciton*, and other genera are known to use their mandibles to vigorously clamp the female during copulation (e.g., Kronauer, 2020; Kronauer et al., 2007; Schneirla, 1971). We note here that reproductive-limited larval mandibular forms are not developed in ants generally (Wheeler & Wheeler, 1976) and for doryline army ants specifically (Cohic, 1948; Tafuri, 1957; Wheeler, 1943; Wheeler & Wheeler, 1964, 1974, 1984), thus it is unlikely that larval ecology plays a role in evolution of queen falcate mandibles. If the development of the male and queen phenotypes is indeed partially coupled, then development of the queen mandibular phenotype is expected to be constrained, as mutations interrupting mandible morphogenesis in males would be catastrophic for reproduction. The comparatively functionless queen-falcate phenotype would thus be coincidentally canalized, and would therefore be an "evolutionary spandrel," akin to the male nipples in therian Mammalia as hypothesized by Gould (Gould, 1993; Gould & Lewontin, 1979). Overall, that sexually selected phenotypes are consistently diagnostic of army ants indicates that alternative reproductive strategies, such as obligate polyandry, may be necessary to derive extremely complex patterns of caste differentiation.

4.3.2 | Mandible patterning

Photomicrographic and SEM comparison reveals conserved development of a mandibular carina (III, Figure 2c; II, Figure 6a). The medial portion of this carina is in the form of a longitudinal costate or ridged line that is edentate in the male but dentate in the worker (state 11, Section 3.2.1). Based on the specific position and orientation of this structure, we hypothesize that the expression of the mandibular carina is caused by a homologous developmental process, for which reason we tentatively term the medial portion the "carinate tooth line" for the purposes of discussion. We observe that, in workers, carinate tooth line is divided into two subsections with distinct angles relative to one another, which are traditionally referred to as the "basal" and "masticatory" margins in the myrmecological literature (e.g., Bolton, 1994, 2003; bm, mm, Figure 11a). The apex of the mandible in the worker and queen is developed into a distinct, acute angle (tooth; mat, Figure 12e), and such an angle is weakly developed at the apex of the carinate line in the male, where the line distally curves toward the ventrolateral underside of the mandible (aa, Figure 6a). Additional teeth in the worker are developmentally specified on the tooth line, including the "preapical mandibular tooth" ("mpat," Figure 11c, 12c) and the "median mandibular tooth" ("mmt" in Figure 11a). Given the approximately falcate mandibular form of larval *Dorylus* (Wheeler & Wheeler, 1984), the specification and development of worker preapical and median teeth must occur during pupation.

Based on the principles of insect morphology (Snodgrass, 1935, 1958) and contemporary evolutionary developmental theory for the mandibles (see the reviews of Angelini & Smith, 2019 and Prpic, 2019), we propose that the carinate tooth line is homologous with the incisor endite of the Mandibulata, with ant- and Hymenoptera-specific patterning processes. We note also that although Xyelidae have a developed mola, this structure is indistinct in other Hymenoptera (Beutel & Vilhelmsen, 2007), including crown and stem ants (Barden & Grimaldi, 2014; Boudinot et al., 2020; Wilson et al., 1967a, 1967b); if it were present, the mola is of a derived and an as-yet unrecognized form.

Given developmental theory and our observations of mandibular anatomy outlined above, we postulate that a minimum of seven processes are responsible for mandibular patterning across the Formicidae, and for which we encourage review and experimentation. (1) Specification of an apical point or fine area in the mandibular anlage during embryogenesis, with retention of this information or re-expression during pupation. (2) Proximodistal elongation of the mandible at the specified apical point during both embryogenesis and pupation. (3) Torsion/curvature of the mandible around the proximodistal axis during pupation, causing the mandibular apex to appear down- and medially turned when viewed frontally. (4) Specification of the mandibular carina, including the carinate tooth line (incisor) on the medial surface of the mandible during embryogenesis, with retention of this information or re-expression during pupation; this step is presumably necessary and prior to tooth development. (5) Specification of the basal angle on the tooth line via a proximodistal position-dependent mechanism. (6) Lateromedial blade-width expansion at the basal angle. (7) Development of adult teeth along the carinate tooth line during pupation, with some teeth canalized (e.g., the apical tooth) and some teeth iterated and space-dependent (e.g., denticles between the apical tooth and basal angle).

Table S3 summarizes hypotheticodeductive extensions of these postulated processes. Additional processes must be necessary to cause development of other mandibular structures, including specification the submarginal sensilla line, diffusion of a sensilla-differentiating morphogen across the frontal and abfrontal mandibular fields, specification of the mandalus position and its subsequent differentiation, and critically, the development of the craniomandibular articulations and mandibular apodemes, among others. Developmental experimentation on mandible growth and patterning will have significant explanatory power, given critical role of mandibles in evolution of the ants (e.g., Booher et al., 2021; Wilson, 1987), and their vast range of structural and functional variation (e.g., Bolton, 1994; Gronenberg et al., 1997; Perrichot et al., 2020; Zhang et al., 2020,b).

4.4 | Head evolution

4.4.1 | Head-shape

The male-phenotypic head shape of *Dorylus* is highly distinctive, being lateromedially transverse with a broad frontal bulge (fb, Figure 2d,e). Through comparison of males across the Dorylinae via AntWeb and Borowiec (2016), we observe that the transverse condition is also shared with *Aenictus*, *Cheliomyrmex*, *Eciton*, *Labidus*, *Nomamyrmex*, and various *Neivamyrmex*, all of which are known army ants, and that have falcate mandibles. Given these observations and the known phylogenetic relationships of these genera (see Section 2.4.7; Figure 16), we hypothesize the following: **(1)** that the transverse shape is an adaptation of the cranium to allow for the massively enlarged mandibular adductor (closer) muscles (0md1) that we observe in *Dorylus*; **(2)** that the transverse shape maximizes the mechanical advantage of the mandibular lever system; **(3)** that the transverse shape allows the male to grasp the similarly thick queen; and **(4)** that the location of the ocular nervous tissue constrains the cranium from accommodating enlarged mandibular adductors by elongating dorsally.

The first hypothesis (1) is supported by the observation that sister groups of the Western and Eastern clades are not army ants, and do not have the transverse head shape, suggesting that this innovative architectural solution has evolved independently, and that sexual selection is the causative force. The second hypothesis (2) predicts that formal mechanical analysis will find increased advantage from the lever conformation, and that this will allow for comparatively greater muscular force transmission relative to nontransverse crania. The third hypothesis (3) predicts a significant correlation between the distance of the falcate male's mandibular bases, and the thickness of the region clasped on the conspecific queen. The fourth hypothesis (4) predicts that *Aenictogiton* will have evolved a different solution to the spatial constraint problem. We note that external examination of *Aenictogiton* males, which have longitudinally elongate rather than lateromedially elongate heads, does seem to support the third hypothesis, in that the cranium is "prognathous" relative to *Dorylus*; the internal anatomy of this genus is necessary to interrogate in order to properly understand the relative spatial orientations and their mechanical consequences.

As for the frontal bulge of the male cranium, examination of the digital reconstructions reveals that lumenal surface corresponds to the origins of four muscles, while the frontal surfaces of the cranium lateral to the median bulge are devoid of musculature. The frontal bulge muscles are the pharyngeal dilator (**0bu2**, **0bu3**), the posterior oral arm muscle (**0hy1**), and the labral depressor ("closer," **0lb2**) muscles (Figure 10a,c,d,f); the remainder of the frontal bulge is filled with the prepharyngeal gland (phg, Figure 10a–c). Of the four frontal bulge muscles, the labral depressor is largest, suggesting need for tight closure of the labrum, hence protection of the maxillolabial complex. The function of the prepharyngeal gland remains ambiguous but it is clearly retained in the male.

Further comparison

The transverse head shape is not unique to the Dorylinae among Formicidae. The best examples, to our knowledge, are the males of *Carebara sensu stricto*, the *Carebara diversa* species group (formerly *Pheidologeton*), various *Cephalotes* (such as *C. atratus*, [L.]), and *Daceton*, all of which are taxa in the hyperdiverse subfamily Myrmicinae. The male phenotypes of all of these taxa have small, underdeveloped mandibles, raising the question of the function and

the evolutionary cause of the derived transverse form as compared to *Dorylus*. To address this question, it will be necessary to micro-tomographically sample these taxa and their less-derived relatives.

4.4.2 | Alternative suctorial phenotypes

We observe that both the male and female reproductive phenotypes share a lateromedially broad clypeus (Figures 2d and 11e), a feature distinct from the worker and of functional significance due to the fact that the clypeus bears the origins of some of the suctorial muscles. For this reason, and because suctorial systems of male and female ants have not been compared to date, we provide a coarse functional characterization of the pharyngeal musculature.

The sampled male phenotype displays 13 uniquely identifiable muscles of the cranial digestive tract, for which we broadly recognize three functional groups based on their insertions (Figure 10): (1) five prepharyngeal muscles (extrinsic: **0ci1a, 0ci1b**, **0bu1**, **0bu5**; intrinsic: **Mped**); (2) four oral arm muscles (extrinsic: **0hy1**, **0hy2**; intrinsic: **0hy9**, **Mpel**); and (3) four pharyngeal muscles (extrinsic: **0bu2**, **0bu3**, **0ph1**, **0ph2**). Because all of these muscles distend tube-shaped soft tissue, their contraction is expected to cause localized variation in tube volume, thus producing regions of high and low liquid density. With overall oral-to-anal waves of prepharyngeal to pharyngeal contraction, the musculature is expected to create directional suction, probably modulated by the muscles attaching directly to the sitophore plate and its lateral apophyses (oral arms, oa, Figure 10; mpel, 0hy1, 0hy2, 0hy9). These oral arm muscles are structurally organized such that two of them (mpel, 0hy2) must act antagonistically with one (0hy1), while the transverse oral arm to oral arm muscle probably causes dilation of the ventral region of the prepharynx (0hy9), complementing the complex extrinsic prepharyngeal dilator musculature.

Preliminary scan data of a worker of *D. orientalis* indicate that the suctorial musculature of workers is qualitatively and quantitatively distinct. Two discrete differences are the absence of the apparently male-specific *M. verticopharyngalis* (0ph1) and absence of the portion of *M. clypeopalatalis* closer to the functional mouth opening (0ci1a). Quantitative differences of muscle proportion are also suggested, with the longitudinal prepharyngeal musculature (Mped) and frontopharyngeal muscles (0bu2, 0bu3) appearing large in males, while 0ci1b is especially pronounced in the worker. These differences may be due to functional optimization as a response to size, spatial, and structural constraints. If 0ph1 is indeed widespread among male Formicidae, its absence in workers could easily be explained by structural constraint given the head and brain orientation of the female phenotype. We cannot confidently infer the consequences of these different muscle sets and conformations, because, to our knowledge, only a few attempts at detailed functional analysis of the cranial digestive tract have been undertaken so far (e.g., Paul & Roces, 2019). We do, however, draw attention to the need to explicitly study suctorial system performance, sex-specific differences, and to incorporate queens and an overall wider sample of species for this outstanding issue.

4.5 | Setae and sensilla

4.5.1 | General considerations

"Setation," or sensilla patterning more precisely, is of considerable functional and evolutionary value for the organism and organismal populations. However, the development of the language for discussing sensilla is not at the stage where the terms are anchored in particulate homology. To use the concepts of Linnaeus and Hennig, we do not have a "natural" system for sensilla nomenclature, as any generally accepted formal name can be applied to almost any given hair-like structure, resulting in polyphyletic inclusion of dissimilar entities together under one name. While on external examination a seta or sensilla may appear to be simple, in reality the sensillum is a complex of multiple parts, differentiated from the neuroectodermal cell layer, with biologically meaningful and variable function (e.g., Chapman, 2012). After a review of the literature, we have come to concur with Altner and Prillinger (1980) that the formal terminology for setation betrays homology via the considerable possibility for paraphyly and polyphyly of the classification of phenotypic objects (anatomical entities). All of this is to say that considerable terminological chaos and contradiction exists for the nomenclature of sensilla, with conflict remaining after over a century and a half of research (e.g., Forel, 1885; Leydig, 1850), and even at the level of Ontology (e.g., DAO, HAO). We therefore call for focused effort for resolution.

In an attempt to find at least some degree of said resolution, we recorded the external properties which were used to apply formal sensilla names in the literature (e.g., *sensillum trichodeum*, *s. basiconicum*, *s. coeloconicum*, *s. styloconicum*, etc.) and considered the consequences of word choice. We found that the properties used to observationally differentiate the sensilla are both variable and insufficient to consistently categorize and designate a name for an observed sensillum. In our opinion, Altner and Prillinger (1980)—with Kraepelin (1883) far before—provided the most coherent general classification for sensilla, recognizing the following broad groups, with further subdivision based on innervation: (1) no pore, socket flexible, mechanosensitive ("NP-f"); (2) no pore, socket inflexible, thermo- and hygrosensitive ("NP-if"); (3) terminal pore, socket flexible, mechanosensitive and gustatory ("TP-f"); (4) terminal pore, socket inflexible, gustatory ("TP-if"); (5) wall (i.e., lateral) pores, socket inflexible, single-walled, olfactory ("WP-sw"); and (6) wall pores, socket inflexible, double-walled, olfactory or olfactory and thermosensitive ("WP-dw"). Consequently, we recognize that in order to obtain a complete and "natural" (monophyletic) classification, it is necessary to evaluate the ultra-scale anatomy, genetic, developmental, and phylogenetic history of "setae" or sensilla.

4.5.2 | Broader concepts

To evaluate the degree of seta class distinction, we borrowed the population biological concepts of sympatry and allopatry, that is, co-occurrence of two or more distinct populations in a given area or non-

co-occurrence. We used these as heuristics for determining independent setation groups. We considered setae allopatrically "distinct" if they displayed discrete properties from other setae on nearby structures, such as the spine-like galeal setae (mxs3c) relative to the hair-like setae (mxs1d) of the galeal crown (gacr; Figure 7). The strongest evidence for fully distinct setae is the retention of discrete differences between two seta classes expressed in anatomical sympatry, that is, in the same setational field, such as the thicker and more-erect hair-like setae of the proximal labral margin (ls1), which co-occur (are surrounded by) thinner, less-erect hair-like setae (ls2) (Figure 4a). More broadly, we conceive of the process of seta class evolution as the process of phenotypic object individuation (speciation), as invoked by Wagner (2014). For the purposes of initiating an approach which might be fruitful, we suggest that the anatomical and physiological properties used to define sensilla in the system of Altner and Prillinger (1980) be used to define homologous *Sensilla Genera*, and other patterns such as shape, form, pore arrangement, cell structure, and so forth, be used to define homologous *Sensilla species*, all to be informed by the underlying genetic architecture and phylogenetic history.

4.5.3 | Specific results and comparisons

With a focused *Sensilla Genus species* approach, we parse the literature and evaluate our observations. First, the broadest phenotypic categories of sensilloid structures or sensilla that we can recognize based on our present observations are **(i)** "hair-," "spine-," or "bristle-like," **(ii)** "button-like," and **(iii)** "blade-like." Across all setose head parts of *Dorylus*, the first category includes 19 classes (*hs1–2*, *as1–6*, *ls1–2*, *mds1–3*, *mxs1–4*, *lbs1–4*), the second category includes one class (*mxs5*), and the third includes two classes (*as7*, *as8*), for a total of 23 observed classes, with considerable intra-class variation for the first maxillary class (*mxs1*). Sensilla diversity was greatest on the antenna (eight classes), followed by the maxilla (five classes), then by the labium (four classes). We recognize that further categories of sensilla should be considered in future comparative work on ants and other Hymenoptera. These categories, from Romani et al. (2010) are as follows: (**iv**) the aporous "campaniform" and "coeloconic" sensilla; (**v**) the uniporous gustatory sensilla; (**vi**) the multiporous single-walled "trichoid," plate, and gustatory sensilla; and (**vii**) the multiporous double-walled grooved-peg sensilla. An additional category, (**viii**) the "ampoule," has been observed in ants (e.g., Forel, 1885; Hashimoto, 1991; Kraepelin, 1883; Lubbock, 1877; Ramirez-Esquivel et al., 2014; Romani et al., 2010), and is known to be sensitive to CO_2 (Kleineidam et al., 2000; Kleineidam & Tautz, 1996).

The first of our observed categories (i) is variably referred to as "*s. trichodeum*" ("*s. trichoideum*") or "*s. chaeticum*" (e.g., Altner & Prillinger, 1980), which we here consider to be synonyms of the analogous English words, and thus are not taxa of the proposed *Sensilla* taxonomy. The function of hair-like sensilla is variable and depends on the pore patterning. Tip-pore sensilla are generally appreciated to be gustatory chemoreceptors, wall-pore sensilla as olfactory chemoreceptors, and aporous sensilla as variable in function (Altner & Prillinger, 1980; Romani et al., 2010). Given that the bulbus (*as1*), pedicellar base (*as2*), and pedicel bell and proximal flagellar (*as3*) setae occur on contact surfaces, it is probable that they are mechanosensory and have a proprioceptive function. Certain of such proprioceptive bristles or hairs have been called the "hair plate" or "Böhm's sensilla" (Schneider, 1964). Because we were unable to observe pore patterning for the other classes of first category (i) setae, we are unable to provide strong functional interpretations.

We do note, out of interest, that the patterning of the short, leaning, hair-like (*hs1*, *as4*, *ls1*) setae with interspersed long, erect, hair-like (*hs2*, *as5*, *ls2*) setae is commonly observed in other ants (e.g., the "*crinosa* group pilosity" of *Crematogaster*, Longino, 2003; various other Myrmicinae, Bolton, 1987), and is similar to the "ground" and "guard" hair pattern of mammalian pelage. For mammals, it is generally accepted that, in addition to mechanosensation (touch), the ground hairs have a thermoregulatory function, and the guard hairs repels water from the skin. An analogous water repellence function for single or double layer setation on ants makes sense for the cranium, mesosoma, and metasoma, but less so for the antennae and labrum. Regarding the antennae, the collective function of the double layer pattern of hair-like setae is dependent on the pore and innervation patterning. With respect to the labrum, the double layer may provide the animal with a spatially refined sense of touch, which is also possibly applicable to other structures, such as the mandibles. The positioning of the longer, sparser labral setae matches that of the "labral pegs," "spicules," "traction setae," or "chaetae" of Amblyoponinae, Leptanillinae, and various stem Formicidae (Boudinot et al., 2020), which suggests that at least the double-layer labral patterning is conserved across the ants. A final note for the double-layer pattern is that the villous "guard setae" of the male *Dorylus* cranium is highly unusual and suggests that a male-specific function is under sexual selection in the genus.

The "button-like" moniker for the second observed category (ii) was first used by Hashimoto (1991) to describe sensilla that he observed on the labial palps of ants. The sensilla is possibly conserved among ants, as Hashimoto (1991) observed these to be present on species spanning the crown and poneroformicine nodes of the Formicidae (i.e., including Leptanillinae and Amblyoponinae, as well as Dorylinae). However, Hashimoto (1991) did not evaluate maxillary palps, so it is possible that the sensilla are more widespread than currently appreciated. Comparing with other Hymenoptera, the external form resembles that of the *Aporous Sensilla* referred to by Romani et al. (2010) as "coeloconic sensilla" and reported to have hygro- and thermoreceptive function (e.g., Ruchty et al., 2008). Indeed, the "button-like" and "coeloconic" sensilla may be homologous with the similarly shaped hygroreceptive "*s. coelocapitula*" of *Apis mellifera* (Yokohari, 1983; Yokohari et al., 1982), and the dissimilarly shaped but also hygroreceptive "*s. styloconica*" observed in *Bombyx* (Steinbrecht, 1989). A complication with this potential interpretation is the apparent doubled state of some of these sensilla on the palp of *Dorylus* (*mxs5*, Figure 7). Among our foundational references for head anatomy, similar appearing short, apparently socketed, conical-to-

TABLE 4 Some priorities and questions for the study of ant caste dimorphism and polyphenism, from the perspective of male phenotypic diversity.

Male-specific phenotype mapping
• Anatomical atlas construction for the mesosoma and metasoma, especially the genitalia (Boudinot, 2013), and for the developmental process—These will be of fundamental importance for establishing the phenotype–genotype map in Formicidae.
• Functional/mechanical analysis of anatomical systems—Within the context of the present work, skeletomusculature and sensilla function are key; other physiological processes should not be ignored however.
• Systematic documentation of conservation and variation through replication of the atlasing process for other taxa, and through taxonomic works (sorting, comparison, imaging, description)—The treatment of morphospecies (i.e., informal groups without an applied binomen) is as high priority as treatment of males with known species identity, as the development of a male phenotype classification is critical for incorporating this caste into the study of ant evolution.
• Ease male ant identification through the construction of keys to genus and (morpho)species (key to subfamilies: Boudinot, 2015)—Global treatments are higher priority than regional treatments, but the latter are also necessary (see Bolton, 2007 for extremely useful guidelines on the revisionary process).
• With respect to *Dorylus* and other army ants addressed in the present work, systematically document the male phenotypes non-army-ant Dorylinae, especially those genera that are closely related to the Eastern and Western clades (Borowiec, 2019)—For example, *Yunodorylus* is in the sister group to the Eastern clade (Borowiec, 2019) and has subdichthadiiform queens (Eguchi et al., 2016; Satria et al., 2018), but only one male has been documented (Borowiec, 2016).
Intercaste phenotype mapping
• Test the generality of the observation that males and workers share no unique states relative to the queen (Section 4.3).
• Evaluate and quantify covariation of male, queen, and worker phenotypes—Are doryline army ants unique in having derived reproductive-limited states?
• Comparatively document cranial musculature—What is the phylogenetic distribution of the two unique muscles of male *Dorylus* (Section 4.2); do all males lack the eight muscles recorded in Table 3? Are all ants characterized by inter-sex alternative suctorial phenotypes (Section 4.4.2); do queen doryline army ants also have the male suctorial phenotype?
• Focused, fine-scale, and quantitative evaluation of worker, queen, and male anatomy and anatomical covariation for the entire body within colonies and across species, whether at the scale of atlas or alpha taxonomic treatment—As we have shown, male ants are informative yet are mentioned peripherally or not at all in works addressing ant morphology and phenotypic diversity (see the second epigraph for a poetic dismissal of this sexual caste).
• Evaluation of worker, queen, and male mandible variation for Dorylinae specifically, particularly *Leptanilloides*—Did the origin of the falcate male phenotype precede or follow the evolution of highly domesticated (specialized) dichthadiiform queens?
Evolutionary developmental biology
• Account for males in the study of caste development and differentiation.
• Document the sequence and timing of anatomical transformation for all castes at the atlas scale.
• Test the general mandible patterning processes for ants postulated in Section 4.3.2.
• Test the specific mandible development hypotheses for *Dorylus* proposed in Section 4.3.1.
Questions of ant evolutionary biology
• What are the developmental and evolutionary causes of the transverse head form of *Dorylus* and other doryline army ant males (Section 4.4.1)?
• What roles do sexual selection and extreme male phenotypes play in the evolution of worker polyphenic complexity, as in doryline army ants and leafcutters?—Are extreme male phenotypes a response to or are they necessary for this evolutionary process?
• Why do some male ants evolve elaborations of the genitalia—Is there a general pattern, or are these elaborations experiencing different selection dynamics?—An inexhaustive list includes: Leptanillinae, *Diacamma*, *Dinoponera*, doryline army ants, Myrmeciomorpha, *Leptomyrmex*, *Liometopum*, *Myrmelachista*, *Cataglyphis*, *Acropyga*, *Aphaenogaster*, *Atta*, *Carebara*.
• Why do some male ants evolve simplified genitalia?—An inexhaustive list includes: *Leptanilloides*, *Simopelta*, *Pseudolasius*, *Oecophylla*.
• What are the interorgan developmental tradeoffs between the head, mesosoma, and genitalia?—How are these regulated?
Sensilla patterning and evolution
• Construct a comparative atlas of sensilla in Formicidae (initiated by Hashimoto, 1991) and the Aculeata more broadly, applying SEM, TEM, physiology, and the principles of sensilla classification from Altner and Prillinger (outlined in Section 4.5.1).
• Reconstruct the history of sensilla class individuation among Formicidae and other Hymenoptera.
• Confirm the identity of the male blade-like sensilla of *Dorylus*.

Note: With a multimodal approach, as taken in the present study, it will be possible to bring the study of morphology closer to the objective of phenotype–genotype mapping—A critical interface for unlocking the causes and patterns of anatomical development and form (see, e.g., Sanger & Rajakumar, 2019). Other, less technical, approaches are necessary, however, to manifest a complete theory of ant diversity and evolution. Because males are understudied in general, non-head tagmata and structures are also addressed.

button-shaped sensilla have also been observed on the galea of *Wasmannia* and *Brachyponera*, as well as on the oral labral surface of *Wasmannia*, *Formica*, *Brachyponera* and the proximal maxillary palpomere of *Protanilla* (Richter et al., 2019, 2020, 2021). Higher resolution SEM imaging is needed to determine if these sensilla are porous or aporous, and TEM is further needed to determine the sagittal cross-section and innervation patterns (e.g., Altner et al., 1983).

Finally, the third observed category (iii) comprises those sensilla which resemble thick blades. Broadly, these match the "*s. basiconica*" of the ant literature (e.g., Dumpert, 1972; Hashimoto, 1991; Nakanishi et al., 2009; Ramirez-Esquivel et al., 2014; Renthal et al., 2003; Romani et al., 2010). The general definition provided in these works is that an "*s. basiconica*" has a "peg" and a "socket," the latter resembling a disc or a pedestal. However, one of the two seta classes we observed was expressed by the male; previous studies comparing male and female ant antenna sensilla have not observed "*s. basiconica*" on the male (Barsagade et al., 2010; Ghaninia et al., 2018; Nakanishi et al., 2009; Okada et al., 2006; Renthal et al., 2003; Walther, 1985). This implies that either the female specificity of "*s. basiconica*" is not generally true, or that the apparent basiconic sensilla of the male is homologous to another *Sensilla species*. We hypothesize that the male "*s. basiconica*" is homologous with the "*s. trichodea curvatum*," a well-defined *Sensilla species*, which is known to occur in other Hymenoptera and to be multiporous, single-walled, and to have an olfactory function (Romani et al., 2010). This is circumstantially supported, as Bin et al. (1989) observed that the male of *Trissolcus basalis* (Scelionidae) has an order of magnitude more of these "curvate" sensilla than the female. Further, Hashimoto (1991) explicitly and Romani et al. (2010) implicitly hypothesized that the "*s. t. curvatum*" is homologous with the placodeal sensilla due to the multiporous condition and presence of internal longitudinal ridges ("ledges"), suggesting that the two would form a *Sensilla Genus*. Future study of *Dorylus* antennal sensilla are necessary to confirm the identity of the male blade-like sensilla.

5 | CONCLUSION

Collectively, ants are exquisitely plastic animals, displaying temporal, ergonomic, physiological, reproductive, and anatomical polyphenism. Missing from the equation of the study of ant phenotypic plasticity are males, and consequently, the phenomenon of ant sexual dimorphism and entire ranges of variation and trait limitation in the Formicidae (Table 4). Our detailed analysis of the male head anatomy of *D. helvolus*, with subsequent comparison to females, revealed to us unexpected and complex patterns of conservation and variation in the genus, and among the Formicidae more broadly.

Conservation of a carinate line on the mandible of the male has led us to postulate and elaborate on a set of necessary developmental processes for mandible patterning. We discovered that the head architecture of the male is fundamentally different than that of workers, with discrete muscle presences and absences, and critically, that not a single specific state is uniquely shared between the two castes to the exclusion of the queen. These findings indicate that males are a true developmental caste of Formicidae, with a discrete pathway of development relative to the conspecific queen and worker castes. We observe that the developmental patterning of the phenotypic castes of ants is similar to the population-biological concept of "ring species," where a morphological gradient can be traced from the worker phenotype to the queen, and from the queen to the male, but not between the male and the worker (Figure 14).

Based on our observations and broad phylogenetic comparisons, we hypothesize that the male mandible in ants is generally an "evolutionary spandrel," akin to male nipples in mammals. That this pattern has become inverted in the army ants is apparent, with strong sexual selection possibly causing canalization of the falcate phenotype in the reproductives, thus partially decoupling the development of the queen and worker castes. We conclude that the falcate phenotype independently originated in the reproductive- and worker-specific developmental cascades, and that this pattern has convergently evolved in the Eastern and Western army ant clades. Finally, we recognize that there is a need for histological and experimental determination of sensilla classes in order to understand sensilla identity and evolution in the ants and Hymenoptera more broadly. In sum, while males may not have ergonomic value for the superorganism, their potential for deepening our understanding of ant evolutionary and developmental biology is clear.

ACKNOWLEDGMENTS

This work represents anastomosis of several streams of thought, whose sources and encouragement are appreciated. Any errors are ours alone. We thank the following people: Roberto Keller for his inspirational mode of thought and for sharing his SEM Atlas; Heather S. Bruce, Daniel Kronauer, Rajendhran Rajakumar, and Buck Trible for stimulating our thinking about development and subsequent insightful and inspiring discussion; Günter Wagner for sharing his thoughts on and vocabulary for homology; Jack Longino and Phil Ward for years of advising, support, and discussion provided to BEB; Barry Bolton for demonstrating the revisionary process of systematics and for collegial communication; Brian Fisher and Michelle Esposito for AntWeb and AntCat, two critical resources for all of Myrmecology; Lars Vilhelmsen for constructive feedback on the digestive tract; Pawel Jałoszyński for providing the male specimens used; Michael Weingardt for repeated discussion about a variety of germane topics; Kenny Jandausch for assisting with Phyletisches Museum matters; Zach Griebenow for constructive comments of an early version of this manuscript; and Jill Oberski for hearing and suggesting useful improvements to this work. Two anonymous reviewers, particularly the second, are gratefully acknowledged for their constructive criticisms. Finally, we thank the editor in chief, Matthias Stark, for improving the consistency of our labeling and figure references. BEB acknowledges a Research Fellowship from the Alexander von Humboldt Stiftung; he is further grateful to circumstance for, as example, his working computer resuscitated unexpectedly after dying. OTDM thanks Hans Pohl for assisting with photomicrography during her bachelor's project, which itself formed the basis for the present contribution; OTDM also thanks her brother

Conrad for the drawings of male *Dorylus* heads represented in the supplementary figure. AR gratefully acknowledges a scholarship by the Evangelisches Studienwerk Villigst eV. The authors declare no conflict of interest. Collectively, we hope that the style of the writing or the language used does not obscure the substance of the work.

AUTHOR CONTRIBUTIONS

Brendon Boudinot: Conceptualization (lead); formal analysis (lead); funding acquisition (equal); investigation (lead); methodology (supporting); visualization (equal); writing – original draft (lead); writing – review and editing (lead). **Olivia Moosdorf:** Conceptualization (supporting); data curation (lead); formal analysis (supporting); investigation (supporting); methodology (equal); validation (supporting); visualization (equal); writing – original draft (supporting); writing – review and editing (supporting). **Rolf Beutel:** Conceptualization (supporting); funding acquisition (equal); project administration (supporting); resources (lead); software (lead); supervision (supporting); validation (supporting); writing – review and editing (supporting). **Adrian Richter:** Conceptualization (supporting); data curation (equal); formal analysis (equal); funding acquisition (equal); investigation (equal); methodology (equal); project administration (equal); supervision (lead); validation (supporting); visualization (equal); writing – review and editing (supporting).

PEER REVIEW

The peer review history for this article is available at https://publons.com/publon/10.1002/jmor.21410.

DATA AVAILABILITY STATEMENT

Data sharing is not applicable to this article as no new data were created or analyzed in this study.

ORCID

Brendon Elias Boudinot https://orcid.org/0000-0002-4588-0430
Rolf Georg Beutel https://orcid.org/0000-0002-0433-7626
Adrian Richter https://orcid.org/0000-0001-5627-2302

REFERENCES

Abouheif, A., & Wray, G. A. (2002). Evolution of the gene network underlying wing polyphenism in ants. *Science*, *297*, 249–252. https://doi.org/10.1126/science.1071468

Agosti, D., & Hauschteck-Jungen, E. (1987). Polymorphism of males in *Formica exsecta* Nyl. (Hym.: Formicidae). *Insectes Sociaux*, *34*, 280–290.

Altner, H., & Prillinger, L. (1980). Ultrastructure of invertebrate chemo-, thermo-, and hygroreceptors and its functional significance. *International Review of Cytology*, *67*, 69–139.

Altner, H., Schaller-Selzer, L., Stetter, H., & Wohlrab, I. (1983). Poreless sensilla with inflexible sockets. *Cell and Tissue Research*, *234*, 279–307.

André, E. (1885). *Les Fourmis. Bibliothèque des Merveilles* (p. 347). Hachette & Cie.

Angelini, D. R., & Smith, F. W. (2019). Theme and variation in the development of insect mouthparts. In H. W. Krenn (Ed.), *Insect mouthparts. Zoological monographs* (Vol. 5, pp. 127–174). Cham: Springer. https://doi.org/10.1007/978-3-030-29654-4_5

AntWeb. (2021). *AntWeb. Version 8.48.3*. California Academy of Science. Available from. https://www.antweb.org

Arnold, G. (1915). A monograph of the Formicidae of South Africa. Part I. Ponerinae, Dorylinae. *Annals of the South African Museum*, *14*, 1–159.

Arnold, G. (1946). New species of African hymenoptera. No. 6. *Occasional Papers of the National Museum of Southern Rhodesia*, *2*, 49–97.

Asplen, M. K., Whitfield, J. B., de Boer, J. G., & Heimpel, G. E. (2009). Ancestral state reconstruction analysis of hymenopteran sex determination mechanisms. *Journal of Evolutionary Biology*, *22*, 1762–1769. https://doi.org/10.1111/j.1420-9101.2009.01774.x

Barden, P., & Grimaldi, D. (2014). A diverse ant fauna from the mid-cretaceous of Myanmar (Hymenoptera: Formicidae). *PLoS One*, *9*, e93627. https://doi.org/10.1371/journal.pone.0093627

Barden, P., & Grimaldi, D. A. (2016). Adaptive radiation in socially advanced stem-group ants from the Cretaceous. *Current Biology*, *26*, 515–521. https://doi.org/10.1016/j.cub.2015.12.060

Barden, P., Perrichot, V., & Wang, B. (2020). Specialized predation drives aberrant morphological integration and diversity in the earliest ants. *Current Biology*, *30*, 3818–3824. https://doi.org/10.1016/j.cub.2020.06.106

Baroni Urbani, C., Bolton, B., & Ward, P. S. (1992). The internal phylogeny of ants (Hymenoptera: Formicidae). *Systematic Entomology*, *17*, 301–329.

Barsagade, D. D., Tembhare, D. B., & Kadu, S. G. (2010). SEM structure of mandibular sensilla in the carpenter ant, *Camponotus compressus* (Fabricius) (Formicidae: Hymenoptera). *Halteres*, *1*, 53–57.

Béhague, J., Fisher, B. L., Péronnet, R., Rajakumar, R., Abouheif, E., & Molet, M. (2018). Lack of interruption of gene network underlying wing polyphenism in an early-branching ant genus. *Journal of Experimental Zoology (Molecular Developmental Evolution)*, *330*, 109–117. https://doi.org/10.1002/jez.b.22794

Berghoff, S. M. (2002). Nesting habits and colony composition of the hypogaeic army ant *Dorylus* (*Dichthadia*) *laevigatus* Fr. Smith. *Insectes Sociaux*, *49*, 380–387.

Beutel, R. G., Friedrich, F., Ge, S.-Q., & Yang, X.-K. (2014). *Insect morphology and phylogeny* (p. xv, 516). Walter de Gruyter.

Beutel, R. G., & Vilhelmsen, L. (2007). Head anatomy of Xyelidae (Hexapoda: Hymenoptera) and phylogenetic implications. *Organisms, Diversity and Evolution*, *7*, 207–230. https://doi.org/10.1016/j.ode.2006.06.003

Bin, F., Colazza, S., Isidoro, N., Solinas, M., & Vinson, S. B. (1989). Antennal chemosensillar and glands, and their possible meaning in the reproductive behavior of *Trissolcus basalis* (Woll.) (Hym.: Scelionidae). *Entomologica*, *24*, 33–97.

Bolton, B. (1987). A review of the *Solenopsis* genus-group and revision of Afrotropical *Monomorium* Mayr (Hymenoptera: Formicidae). *Bulletin of the British Museum (Natural History) Entomology*, *52*, 263–452.

Bolton, B. (1994). *Identification guide to the ant genera of the world* (p. 222). Harvard University Press.

Bolton, B. (2000). The ant tribe Dacetini. *Memoirs of the American Entomological Institute*, *65*, 1–1028.

Bolton, B. (2003). Synopsis and classification of Formicidae. *Memoirs of the American Entomological Institute*, *71*, 1–370.

Bolton, B. (2007). How to conduct large-scale taxonomic revisions in Formicidae. pp. 52–71. In R. R. Snelling, B. L. Fisher, & P. S. Ward (Eds.), *Advances in ant systematics (Hymenoptera: Formicidae): Homage to E.O. Wilson – 50 years of contributions* (Vol. 80, p. 690). *Memoirs of the American Entomological Institute*.

Bolton, B. (2021). An online catalog of the ants of the world. Available from https://www.antcat.org.

Booher, D. B., Gibson, J. C., Liu, C., Longino, J. T., Fisher, B. L., Janda, M., Narula, N., Toulkeridou, E., Mikheyev, A. S., Suarez, A. V., & Economo, E. P. (2021). Functional innovation promotes diversification of form in the evolution of an ultrafast trap-jaw mechanism in ants.

PLoS Biology, *19*, e3001031. https://doi.org/10.1371/journal.pbio.3001031

Boomsma, J. J., Baer, B., & Heinze, J. (2005). The evolution of male traits in social insects. *Annual Review of Entomology*, *50*, 395–420.

Boomsma, J. J., & Gawne, R. (2018). Superorganismality and caste differentiation as points of no return: How the major evolutionary transitions were lost in translation. *Biological Reviews*, *93*, 28–54. https://doi.org/10.1111/brv.12330

Borgmeier, T. (1955). Die Wanderameisen der neotropischen Region. *Studia Entomologica*, *3*, 1–720.

Borowiec, M. L. (2016). Generic revision of the ant subfamily Dorylinae (Hymenoptera, Formicidae). *ZooKeys*, *2016*, 1–280. https://doi.org/10.3897/zookeys.608.9427

Borowiec, M. L. (2019). Convergent evolution of the army ant syndrome and congruence in big-data phylogenetics. *Systematic Biology*, *68*, 642–656. https://doi.org/10.1093/sysbio/syy088

Borowiec, M. L., & Longino, J. T. (2011). Three new species and reassessment of the rare Neotropical ant genus *Leptanilloides* (Hymenoptera, Formicidae, Leptanilloidinae). *ZooKeys*, *133*, 19–48. https://doi.org/10.3897/zookeys.133.1479

Borowiec, M. L., Rabeling, C., Brady, S. G., Fisher, B. L., Schultz, T. R., & Ward, P. S. (2019). Compositional heterogeneity and outgroup choice influence the internal phylogeny of the ants. *Molecular Phylogenetics and Evolution*, *134*, 111–121. https://doi.org/10.1016/j.ympev.2019.01.024

Boudinot, B. E. (2013). The male genitalia of ants: Musculature, homology, and functional morphology (Hymenoptera, Aculeata, Formicidae). *Journal of Hymenoptera Research*, *30*, 29–49. https://doi.org/10.3897/JHR.30.3535

Boudinot, B. E. (2015). Contributions to the knowledge of Formicidae (Hymenoptera, Aculeata): A new diagnosis of the family, the first global male-based key to subfamilies, and a treatment of early branching lineages. *European Journal of Taxonomy*, *120*, 1–62.

Boudinot, B. E. (2018). A general theory of genital homologies for the Hexapoda (Pancrustacea) derived from skeletomuscular correspondences, with emphasis on the Endopterygota. *Arthropod Structure & Development*, *47*, 563–613. https://doi.org/10.1016/j.asd.2018.11.001

Boudinot, B.E. (2020). *Systematic and Evolutionary Morphology*: *Case Studies on Formicidae*, *Mesozoic Aculeata*, *and Hexapodan Genitalia*. (Dissertation) University of California, Davis, ix + 562 pp.

Boudinot, B. E., Perrichot, V., & Chaul, J. C. M. (2020). *Camelosphecia* gen. nov., lost ant-wasp intermediates from the mid-cretaceous (Hymenoptera, Formicidae). *ZooKeys*, *1005*, 21–55.

Brady, S. G., Schultz, T. R., Fisher, B. L., & Ward, P. S. (2006). Evaluating alternative hypotheses for the early evolution and diversification of ants. *Proceedings of the National Academy of Sciences of the United States of America*, *103*, 18172–18177. https://doi.org/10.1073/pnas.0605858103

Branstetter, M. G., Danforth, B. N., Pitts, J. P., Faircloth, B. C., Ward, P. S., Buffington, M. L., Gates, M. W., Kula, R. R., & Brady, S. G. (2017). Phylogenomic insights into the evolution of stinging wasps and the origins of ants and bees. *Current Biology*, *27*, 1019–1025. https://doi.org/10.1016/j.cub.2017.03.027

Branstetter, M. G., Longino, J. T., Ward, P. S., & Faircloth, B. C. (2017). Enriching the ant tree of life: Enhanced UCE bait set for genome-scale phylogenetics of ants and other Hymenoptera. *Methods in Ecology and Evolution*, *8*, 768–776. https://doi.org/10.1111/20141-210X.12742

Bruch, C. (1934). Las formas femeninas de *Eciton*. Descripción y redescripción de algunas especies de la Argentina. *Anales de la Sociedad Cientifica Argentina*, *118*, 113–135.

Chapman, R. F. (2012). In S. J. Simpson & A. E. Douglas (Eds.), *The insects: Structure and function* (5th ed., pp. 929–xxxi). Cambridge University Press.

Cohic, F. (1948). Observations morphologiques et écologiques sur *Dorylus* (*Anomma*) *nigricans* Illiger (Hymenoptera: Dorylidae). *Revue Française d'Entomologie*, *14*, 229–276.

Cornette, R., Gotoh, H., Koshikawa, S., & Miura, T. (2008). Juvenile hormone titers and caste differentiation in the damp-wood termite *Hodotermopsis sjostedti* (Isoptera, Termopsidae). *Journal of Insect Physiology*, *54*, 922–930. https://doi.org/10.1016/j.insphys.2008.04.017

Corson, F., Couturier, L., Rouault, H., Mazouni, K., & Schweisguth, F. (2017). Self-organized notch dynamics generate stereotyped sensory organ patterns in *Drosophila*. *Science*, *356*, eaai7407. https://doi.org/10.1126/science.aai7407

Costa, M., Reeve, S., Grumbling, G., & Osumi-Sutherland, D. (2013). The *Drosophila* anatomy ontology. *Journal of Biomedical Semantics*, *4*, 32. https://doi.org/10.1186/2041-1480-4-32

Coyne, J. A., Kay, E. H., & Pruett-Jones, S. (2007). The genetic basis of sexual dimorphism in birds. *Evolution*, *62*, 214–219. https://doi.org/10.1111/j.1558-5646.2007.00254.x

De Andrade, M. L., & Baroni Urbani, C. (1999). Diversity and adaptation in the ant genus *Cephalotes*, past and present. *Stuttgarter Beiträge zur Naturkunde, Serie B (Geologie und Paläontologie)*, *271*, 1–889.

Divieso, R., Silva, T. S. R., & Pie, M. R. (2020). Morphological evolution in the ant reproductive caste. *Biological Journal of the Linnean Society*, *131*, 465–475. https://doi.org/10.1093/biolinnean/blaa138

Dumpert, K. (1972). Bau und Verteilung der Sensillen auf der Antennengeißel von *Lasius fuliginosus* (Latr.) (Hymenoptera: Formicidae). *Zeitschrift für Morphologie der Tiere*, *73*, 95–116.

Eguchi, K., Bui, V. T., Oguri, E., Maruyama, M., & Yamane, S. (2014). A new data of worker polymorphism in the ant genus *Dorylus* (hymenoptera: Formicidae: Dorylinae). *Journal of Asia-Pacific Entomology*, *17*, 31–36. https://doi.org/10.1016/j.aspen.2013.09.004

Eguchi, K., Mizuno, R., Ito, F., Satria, R., Van An, D., Tuan Viet, B., & Luong, P. T. H. (2016). First disco of subdichthadiigyne in *Yunodorylus* Xu, 2000 (Formicidae: Dorylinae). *Revue Suisse de Zoologie*, *123*, 307–314. https://doi.org/10.5281/zenodo.155307

Emlen, D. J., Hunt, J., & Simmons, L. W. (2005). Evolution of sexual dimorphism and male dimorphism in the expression of beetle horns: Phylogenetic evidence for modularity, evolutionary lability, and constraint. *American Naturalist*, *166*, S42–S68.

Fabricius, J.C. (1793). Entomologia systematica emendate et aucta. Secundum classes, ordines, genera, species, adjectis synonimis, locis observationibus, descriptionibus. Tome 2 *Hafniae [= Copenhagen]*, *C. G. Proft*, 519 *pp*.

Forel, A. (1885 1884). Études myrmécologiques en 1884 avec une description des organes sensoriels des antennes. *Bulletin de la Societe Vaudoise des Sciences Naturelles*, *20*, 316–380.

Fortelius, W., Pamilo, P., Rosengren, R., & Sundström, L. (1987). Male size dimorphism and alternative reproductive tactics in *Formica exsecta* ants (hymenoptera: Formicidae). *Annales Zoologici Fennici*, *24*, 45–54.

Gerstäcker, A. (1859). Untitled. Introduced by: "Hr. Peters berichtete über sein Reisewerk, von dem die Insekten bis zum 64., die Botanik bis zum 34. Bogen gedruckt sind und theillte den Schluss der Diagnosen der von Hrn. Dr. Gerstäcker bearbeiteten Hymenopteren mit.". *Monatsberichte der Königlichen Preussischen Akademie der Wissenschaften zu Berlin*, *1858*, 261–264.

Ghaninia, M., Berger, S. L., Reinberg, D., Zwiebel, L. J., Ray, A., & Liebig, J. (2018). Antennal olfactory physiology and behavior of males of the ponerine ant *Harpegnathos saltator*. *Journal of Chemical Ecology*, *44*, 999–1007. https://doi.org/10.1007/s10886-018-1013-6

Gotoh, H., Cornette, R., Koshikawa, S., Okada, Y., Lavine, L. C., Emlen, D. J., & Miura, T. (2011). Juvenile hormone regulates extreme mandible growth in male stag beetles. *PLoS One*, *6*, e21139. https://doi.org/10.1371/journal.pone.0021139

Gotoh, H., Miyakawa, H., Ishikawa, A., Ishikawa, Y., Sugime, Y., Emlen, D. J., Lavine, L. C., & Miura, T. (2014). Developmental link between sex and nutrition; *doublesex* regulates sex-specific mandible growth via juvenile hormone signaling in stag beetles. *PLoS Genetics*, *10*, e1004098. https://doi.org/10.1371/journal.pgen.1004098

Gotoh, H., Zinna, R. A., Ishikawa, Y., Miyakawa, H., Ishikawa, A., Sugime, Y., Emlen, D. J., Lavine, J. C., & Miura, T. (2017). The function of appendage patterning genes in mandible development of the sexually dimorphic stag beetle. *Developmental Biology*, *422*, 24–32. https://doi.org/10.1016/j.ydbio.2016.12.011

Gotwald, W. H., Jr. (1982). Army ants. Pp. 157–254. In H. R. Hermann (Ed.), *Social insects* (Vol. 4, p. 385). Academic Press.

Gotwald, W. H., Jr., & Kupiec, B. M. (1975). Taxonomic implications of doryline worker ant morphology: *Cheliomyrmex morosus* (Hymenoptera: Formicidae). *Annals of the Entomological Society of America*, *68*, 961–971.

Gotwald, W. H., Jr., & Schaefer, R. F., Jr. (1982). Taxonomic implications of doryline worker ant morphology: *Dorylus* subgenus *Anomma* (Hymenoptera: Formicidae). *Sociobiology*, *7*, 187–204.

Gould, S. J. (1993). Male nipples and clitoral ripples. *Columbia: A Journal of Literature and Art*, *20*, 80–96.

Gould, S. J., & Lewontin, R. (1979). The spandrels of san Marco and the Panglossian paradigm: A critique of the adaptationist programme. *Proceedings of the Royal Society of London B*, *205*, 581–598. https://doi.org/10.1098/rspb.1979.0086

Gronenberg, W. (2008). Structure and function of ant (Hymenoptera: Formicidae) brains: Strength in numbers. *Myrmecological News*, *11*, 25–36.

Gronenberg, W., Brandão, C. R. F., Dietz, B. H., & Just, S. (1998). Trap-jaws revisited: The mandible mechanism of the ant *Acanthognathus*. *Physiological Entomology*, *23*, 227–240. https://doi.org/10.1046/j.1365-3032.1998.233081.x

Gronenberg, W., & Hölldobler, B. (1999). Morphologic representation of visual and antennal information in the ant brain. *Journal of Comparative Neurology*, *412*, 229–240.

Gronenberg, W., Paul, J., Just, S., & Hölldobler, B. (1997). Mandible muscle fibers in ants: Fast or powerful? *Cell and Tissue Research*, *289*, 347–361.

Guénard, B., Weiser, M., Gomez, K., Narula, N., & Economo, E. P. (2017). The global ant biodiversity informatics (GABI) database: A synthesis of ant species geographic distributions. *Myrmecological News*, *24*, 83–89.

Harris, R. A. (1979). *A glossary of surface sculpturing* (Vol. 28, pp. 1–31). California Department of Food & Agriculture, Bureau of Entomology.

Hashimoto, Y. (1990). Unique features of sensilla on the antennae of Formicidae (Hymenoptera). *Applied Entomology and Zoology*, *25*, 491–501.

Hashimoto, Y. (1991). Phylogenetic study of the family Formicidae based on the sensillum structures on the antennae and labial palpi (Hymenoptera, Aculeata). *Japanese Journal of Entomology*, *59*, 125–140.

Heimpel, G. E., & de Boer, J. G. (2008). Sex determination in the Hymenoptera. *Annual Review of Entomology*, *53*, 209–230. https://doi.org/10.1146/annurev.ento.53.103106.093441

Helms Cahan, S., & Keller, L. (2003). Complex hybrid origin of genetic caste determination in harvester ants. *Nature*, *424*, 306–309. https://doi.org/10.1038/nature01744

Höhna, S., Stadler, T., Ronquist, F., & Britton, T. (2011). Inferring speciation and extinction rates under different sampling schemes. *Molecular Biology and Evolution*, *28*, 2577–2589. https://doi.org/10.1093/molbev/msr095

Hollingsworth, M. J. (1960). Studies on the polymorphic workers of the army ant *Dorylus* (*Anomma*) *nigricans* Illiger. *Insectes Sociaux*, *6*, 2–37.

Jaitrong, W., & Ruangsittichai, J. (2018). Two new species of the *Aenictus wroughtonii* species group (Hymenoptera, Formicidae, Dorylinae) from Thailand. *ZooKeys*, *775*, 103–115. https://doi.org/10.3897/zookeys.775.26893

Jaitrong, W., & Yamane, S. (2013). The *Aenictus ceylonicus* species group (Hymenoptera: Formicidae, Aenictinae) from Southeast Asia. *Journal of Hymenoptera Research*, *31*, 165–233.

Janicki, J., Narula, N., Ziegler, M., Guénard, B., & Economo, E. P. (2016). Visualizing and interacting with large-volume biodiversity data using client-server web-mapping applications: The design and implementation of antmaps.org. *Ecological Informatics*, *32*, 185–193.

Johnson, B. R., Borowiec, M. L., Chiu, J. C., Lee, E. K., Atallah, J., & Ward, P. S. (2013). Phylogenomics resolves evolutionary relationships among ants, bees, and wasps. *Current Biology*, *23*, 2058–2062. https://doi.org/10.1016/j.cub.2013.08.050

Kajimoto, T., Moczek, A. P., & Andrews, J. (2012). Diversification of *doublesex* function underlies morph-, sex-, and species-specific development of beetle horns. *Proceedings of the National Academy of Sciences of the United States of America*, *109*, 20526–20531. https://doi.org/10.1073/pnas.1118589109

Keller, R. A. (2011). A phylogenetic analysis of ant morphology (Hymenoptera: Formicidae) with special reference to the poneromorph subfamilies. *Bulletin of the American Museum of Natural History*, *355*, 1–90. https://doi.org/10.1206/355.1

Keller, R. A., Peeters, C., & Beldade, P. (2014). Evolution of thorax architecture in ant castes highlights trade-off between flight and ground behaviors. *eLife*, *3*, e01539. https://doi.org/10.7554/eLife.01539

Klein, A., Schultner, E., Lowak, H., Schrader, L., Heinze, J., Holman, L., & Oettler, J. (2016). Evolution of social insect polyphenism facilitated by the sex differentiation cascade. *PLoS Genetics*, *12*, e1005952. https://doi.org/10.1371/journal.pgen.1005952

Kleineidam, C., Romani, R., Tautz, J., & Isidoro, N. (2000). Ultrastructure and physiology of the CO_2 sensitive sensillum ampullaceum in the leaf-cutting ant *Atta sexdens*. *Arthropod Structure & Development*, *29*, 43–55.

Kleineidam, C., & Tautz, J. (1996). Perception of carbon dioxide and other "air-condition" parameters in the leaf cutting ant *Atta cephalotes*. *Naturwissenschaften*, *83*, 566–568.

Koch, S., Tahara, R., Vasquez-Correa, A. & Abouheif, E. (2021). Nano-CT characterization reveals coordinated growth of a rudimentary organ necessary for soldier development in the ant *Pheidole hyatti*. *BioRxiv*, doi: https://doi.org/10.1101/2021.03.05.434146.

Kraepelin, K. (1883). Ueber die Geruchsorgane der Gliederthiere. Eine historisch-kritische Studie. Hamburg: Th. G. Meißner, 1–48.

Kronauer, D. J. C. (2009). Recent advances in army ant biology (Hymenoptera: Formicidae). *Myrmecological News*, *12*, 51–65.

Kronauer, D. J. C. (2020). *Army ants: Nature's ultimate social hunters* (p. 384). Harvard University Press.

Kronauer, D. J. C., Schöning, C., Vilhelmsen, L. B., & Boomsma, J. J. (2007). A molecular phylogeny of *Dorylus* army ants provides evidence for multiple evolutionary transitions in foraging niche. *BMC Evolutionary Biology*, *7*, 56. https://doi.org/10.1186/1471-2148-7-56

Kubota, H., Yoshimura, J., Niitsu, S., & Shimizu, A. (2019). Morphology of the tentorium in the ant genus *Lasius* Fabricius (Hymenoptera: Formicidae). *Scientific Reports*, *9*, 6722. https://doi.org/10.1038/s41598-019-43175-w

Laciny, A. (2021). Among the shapeshifters: Parasite-induced morphologies in ants (Hymenoptera, Formicidae) and their relevance within the EcoEvoDevo framework. *EvoDevo*, *12*, 2. https://doi.org/10.1186/s13227-021-00173-2

Leydig, F. (1850). Zum feinen Aufbau der Arthropoden. [Müller's] Archiv für Anatomie. *Physiologie und wissenschaftliche Medizin, Berlin*, *1855*, 376–480.

Lillico-Ouachour, A., & Abouheif, E. (2017). Regulation, development, and evolution of caste ratios in the hyperdiverse ant genus *Pheidole*. *Current Opinion in Insect Science*, *19*, 43–51. https://doi.org/10.1016/j.cois.2016.11.003

Linnaeus, C. (1761). Fauna suecica sistens animalia Sueciae regni: Mammalia, Aves, Amphibia, Pisces, Insecta, Vermes. Editio altera, auctior. Stockholmiae: L. Salvii, 48–587 pp.

Linnaeus, C. (1764). Museum S;ae R:ae M:tis Ludovicae Ulricae Reginae Svecorum, Gothorum, Vandalorumque, &c. In quo animalia rariora, exotica, imprimis. Insecta & Conchilia describuntur & determinatur. Prodromi instar. Holmiae [= Stockholm]: Salvius, 8 + 720 pp.

Longino, J. T. (2003). The *Crematogaster* (Hymenoptera, Formicidae, Myrmicinae) of Costa Rica. *Zootaxa*, *151*, 1–150.

Longino, J. T., & Boudinot, B. E. (2013). New species of central American *Rhopalothrix* Mayr, 1870 (Hymenoptera, Formicidae). *Zootaxa*, *3616*, 301–324. https://doi.org/10.11646/Zootaxa.3616.4.1

Lösel, P. D., van de Kamp, T., Jayme, A., Ershov, A., Faragó, T., Pichler, O., Jerome, N. T., Aadepu, N., Bremer, S., Chilingaryan, S. A., Heethoff, M., Kopmann, A., Odar, J., Schmelzle, S., Zuber, M., Wittbrot, J., Baumbach, T., & Heuveline, V. (2020). Introducing Biomedisa as an open-source online platform for biomedical image segmentation. *Nature Communications*, *11*, 5577. https://doi.org/10.1038/s41467-020-19303-w

Lösel, P. & Heuveline, V. (2016). Enhancing a diffusion algorithm for 4D image segmentation using local information. In Medical imaging 2016: Image processing (International Society for Optics and Photonics), 9784, 97842L.

Lubbock, J. (1877). On some points in the anatomy of ants. *Monthly Microscopical Journal*, *18*, 121–142.

McKenna, K. Z., Wagner, G. P., & Cooper, K. L. (2021). A developmental perspective of homology and evolutionary novelty. *Current Topics in Developmental Biology*, *141*, 1–38. https://doi.org/10.1016/bs.ctdb.2020.12.001

Miyazaki, S., Okada, Y., Miyakawa, H., Tokuda, G., Cornette, R., Koshikawa, S., Maekawa, K., & Miura, T. (2014). Sexually dimorphic body color is regulated by sex-specific expression of *yellow* gene in ponerine ant, *Diacamma* sp. *PLoS One*, *9*, e92875. https://doi.org/10.1371/journal.pone.0092875

Molet, M., Maicher, V., & Peeters, C. (2014). Bigger helpers in the ant *Cataglyphis bombycina*: Increased worker polymorphism or novel soldier caste? *PLoS One*, *9*, e84929. https://doi.org/10.1371/journal.pone.0084929

Moreau, C. S., Bell, C. D., Vila, R., Archibald, S. B., & Pierce, N. E. (2006). Phylogeny of the ants: diversification in the age of angiosperms. *Science*, *312*(5770), 101–104.

Nakanishi, A., Nishino, H., Watanabe, H., Yokohari, F., & Nishikawa, M. (2009). Sex-specific antennal sensory system in the ant *Camponotus japonicus*: Structure and distribution of sensilla on the flagellum. *Cell and Tissue Research*, *338*, 79–97. https://doi.org/10.1007/s00441-009-0863-1

Narendra, A., Reid, S. F., Greiner, B., Peters, R. A., Hemmi, J. M., Ribi, W. A., & Zeil, J. (2011). Caste-specific visual adaptations to distinct daily activity schedules in Australian *Myrmecia* ants. *Proceedings of the Royal Society B*, *278*, 1141–1149. https://doi.org/10.1098/rspb.2010.1378

Nijhout, H. F., & Emlen, D. J. (1998). Competition among body parts in the development and evolution of insect morphology. *Proceedings of the National Academy of Sciences of the United States of America*, *95*, 3685–3689.

Nipitwattanaphon, M., Wang, J., Ross, K. G., Riba-Grognuz, O., Wurm, Y., Khurewathanaku, C., & Keller, L. (2014). Effects of ploidy and sex-locus genotype on gene expression patterns in the fire ant *Solenopsis invicta*. *Proceedings of the Royal Society B*, *281*, 2014177. https://doi.org/10.1098/rspb.2014.1776

Nylander, W. (1846). Adnotationes in monographiam formicarum borealium Europae. *Acta Societatis Scientiarum Fennicae*, *2*, 875–944.

Oettler, J., Platschek, T., Schmidt, C., Rajakumar, R., Favé, M.-J., Khila, A., Heinze, J., & Abouheif, E. (2018). Interruption points in the wing gene regulatory network underlying wing polyphenism evolved independently in male and female morphs in *Cardiocondyla* ants. *Journal of Experimental Zoology Part B: Molecular & Developmental Evolution*, *332*, 7–16. https://doi.org/10.1002/jez.b.22834

Okada, Y., Tsuji, K., & Miura, T. (2006). Morphological differences between sexes in the ponerine ant *Diacamma* sp. (Formicidae: Ponerinae). *Sociobiology*, *48*, 527–541.

Oliver, J. C., & Monteiro, A. (2011). On the origins of sexual dimorphism in butterflies. *Proceedings of the Royal Society B*, *278*, 1981–1988. https://doi.org/10.1098/rspb.2010.2220

Ortius-Lechner, D., Rüger, M., & Wanke, T. (2003). Sexing at the larval stage in two ant species of the Formicoxenini. *Zoomorphology*, *122*, 41–45. https://doi.org/10.1007/s00435-002-0067-7

Owens, I. P. F., & Hartley, I. R. (1998). Sexual dimorphism in birds: Why are there so many different forms of dimorphism? *Proceedings of the Royal Society B*, *265*, 397–407.

Passera, L., & Suzzoni, J. P. (1979). La role de la reine de *Pheidole pallidula* (Nyl.) (Hym., Form.) dans la sexualization du couvain après traitement par l'hormone juvenile. *Insectes Sociaux*, *26*, 343–353.

Patrella, V., Aceto, S., Colonna, V., Saccone, G., Sanges, R., Polanska, N., Volf, P., Gradoni, L., Bongiorno, G., & Salvemini, M. (2019). Identification of sex determination genes and their evolution in Phlebotominae sand flies (Diptera, Nematocera). *BMC Genomics*, *20*, 522. https://doi.org/10.1186/s12864-019-5898-4

Paul, J., & Roces, F. (2019). Comparative functional morphology of ant mouthparts and significance for liquid food intake. In H. W. Krenn (Ed.), *Insect mouthparts. Zoological monographs 5* (pp. 335–359). Springer.

Peeters, C., Keller, R. A., Khalife, A., Fischer, G., Katzke, J., Blanke, A., & Economo, E. P. (2020). The loss of flight in ant workers enabled an evolutionary redesign of the thorax for ground labor. *Frontiers in Zoology*, *17*, 33. https://doi.org/10.1186/s12983-020-00375-9

Penick, C. A., Ebie, J., & Moore, D. (2014). A non-destructive method for identifying the sex of ant larvae. *Insectes Sociaux*, *61*, 51–55. https://doi.org/10.1007/s00040-013-0323-5

Perfilieva, K. S. (2010). Trends in evolution of ant wing venation (Hymenoptera: Formicidae). *Entomological Review*, *90*, 965–977.

Perrichot, V., Wang, B., & Barden, P. (2020). New remarkable hell ants (Formicidae: Haidomyrmecinae stat. nov.) from mid-cretaceous amber of northern Myanmar. *Cretaceous Research*, *109*, 104381. https://doi.org/10.1016/j.cretres.2020.104381

Peters, R. S., Krogmann, L., Mayer, C., Donath, A., Gunkel, S., Meusemann, K., Kozlov, A., Podsiadlowski, L., Petersen, M., Lanfear, R., Diez, P. A., Heraty, J., Kjer, K., Klopfstein, S., Meier, R., Polidori, C., Schmitt, T., Liu, S., Zhou, X., … Niehuis, O. (2017). Evolutionary history of the Hymenoptera. *Current Biology*, *27*, 1013–1018. https://doi.org/10.1016/j.cub.2017.01.027

Pohl, H. (2010). A scanning electron microscopy specimen holder for viewing different angles of a single specimen. *Microscopy Research & Technique*, *73*, 1073–1076.

Pontieri, L., Rajakumar, A., Rafiqi, A.M., Larsen, R.S., Abouheif, E. & Zhang, G. (2020). From egg to adult: A developmental table of the ant *Monomorium pharaonis*. *bioRxiv*. Doi: https://doi.org/10.1101/2020.12.22.423970.

Powell, S., & Franks, N. R. (2006). Ecology and the evolution of worker morphological diversity: A comparative analysis with *Eciton* army ants. *Functional Ecology*, *20*, 1105–1114.

Prpic, N.-M. (2019). Homology of endites and palps in insect mouthparts: Recent advances based on gene expression studies. In A. Fusco (Ed.), *Perspectives on evolutionary and developmental biology. Essays for Alessandro Minelli* (pp. vi–388). Padova University Press.

Rajakumar, R., Koch, S., Couture, M., Favé, M.-J., Lillico-Ouachour, A., Chen, T., de Blassis, G., Rajakumar, A., Oullette, D., & Abouheif, E. (2018). Signal regulation of a rudimentary organ generates complex worker-caste systems in ants. *Nature*, *562*, 574–577.

Ramirez-Esquivel, F., Zeil, J., & Narendra, A. (2014). The antennal sensory array of the nocturnal bull ant *Myrmecia pyriformis*. *Arthropod Structure & Development*, *43*, 543–558. https://doi.org/10.1016/j.asd.2014.07.004

Réaumur, R. A. F. de (1926). The natural history of ants: from an unpublished manuscript in the archives of the Academy of Sciences of Paris, translated and annotated by William Morton Wheeler. Alfred A. Knopf, New York.

Reichensperger, A. (1924). Das Weibchen von *Eciton quadriglume* Hal. Einige neue ecitophile Histeriden und allgemeine Bemerkungen. *Zoologischer Anzeiger*, *60*, 201–213.

Remane, A. (1956). *Die Grundlagen des Natürlichen Systems, der Vergleichenden Anatomie, und der Phylogenetik: Theoretische Morphologie und Systematik I* (p. 364). Akademische Verlagsgesellschaft.

Renthal, R., Velasquez, D., Olmos, D., Hampton, J., & Wergin, W. P. (2003). Structure and distribution of antennal sensilla of the red imported fire ant. *Micron*, *34*, 405–413. https://doi.org/10.1016/S0968-4328(03)00050-7

Richter, A., Hita Garcia, F., Keller, R. A., Billen, J., Economo, E. P., & Beutel, R. G. (2020). Comparative analysis of worker head anatomy of *Formica* and *Brachyponera* (Hymenoptera: Formicidae). *Arthropod Systematics & Phylogeny*, *78*, 133–170. https://doi.org/10.26049/ASP78-1-2020-06

Richter, A., Keller, R. A., Hita Garcia, F., Billen, J., Katzke, J., Boudinot, B. E., Economo, E. P., & Beutel, R. G. (2021). Head anatomy of *Protanilla lini* (Leptanillinae, Formicidae, Hymenoptera) and a hypothesis of their mandibular movement. *Myrmecological News*, *31*, 107–136. https://doi.org/10.25849/myrmecol.news_031:107

Richter, A., Keller, R. A., Rosumek, F. B., Economo, E. P., Hita Garcia, F., & Beutel, R. G. (2019). The cephalic anatomy of workers of the ant species *Wasmannia affinis* (Formicidae, Hymenoptera, Insecta) and its evolutionary implications. *Arthropod Structure & Development*, *49*, 26–49. https://doi.org/10.1016/j.asd.2019.02.002

Roger, J. (1859). Beiträge zur Kenntniss der Ameisenfauna der Mittelmeerländer. I. *Berliner Entomologische Zeitschrift*, *3*, 225–259.

Romani, R., Isidoro, N., & Bin, F. (2010). Antennal structures used in communication by egg parasitoids. In F. Consoli, J. Parra, & R. Zucchi (Eds.), *Egg parasitoids in Agroecosystems with emphasis on Trichogramma* (Vol. 9, pp. 57–96). Springer. Progress in Biological Control. https://doi.org/10.1007/978-1-4020-9110-0_3

Ruchty, M., Romani, R., Kuebler, L. S., Ruschioni, S., Roces, F., Isidoro, N., & Kleineidam, C. J. (2008). The thermo-sensitive sensilla coeloconica of leaf-cutting ants (*Atta vollenweideri*). *Arthropod Structure & Development*, *38*, 195–205. https://doi.org/10.1016/j.asd.2008.11.001

Sánchez, L. (2008). Sex-determining mechanisms in insects. *International Journal of Developmental Biology*, *52*, 837–586. https://doi.org/10.1387/ijdb.072396ls

Sanger, T. J., & Rajakumar, R. (2019). How a growing organismal perspective is adding new depth to integrative studies of morphological evolution. *Biological Reviews*, *94*, 184–198. https://doi.org/10.1111/brv.12442

Santschi, F. (1917). Note sur *Dorylus affinis* Shuckard mâle et ses variétés. *Bulletin de la Société d'Histoire Naturelle de l'Afrique du Nord*, *8*, 18–21.

Santschi, F. (1939). Contribution au sous-genre *Alaopone* Emery. *Revue Suisse de Zoologie*, *46*, 143–154.

Satria, R., Itioka, T., Meleng, P., & Eguchi, K. (2018). Second disco of the subdichthadiigyne in *Yunodorylus* (Borowiec, 2009) (Formicidae: Dorylinae). *Revue Suisse de Zoologie*, *125*, 73–78. https://doi.org/10.5281/zenodo.1196017

Savage, T. S. (1849). The driver ants of western Africa. *Proceedings of the Academy of Natural Sciences of Philadelphia*, *4*, 195–200.

Schneider, D. (1964). Insect antennae. *Annual Review of Entomology*, *9*, 103–122.

Schneirla, T. C. (1971). In H. R. Topoff (Ed.), *Army ants. A study in social organization* (pp. xx–349). W. H. Freeman & Co.

Schöning, C., Gotwald, W. J., Jr., Kronauer, D. J. C., & Vilhelmsen, L. (2008). Taxonomy of the African army ant *Dorylus gribodoi* Emery, 1892 (Hymenoptera, Formicidae) — New insights from DNA sequence data and morphology. *Zootaxa*, *1749*, 39–52.

Shik, J., Donoso, D., & Kaspari, M. (2013). The life history continuum hypothesis links traits of male ants with life outside the nest. *Entomologia Experimentalis et Applicata*, *149*, 99–109. https://doi.org/10.1111/eea.12117

Shik, J. Z., Flatt, D., Kay, A., & Kaspari, M. (2012). A life history continuum in the males of a Neotropical ant assemblage: Refuting the sperm vessel hypothesis. *Naturwissenschaften*, *99*, 191–197. https://doi.org/10.1007/s00114-012-0884-6

Shuckard, W. E. (1840). Monograph of the Dorylidae, a family of the Hymenoptera Heterogyna. *Annals of Natural History*, *5*, 188–201.

Simpson, S. J., Sword, G. A., & Lo, N. (2011). Polyphenism in insects. *Current Biology*, *21*, R738–R749. https://doi.org/10.1016/j.cub.2011.06.006

Snelling, G. C., & Snelling, R. R. (2007). New synonymy, new species, new keys to *Neivamyrmex* army ants of the United States. In R. R. Snelling, B. L. Fisher, & P. S. Ward (Eds.), *Advances in ant systematics (Hymenoptera: Formicidae): Homage to E. O. Wilson – 50 years of contributions* (pp. 459, 80–550). Memoirs of the American Entomological Institute.

Snodgrass, R. E. (1935). *The principles of insect morphology* (p. 667). McGraw-Hill Book Company.

Snodgrass, R. E. (1954). Insect metamorphosis. *Smithsonian Miscellaneous Collections*, *122*, 1–122.

Snodgrass, R. E. (1958). Evolution of arthropod mechanisms. *Smithsonian Miscellaneous Collections*, *138*, 1–77.

Sokolowski, A., & Wisniewski, J. (1975). Teratologische Untersuchungen an Ameisen-Arbeiterinnen aus der *Formica rufa*-Gruppe (Hymenoptera: Formicidae). *Insectes Sociaux*, *22*, 117–134.

Stearns, S. C. (1989). The evolutionary significance of phenotypic plasticity. *Bioscience*, *39*, 436–445.

Steinbrecht, R. A. (1989). The fine structure of thermo−/hygrosensitive sensilla in the silkmoth *Bombyx mori*: Receptor membrane substructure and sensory cell contacts. *Cell and Tissue Research*, *225*, 49–57.

Strenger, P. P., & Menzel, F. (2020). Cuticular hydrocarbons in ants (hymenoptera: Formicidae) and other insects: How and why they differ among individuals, colonies, and species. *Myrmecological News*, *30*, 1–26. https://doi.org/10.25849/myrmecol.news_030:001

Stubblefield, J. W., & Seger, J. (1994). Sexual dimorphism in Hymenoptera. In R. V. Short & E. Balaban (Eds.), *The differences between the sexes* (pp. 71–103). Cambridge University Press.

Tafuri, J. F. (1957, 1955). Growth and polymorphism in the larva of the army ant (*Eciton* [*E.*] *hamatum* Fabricius). *Journal of the New York Entomological Society*, *63*, 21–41.

Topoff, H. (1971). Polymorphism in army ants related to division of labor and colony cyclic behavior. *American Naturalist*, *105*, 529–548.

Verhulst, E. C., van de Zande, L., & Beukeboom, L. W. (2010). Insect sex determination: It all evolves around *transformer*. *Current Opinion in Genetics & Development*, *20*, 376–383. https://doi.org/10.1016/j.gde.2010.05.001

Vilhelmsen, L. (1996). The preoral cavity of lower Hymenoptera (Insecta): Comparative morphology and phylogenetic significance. *Zoologica Scripta*, *25*, 143–170.

Wagner, G. (2007). The road to modularity. *Nature Reviews Genetics*, *8*, 921–931. https://doi.org/10.1038/nrg2267

Wagner, G. (2014). *Homology, genes, and evolutionary innovation* (p. 478). Princeton University Press.

Walther, J. R. (1985). The antennal pattern of sensilla of the ants (Formicoidea, hymenoptera). *Mitteilungen der Deutschen Gesellschaft für Allgemeine und Angewandte Entomologie*, *4*, 173–176.

Weber, N. A. (1941). The redisco of the queen of *Eciton* (*Labidus*) *coecum* Latr. (Hym.: Formicidae). *American Midland Naturalist*, *26*, 325–329.

Westwood, J. O. (1835). Untitled. Introduced by: "Specimens were exhibited, partly from the collection of the Rev. F. W. Hope, and partly from that of Mr. Westwood, of various Hymenopterous insects, which Mr. Westwood regarded as new to science.". *Proceedings of the Zoological Society of London*, *3*, 68–72.

Wheeler, D. E. (1986). Developmental and physiological determinants of caste in social Hymenoptera: Evolutionary implications. *The American Naturalist*, *128*, 13–34.

Wheeler, D. E. (1991). The developmental basis of worker caste polymorphism in ants. *The American Naturalist*, *138*, 1218–1238.
Wheeler, D. E., & Nijhout, H. F. (1983). Soldier determination in the ant *Pheidole bicarinate*: Hormonal control of caste and size within castes. *Journal of Insect Physiology*, *29*, 847–854.
Wheeler, G. C. (1943). The larvae of the army ants. *Annals of the Entomological Society*, *36*, 319–332.
Wheeler, G. C., & Wheeler, J. (1964). The ant larvae of the subfamily Dorylinae: Supplement. *Proceedings of the Entomological Society of Washington*, *66*, 129–137.
Wheeler, G. C., & Wheeler, J. (1974). Ant larvae of the subfamily Dorylinae: Second supplement (Hymenoptera: Formicidae). *Journal of the Kansas Entomological Society*, *47*, 166–172.
Wheeler, G. C., & Wheeler, J. (1976). Ant larvae: Review and synthesis. *Memoirs of the Entomological Society of Washington*, *7*, 1–108.
Wheeler, G. C., & Wheeler, J. (1984). The larvae of army ants (Hymenoptera: Formicidae): A revision. *Journal of the Kansas Entomological Society*, *57*, 263–275.
Wheeler, W. M. (1903). Extraordinary females in three species of *Formica*, with remarks on mutation in the Formicidae. *Bulletin of the American Museum of Natural History*, *19*, 639–651.
Wheeler, W. M. (1910). *Ants: Their structure, development and behavior* (pp. 1–663 +xxv). Columbia University Press.
Wheeler, W. M. (1921). Observations on army ants in British Guiana. *Proceedings of the American Academy of Arts and Sciences*, *56*, 291–328.
Wheeler, W. M. (1922). *Ants of the American museum Congo expedition* (p. 1139). Bulletin of the American Museum of Natural History.
Wheeler, W. M. (1925). The finding of the queen of the army ant *Eciton hamatum* Fabricius. *Biological Bulletin (Woods Hole)*, *49*, 139–149.
Williams, T. M., & Carrol, S. B. (2009). Genetic and molecular insights into the development and evolution of sexual dimorphism. *Nature Reviews Genetics*, *10*, 797–804. https://doi.org/10.1038/nrg2687
Wilson, E. O. (1955). A monographic revision of the ant genus *Lasius*. *Bulletin of the Museum of Comparative Zoology at Harvard College*, *113*, 3–199.
Wilson, E. O. (1964). The true army ants of the indo-Australian area. *Pacific Insects*, *6*, 427–483.
Wilson, E. O. (1987). Causes of ecological success: The case of the ants. *Journal of Animal Ecology*, *56*, 1–9.
Wilson, E. O., Carpenter, F. M., & Brown, W. L., Jr. (1967a). The first Mesozoic ants, with the description of a new subfamily. *Psyche*, *74*, 1–19.
Wilson, E. O., Carpenter, F. M., & Brown, W. L., Jr. (1967b). The first Mesozoic ants. *Science*, *157*, 1038–1040.
Yoder, M., Mikó, I., Seltmann, K. C., Bertone, M. A., & Deans, A. R. (2010). A gross anatomy ontology for Hymenoptera. *PLoS ONE*, *5*(12), e15991.
Yokohari, F. (1983). The coelocapitular sensillum, an antennal hygro- and thermoreceptive sensillum of the honey bee, *Apis mellifera* L. *Cell and Tissue Research*, *233*, 355–365.
Yokohari, F., Tominaga, Y., & Tateda, H. (1982). Antennal hygroreceptors of the honey bee, *Apis mellifera* L. *Cell and Tissue Research*, *226*, 63–73.
Zhang, W., He, Z., Sun, Y., Wu, J., & Wu, Z. (2020). A mathematical modeling method elucidating the integrated gripping performance of ant mandibles and bio-inspired grippers. *Journal of Bionic Engineering*, *17*, 1–15. https://doi.org/10.1007/s42235-020-0065-9
Zhang, W., Li, M., Zheng, G., Guan, Z., Wu, J., & Wu, Z. (2020). Multifunctional mandibles of ants: Variation in gripping behavior facilitated by specific microstructures and kinematics. *Journal of Insect Physiology*, *120*, 103993. https://doi.org/10.1016/h.jinsphys.2019.103993
Zimmermann, D., & Vilhelmsen, L. (2016). The sister group of Aculeata (Hymenoptera) – Evidence from internal head anatomy, with emphasis on the tentorium. *Arthropod Systematics & Phylogeny*, *74*, 195–218.

SUPPORTING INFORMATION

Additional supporting information may be found in the online version of the article at the publisher's website.

How to cite this article: Boudinot, B. E., Moosdorf, O. T. D., Beutel, R. G., & Richter, A. (2021). Anatomy and evolution of the head of *Dorylus helvolus* (Formicidae: Dorylinae): Patterns of sex- and caste-limited traits in the sausagefly and the driver ant. *Journal of Morphology*, *282*(11), 1616–1658. https://doi.org/10.1002/jmor.21410